ROADMAP • OPEN ACCESS

Roadmap on nonlinear optics–focus on Chinese research

To cite this article: Mengxin Ren *et al* 2023 *J. Phys. Photonics* **5** 032501

View the article online for updates and enhancements.

Journal of Physics: Photonics

ROADMAP

Roadmap on nonlinear optics–focus on Chinese research

Mengxin Ren[1] , Jingjun Xu[1,*], Pengfei Lan[2], Peixiang Lu[2], Zhi-Yuan Li[3], Li-Hong Hong[3], Yulei Wang[4,5], Zhenxu Bai[4,5], Zhiwei Lv[4,5], Zhi-Yuan Zhou[6], Bao-Sen Shi[6] , Yong Zhang[7] , Shining Zhu[7], Min Xiao[7,8] , Satoshi Aya[9,10], Yan-qing Lu[7,11], Huixin Fan[12], Min Luo[12], Ning Ye[13], Zeyuan Sun[14], Wei-Tao Liu[14], Shiwei Wu[14] , Qingyun Li[15], Hui Hu[15] , Yuanlin Zheng[16], Xianfeng Chen[16], Xiaoyong Hu[17] , Chuanshan Tian[14], Zixian Hu[18], Guixin Li[18], Yi Hu[1], Kun Huang[19,20], Heping Zeng[19,20], Zhen-Ze Li[21], Hong-Bo Sun[22] , Lei Dong[23], Runfeng Li[17], Wenkai Yang[17] and Kebin Shi[17]

1   The Key Laboratory of Weak-Light Nonlinear Photonics, Ministry of Education, School of Physics and TEDA Applied Physics Institute, Nankai University, Tianjin 300071, People's Republic of China
2   School of Physics and Wuhan National Laboratory for Optical Electronics, Huazhong University of Science and Technology, Wuhan 430074, People's Republic of China
3   School of Physics and Optoelectronics, South China University of Technology, Guangzhou 510640, People's Republic of China
4   Center for Advanced Laser Technology, Hebei University of Technology, Tianjin 300401, People's Republic of China
5   Hebei Key Laboratory of Advanced Laser Technology and Equipment, Tianjin 300401, People's Republic of China
6   CAS Key Laboratory of Quantum Information, University of Science and Technology of China, Hefei 230026, People's Republic of China
7   National Laboratory of Solid-State Microstructures, College of Engineering and Applied Sciences, Nanjing University, Nanjing 210093, People's Republic of China
8   Department of Physics, University of Arkansas, Fayetteville, AR 72701, United States of America
9   South China Advanced Institute for Soft Matter Science and Technology (AISMST), School of Emergent Soft Matter, South China University of Technology, Guangzhou 510640, People's Republic of China
10   Guangdong Provincial Key Laboratory of Functional and Intelligent Hybrid Materials and Devices, South China University of Technology, Guangzhou 510640, People's Republic of China
11   Key Laboratory of Intelligent Optical Sensing and Manipulation, Nanjing University, Nanjing 210093, People's Republic of China
12   Fujian Institute of Research on the Structure of Matter, Chinese Academy of Sciences, Fuzhou 350002, People's Republic of China
13   Institute of Functional Crystals, Tianjin University of Technology, Tianjin 300384, People's Republic of China
14   State Key Laboratory of Surface Physics, Key Laboratory of Micro and Nano Photonic Structures (MOE), and Department of Physics, Fudan University, Shanghai 200433, People's Republic of China
15   School of Physics, Shandong University, Jinan 250100, People's Republic of China
16   State Key Laboratory of Advanced Optical Communication Systems and Networks, School of Physics and Astronomy, Shanghai Jiao Tong University, Shanghai 200240, People's Republic of China
17   State Key Laboratory for Mesoscopic Physics and Frontiers Science Center for Nano-Optoelectronics, School of Physics, Peking University, Beijing 100871, People's Republic of China
18   Department of Materials Science and Engineering, Southern University of Science and Technology, Shenzhen 518055, People's Republic of China
19   State Key Laboratory of Precision Spectroscopy, East China Normal University, Shanghai 200062, People's Republic of China
20   Chongqing Key Laboratory of Precision Optics, Chongqing Institute of East China Normal University, Chongqing 401121, People's Republic of China
21   State Key Laboratory of Integrated Optoelectronics, College of Electronic Science and Engineering, Jilin University, Changchun 130012, People's Republic of China
22   State Key Laboratory of Precision Measurement Technology and Instruments, Department of Precision Instrument, Tsinghua University, Beijing 100084, People's Republic of China
23   State Key Laboratory of Quantum Optics and Quantum Optics Devices, Institute of Laser Spectroscopy, Shanxi University, Taiyuan 030006, People's Republic of China
*   Author to whom any correspondence should be addressed.

E-mail: jjxu@nankai.edu.cn

Abstract

In nonlinear optical systems, the optical superposition principle breaks down. The system's response (including electric polarization, current density, etc) is not proportional to the stimulus it receives. Over the past half century, nonlinear optics has grown from an individual frequency doubling experiment into a broad academic field. The nonlinear optics has not only brought new physics and phenomena, but also has become an enabling technology for numerous areas that are vital to our lives, such as communications, health, advanced manufacturing, *et al*. This Roadmap surveys some of the recent emerging fields of the nonlinear optics, with a special attention to

studies in China. Each section provides an overview of the current and future challenges within a part of the field, highlighting the most exciting opportunities for future research and developments.

Contents

Introduction

Mengxin Ren and Jingjun Xu*

The Key Laboratory of Weak-Light Nonlinear Photonics, Ministry of Education, School of Physics and TEDA Applied Physics Institute, Nankai University, Tianjin 300071, People's Republic of China

*Email: jjxu@nankai.edu.cn

Nonlinear optics is a branch of optics that describes the behaviors of light in media, in which polarization density **P** responds nonlinearly to the electric field **E** of the light as $\mathbf{P}(\omega) = \in_0[\chi^{(1)}\mathbf{E}(\omega) + \chi^{(2)}\mathbf{E}^2(\omega) + \chi^{(3)}\mathbf{E}^3(\omega) + \ldots]$. The quantity $\chi^{(1)}$ is responsible for the linear optical response and $\in_0$ is the permittivity of free space. The $\chi^{(2)}$ and $\chi^{(3)}$ are knowns as the second- and third-order nonlinear optical (NLO) susceptibilities, respectively. The birth of the nonlinear optics. The birth of the nonlinear optics is often taken to be the discovery of second-harmonic generation (SHG) by Franken *et al* in 1961, shortly after construction of the first laser by Maiman in 1960. As a matter of fact, before the development of the lasers, some nonlinear effects had already been observed without realizing their nonlinear nature. Two examples are DC Kerr effect and Pockels effect discovered in the 19th century. In these effects, the refractive indices of media were found to vary as a result of the external electrostatic fields. The invention of the laser provides a new tool to generate strong optical frequency electric fields comparable to that inside atom ($\sim 10^8$ V m^{-1}), making the nonlinear perturbation noticeable, thus ushering in a golden-rush era of nonlinear optics.

The nonlinear optics developed at an explosive rate in its first decade (1961–1969). During this period, most of the fundamental principles were established, and most of the nonlinear phenomena known today were observed. These include optical harmonics (1961), sum-and difference-frequency generation (DFG) (1962, 1963), multiphoton absorption (1961), stimulated Raman/Brillouin scattering (1962, 1964), self-focusing (1964), optical breakdown (1964), photon echo (1964), optical parametric amplification and oscillation (OPA and OPO) (1965), coherent anti-Stokes Raman spectroscopy (CARS, 1965), photorefractive effect (1966), electromagnetically induced transparency (1967), optical nutation (1966), and optical bistability (1969), etc.

During the 1970s and the following few decades, the establishment of new principles and the discovery of new effects became rare; nevertheless, the understanding of the known effects was dramatically improved. With the amazing advances in tunable and pulsed lasers, people started to exploit nonlinear optics at an astonishing rate in new materials, in new systems, in new configurations, and especially on challenging spatiotemporal scales. During this period, in addition to focusing on its own development, nonlinear optics has penetrated other related disciplines (e.g. solid state physics, plasma physics, integrated optics, acoustics, mechanics, chemistry, biology, etc.).

The golden-rush of nonlinear optics is said to have ended in the 1960s [1, 2]. However, in the recent decades, some things that are truly novel and hardly predicted in the 1960s have appeared. For example, the emergence of photonic crystals, and metamaterials represents an important trend towards artificial designer media with exotic nonlinear performance surpassing the natural materials. Two-dimensional materials, such as graphene, certainly provides a nonlinear framework with ultimate thin thickness, etc.

In this roadmap, we do not intend to outline the global picture of the nonlinear optics, but rather focus on the developments in China. Inspired by the landmark paper of 'Infrared and optical masers' by Schawlow and Townes in 1958, scientists from Changchun Institute of Optics, Fine Mechanics and Physics (CIOMP) began to conceive of optical quantum amplifiers, and successfully built the China's first laser in 1961. In the following 15 years, different lasers were built [3], such as He–Ne laser (1963), Nd–glass laser (1963), GaAs semiconductor laser (1963), Ar$^+$ laser (1965), CO$_2$ laser (1965), dye laser (1974) and excimer laser (1977). The nonlinear effects that are related to improving the performance of high-power lasers were well studied, such as optical breakdown, self-focusing, optical filamentation, parasitic oscillation, etc. However, the researches on nonlinear frequency conversion and nonlinear spectroscopy were largely hindered by the lack of high-quality nonlinear crystals before 1980 in China [4].

In the 1980s, researches of nonlinear crystal flourished with fruitful results. Periodically poled lithium niobate (PPLN) crystals were successfully grown in Nanjing University and the quasi-phase matched SHG was demonstrated experimentally, which provided a new framework for harmonic generation. Nankai University, in cooperation with Norla Institute of Technical Physics, found the high-resistance of optical damage in Mg doped lithium niobate (LN), which opened a new horizon for applications of LN in high power laser and integrated optics. Scientists of the Fujian Institute of Research on the Structure of Matter synthesized barium metaborate (BBO) and lithium triborate (LBO) crystals, which enable the lasers with ultraviolet emission. Potassium titanyl phosphate (KTP) was successfully grown in Shandong University. In the meantime, Chinese researchers made great efforts to catch up with the international counterparts, and

nearly all NLO phenomena that had been observed abroad were successfully reproduced in China in a short period of time. Until the middle of 1980s, Chinese researchers have achieved remarkable progresses in such as optical bistability, four-waves mixing, and stimulated Raman scattering (SRS), etc. By the turn of 21th century, nonlinear optics has become an important academic topic in China. A series of breakthroughs have been made in photorefractive effect and its applications in optical storage and computing, as well as the quasi-phase matching (QPM) frequency conversion and tunable lasers, etc. More progresses of nonlinear optics in China can be found in several review articles and books [5–9].

In this Roadmap, we highlight the status, current and future challenges, and emerging technologies in several research areas of nonlinear optics in China. This roadmap is divided into several topics, grouped thematically.

The first part of the roadmap covers the current progress of lasers, which is an essential tool to produce nonlinearities. In article 1, Pengfei Lan and Peixiang Lu describe the developments of attosecond lasers, which is an ideal tool to study the ultrafast nonlinear dynamics in matters. In article 2, Zhi-Yuan Li and Li-Hong Hong demonstrate an all-spectrum white laser, which has an extremely broadband spectrum like solar radiation but with coherent light. In article 3, Yulei Wang and Zhiwei Lv present an overview of the stimulated Brillouin scattering (SBS) effect and its application in manufacturing lasers with designer performance. The realization of quantum light sources based on nonlinear optics is discussed in article 4 by Zhiyuan Zhou and Baosen Shi.

The second part of the roadmap addresses the field of nonlinear materials. In article 5, Yong Zhang, Shining Zhu and Min Xiao discuss the state-of-the-art three-dimensional artificial microstructures, which is a solid step towards nonlinear optics in three-dimensional space. In article 6, Satoshi Aya and Yanqing Lu introduce emerging polar liquid crystals (LCs) with tunable polarization structures, which are the first class of second-order nonlinear materials in the liquid form. In article 7, Huixin Fan, Min Luo and Ning Ye describe the design of the nonlinear materials for SHG in ultraviolet and deep ultraviolet (DUV). Zeyuan Sun, Weitao Liu and Shiwei Wu present in article 8 the atomically thin two-dimensional materials, which provide a unique opportunity to study various NLO phenomena. Furthermore, this part of the roadmap ends by Qingyun Li and Hui Hu with an introduction to the current status and perspectives of the lithium niobate thin films (LNTFs), which is a promising platform for the next generation integrated photonics.

The third part of the roadmap deals with new nonlinear effects and behaviors. In article 10, Yuanlin Zheng and Xianfeng Chen show the classical and quantum nonlinear frequency conversion by LNTF, which is essential to build all-optical functional chips. In article 11, Xiaoyong Hu surveys the research on ultrafast and giant third-order nonlinearity, which is essential to achieve high-speed and low energy consumption all-optical processing system. Chuanshan Tian describes in article 12 the surface-specific NLO spectroscopy and its implementation in probing the microscopic structure and dynamics at surfaces and interfaces. In article 13, Zixian Hu and Guixin Li review the spin–orbit interaction in the NLO processes, which has been proven as an efficient method to generate and control the angular momentum of the harmonic waves. In the last article of this part, Yi Hu and Jingjun Xu introduce some counterintuitive phenomena by nonlinear light interactions, which manifest synchronized acceleration of optical beams breaking the action-reaction symmetry.

The final part of the roadmap discusses the applications of the nonlinear optics. Kun Huang and Heping Zeng discuss in article 15 how parametric upconversion imaging acts as a promising strategy for mid-infrared (MIR) imaging, where infrared photons are detected by high-performance visible detector. In article 16, Zhenze Li and Hongbo Sun present the status of ultrafast laser nonlinear manufacturing, which represents a promising method to construct next-generation integrated photonic system. In article 17, Lei Dong introduces the application of photoacoustic (PA) effect in sensitive gas spectroscopic sensing. The whole roadmap concludes by Runfeng Li, Wenkai Yang and Kebin Shi with an important application of NLO microscopy for bio-imaging, which is an unparalleled tool for observing biological dynamics *in-vivo* with high spatiotemporal resolution and biomedical specificities.

Nonlinear optics is a flourishing field, which has grown far beyond what we expected at its birth. It not only provides us with new understanding or essence to the light-matter interactions, but also new technique to harness light. We shall not limit the nonlinear optics as an academic subject, but also recognize its power in driving economic development. Its advances have fostered innovations across a broad spectrum of applications in a diverse array of economic sectors. For example, the electro-optical effect, which enables information routing at a hyper-speed in fiber networks, makes the Internet economy thrive. Furthermore, NLO spectroscopy has become a standard method for material inspection, playing a vital role in many aspects of microelectronic industries. There is no doubt that the nonlinear optics will offer greater societal impact over the coming decades, but as highlighted in the following sections there are certainly many new challenges to overcome. The nonlinear optics in China has achieved remarkable achievements during the

past decades. To maintain this encouraging trend and meet the challenges ahead, greater investment in national policy, financial support and intellectual resources are highly desirable in the future.

Acknowledgments

1. High order harmonics and attosecond pulse

Pengfei Lan and Peixiang Lu
School of Physics and Wuhan National Laboratory for Optical Electronics, Huazhong University of Science and Technology, Wuhan 430074, People's Republic of China

Status

At the end of 1980s, high order harmonics were observed in the interaction of strong laser field with atomic gases [10, 11]. Different from the normal perturbation nonlinear effect, the spectra of strong-field high order harmonic generation (HHG) present a broad plateau of nearly constant conversion efficiency, followed by abrupt cut-off. Such a non-perturbation nonlinear optics effect has revolutionized contemporary optics. On the one hand, it produces coherent extremely ultraviolet (XUV) or soft x-ray light sources. As opposed to synchrotron and free-electron laser, which need large-scale facilities, HHG-based x-ray can be much more easily accessed in a small-scale laboratory. On the other hand, the broadband spectrum enables to produce an attosecond ultrashort laser pulse [12, 13]. Attoseconds pulse lies at the current frontier of ultrashort laser and ultrafast science. It enables the attosecond time-resolved metrology that is not possible before, so that the electron motion can be detected in real time. The fast development of attosecond time-resolved measurement has significantly advanced the fundamental understanding of the microscopic dynamics of laser-matter interaction in the past decades.

Generation of HHG and attosecond pulse with shorter duration, higher photon energy, higher single-pulse energy, and higher flux (i.e. higher peak power and average power) has being the important goal. Several methods, e.g. amplitude gating, polarization gating, two-color or multi-color gating, have been demonstrated to control the HHG so as to generate an isolated attosecond pulse. In the first decades of this century, HHG and attosecond pulse is usually produced by using a Ti: Sapphire femtosecond driving laser with a wavelength of 800 nm. In the most recent decades, the MIR optical parametric amplifier (OPA) become the mainstream driving source for HHG. Then the photon energy has been extended the 'water window' region (i.e. 284 eV–583 eV) and the shortest pulse duration is reduced to ~50 as. However, as shown in figure 1(b), the pulse energy of the isolated attosecond pulse is usually at the nanojoule level and the repetition rate is 1 kHz. In recent two experiments, the pulse energy is boosted to 240 nJ and 1.3 μJ by loosely focusing a terawatt (TW) driving laser to the Ar and Xe gases, but the repetition rate is reduced to 10 Hz. The low pulse energy and photon flux is the crucial issue for the applications of attosecond pulses.

Current and future challenges

Applications of HHG and attosecond pulses have enabled lots of break-through achievements ether using attosecond pulse pump near infrared femtosecond pulse probe (or vice versa) and high harmonic spectroscopy. It is previously applied and developed in the field of ultrafast dynamics in atoms and molecules. In very recent years, considerable efforts are devoted to extending the attosecond spectroscopy to more complex systems, including solids and liquids. To this end, it requires to develop the more powerful attosecond laser pulse and attosecond techniques. Currently, it is still very challenging to increase the photon flux, pulse energy and photon energy of the attosecond pulse. The bottleneck is that the generation of isolated attosecond pulse generally requires an ultrashort driving pulse of few-cycle pulse duration and 100 TW cm^{-2} focusing intensity. Therefore, it is typically based on a Ti: Sapphire chirped pulse amplification (CPA) laser system, the pulse energy is at the milijoule level, and the relation rate is at the 1–10 kHz level. The generated attosecond pulse is typically at the nanojoule or tens of nanojoules level and the photon energy is limited to ~100 eV. Using a MIR OPA driving laser pulse is a good way to increase the photon energy and produce the shorter attosecond pulse. However, the efficiency of HHG decreases dramatically as the yield declines approximately by $\lambda^{-5 \text{ to } -6}$ with increasing the driving laser wavelength.

On the other hand, circularly polarized HHG and attosecond pulse are very attracting for the study of ultrafast dynamics in circular dichroism of magnetic materials, chiral molecules. However, due to the 'recollision' mechanism [16], it is more challenging to produce bright circularly polarized high harmonics and attosecond pulses than the linearly polarized one.

Moreover, the observations of high harmonic generation in semiconductors [17], dielectrics, liquids [18] and even glasses pave the way to extend the high harmonic spectroscopy to probing the band structure, topologic state, and electron dynamics to more complex systems. However, it is very challenging to understand the physics underlying the interaction of solids, liquids with strong laser fields. For instance, the mechanism of solid high harmonic generation is still under active discussions [19]. To real these ultrafast processes, advanced time-resolved spectroscopy methods that can capture the electron and nuclear motion are desired.
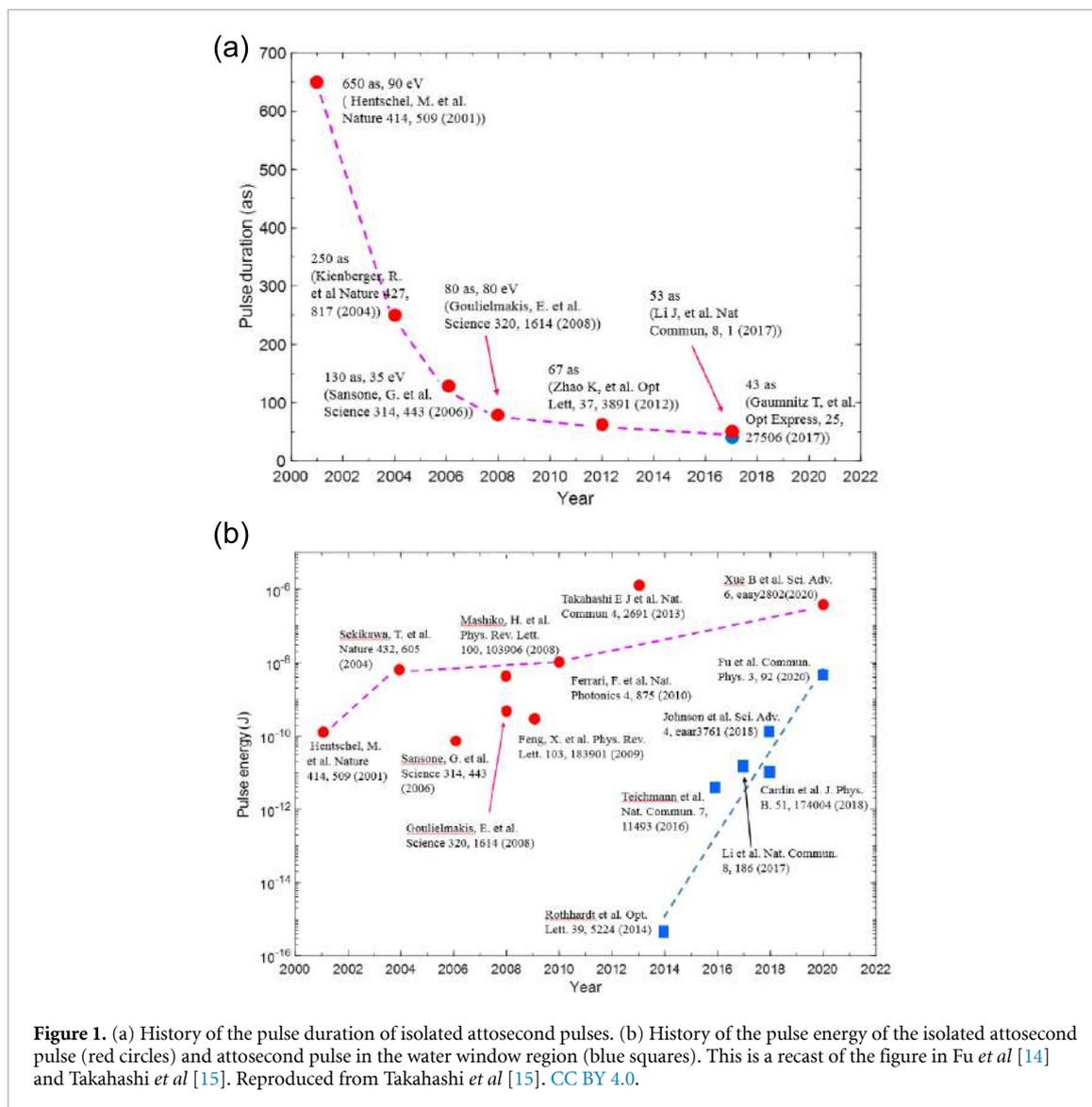
Figure 1. (a) History of the pulse duration of isolated attosecond pulses. (b) History of the pulse energy of the isolated attosecond pulse (red circles) and attosecond pulse in the water window region (blue squares). This is a recast of the figure in Fu *et al* [14] and Takahashi *et al* [15]. Reproduced from Takahashi *et al* [15]. CC BY 4.0.

Advances in science and technology to meet challenges

The recent development of Yb-based CPA laser system (see the recent review [20]), e.g. fiber laser, slab lasers and ultrafast thin-disk laser, has opens a very promising way to produce the attosecond pulses with high-flux and high pulse energy. In compression to Ti: Sapphire CPA, the Yb-based CPA can deliver multi-millijoule, sub-picosecond laser pulse at 100 kHz or even several MHz, so that the average power can be improved by one-to-two orders of magnitude. In combination with the nonlinear pulse compression techniques, e.g. the gas-filled hollow-core-fiber, multipass cell, multipass thin plate, the pulse duration of the Yb-CPA laser can be reduced to several tens of femtoseconds or a few femtoseconds. Several groups have demonstrated the enhancement of photon flux using the Yb-CPA driving laser. Moreover, the coherent beam combination of ultrafast fiber lasers has advanced substantially in very recent years. It becomes an efficient power scaling techniques and enables to produce the 10 mJ pulse at 100 kHz and above 1 J at 1 kHz. Then it becomes possible to improve the single-pulse energy and average power of the attosecond pulse.

An alternative way to implement the high power Yb-CPA is to pump the optical parametric CPA, i.e. OPCPA. Several groups have generated sub-10 fs laser pulse at 100 kHz or MHz and produced HHG and attosecond pulse with OPCPA systems. Moreover, by using different nonlinear materials, OPCPA enables to produce the MIR laser pulse so that to extend the photon energy of HHG to more than 600 eV. It is expected to dramatically boost the peak power to tens TW and average power to more than 3 kW in a concept design, which will become a powerful engine for pushing attosecond science [21]. Another way to boost the photon flux is using cavity-enhanced HHG, which can increase the repetition rate to tens of MHz, but with limited single-pulse energy.

High brilliance attosecond pulses will enable numerous opportunities. By applying the table-top HHG source, one can extend the x-ray techniques, e.g. x-ray absorption spectroscopy, x-ray photoelectron spectroscopy, to the attosecond domain. The increase of the HHG photon energy will enable the time-resolved x-ray absorption near-edge structure and extended x-ray absorption fine structure spectroscopy, providing electronic as well as structural and chemical information with atomic resolution. The combination of the HHG source with the Angle resolved photoemission spectroscopy or photo-emission electron microscopy will provide a powerful tool to investigate the electronic band and structure change of the material. Great progresses can be foreseen in understanding the ultrafast dynamics in chemistry and condense matter physics.

Concluding remarks

Tracking and understanding the ultrafast dynamics in atoms, molecules and condensed matter has been a continuous hot topic of ultrafast science. The last two decades have witnessed the fast advances of attosecond science. New perspective about the hitherto immeasurably ultrafast electronic processes of laser-matter interaction have been obtained. Since HHG has been observed ranging from atoms, molecules to solids and liquids, the field of attosecond sciences becomes much broader and has attracted more interdisciplinary interests. More powerful attosecond laser sources e.g. extreme light infrastructure in Europe, Synergetic Extreme Condition User Facility in China and the attosecond pulse from free electron lasers in USA, are being available, a bright future of attosecond science can be expected.

Acknowledgments

2. All-spectrum white laser and ultra-broadband nonlinear optics

Zhi-Yuan Li and Li-Hong Hong
School of Physics and Optoelectronics, South China University of Technology, Guangzhou 510640, People's Republic of China

Status

Since the invention of ruby laser in 1960 by Maiman, the realm of lasers has continuously advanced into an ever-increasing height and ever-expanding frontiers in terms of laser materials (gas, liquid, solid, semiconductor, and fiber), pulse duration (continuous wave, nanosecond, picosecond, femtosecond, and attosecond), spectral width, power, and energy, thanks to the cooperative efforts from laser technology and nonlinear optics communities. An ordinary laser machine, with fixed design of cavity, gain medium, and pump source, only outputs continuous-wave laser with one or several specific discrete wavelengths or ultrashort pulse laser covering only a limited spectral bandwidth. This shortcoming can be lifted by input these pump lasers into a nonlinear crystal or amorphous material with considerable second and third-order nonlinearity, where NLO interaction will convert part of the energy of pump lasers into new lasers of different discrete wavelengths or spectral bands, leading to significantly expanded windows and bandwidths of lasers. One sees the cooperative action of laser technology and nonlinear optics here.

As the second and third-order nonlinear coefficients are very small compared with the linear susceptibility, it requires the input pump laser beam to have sufficiently high intensity (i.e. power density) in order that the NLO conversion efficiency reaches a high magnitude. Besides, to enlarge the spectral window and bandwidth as much as possible, the pump laser should first have as large as possible bandwidth. A femtosecond pulse laser with pulse duration on the order of 50–100 fs has a bandwidth (measured by the full width at half maximum, FWHM) on the order of 20–50 nm, is suitable for this purpose. If, in addition, the femtosecond laser has its single pulse energy reaching the ∼1 mJ level, then the peak power can be as large as 10 GW, and when focused into a tiny laser beam with spot radius as 1 mm, then the power density (i.e. the optical intensity) can reach 1 TW cm^{-2}, a magnitude sufficiently large to induce both very strong second and third-order NLO effects, so that an input narrow band femtosecond pulse laser can evolve into an output supercontinuum laser with much larger bandwidth.

A great dream of this type of ultra-broadband laser is to construct a supercontinuum white laser possessing an extremely broad spectral bandwidth that covers ultraviolet–visible–infrared (UV–vis–IR), much like the ordinary solar radiation spectrum (which is a completely incoherent light source) does, as illustrated in figure 2.

Current and future challenges

The solar radiation not only has a large bandwidth, but also has a superflat spectral profile, where the FWHM (or 3 dB bandwidth) reaches about 640 nm (320–960 nm). A white laser with this brilliant degree of ultrabroad bandwidth and superflat spectral profile, which can be named as ***all-spectrum white laser***, should represent a milestone in laser science and technology, and undoubtedly will induce a revolution in both basic sciences and practical applications. Yet, it is by no means an easy task to bring this dream into reality, on the contrary, it is a great challenge and difficulty. Notice that an ordinary Ti:Sapphire femtosecond pulse laser with 50 fs pulse duration only has 45 nm 3 dB bandwidth around the central wavelength of 785 nm, a natural question arises: how to expand the bandwidth of pump femtosecond laser into the UV–vis–IR all-spectrum white laser with the similar superflat spectral profile of solar radiation?

In the past history there have appeared many schemes toward supercontinuum white-light laser, but most of them utilize various third-order nonlinear effects (third-NL) (self-phase modulation (SPM), four-wave mixing (FWM), SRS, etc) of high-peak-power picosecond and femtosecond pulse laser interacting with amorphous solid materials (like silica, fluoride, chalcogenide glass) in the form of microstructured photonic crystal fibers or homogeneous plates, or with rare gases (He, Ar, etc) filled within hollow-core silica fibers [22–25]. However, these purely third-NL schemes always encounter certain limitations in the balanced performance of spectral bandwidth, spectral flatness, and pulse energy due to the tiny modal area or the dispersion properties of transport waves. Another more powerful means to expand the spectral range of the laser is various second-order nonlinear effects (second-NL) effects via the promising route of QPM scheme. However, these existing QPM routes also have difficulty in high-quality broadband laser generation with limited spectral bandwidth, not flat enough spectral profile, and reduced conversion efficiency. Frankly speaking, it becomes a great challenge to resolve these bad limitations existing in both second-NL and third-NL regimes and make the best of the both worlds.

Figure 2. A dream supercontinuum white laser with an extremely broad spectral bandwidth that covers UV–vis–IR, resembling the ordinary solar radiation spectrum as displayed in this figure.

Figure 3. Schematic illustration of a roadmap toward construction of all-spectrum white laser via synergic second-NL and third-NL. The second-NL is implemented by pumping a CPPLN crystal by a high peak power mid-IR fs pulse laser and igniting multiple HHG. The third-NL is used to broaden both the pump fs laser pulse and output HHH laser pulse, so that the spectral bands of all harmonics overlap to form a UV–vis-IR supercontinuum white laser.

The above analyses also indicate that if one can dig and explore to make the good figures of both second-NL and third-NL to fully cooperate and operate together, then the synergic action of these two effects might shine a light of explosive power to overcome and exceed all challenges and difficulties standing before the all-spectrum white laser.

Advances in science and technology to meet challenges

Following the roadmap shown in figure 3, the Li team has dug into the physics of ultra-broadband nonlinear optics and made gradual and stable progress toward all-spectrum white laser. In 2014 the team realized that ordinary PPLN with powerful QPM ability is suitable for single-wavelength pump laser (continuous wave, ns and ps) SHG, but not good for either simultaneous SHG and third harmonic generation (THG) for single-wavelength pump laser or broadband fs pulse laser SHG [26, 27]. Yet, introduction of simple modulation to poled structures like chirping leads to a new chirped PPLN (called CPPLN) can largely lift such a limitation of PPLN so that 100 nm bandwidth of SHG and THG (via cascaded SHG and sum-frequency generation (SFG)) can be readily implemented to create red, green, and blue color [28]. In 2015 a mid-IR fs laser of 20 μJ pulse energy and central wavelength 3600 nm was used to pump the CPPLN

with a multiple QPM bands covering an extremely broad bandwidth and simultaneous 2–8 harmonics was observed with high efficiency [29]. This was the first experimental demonstration of high harmonics generation in a single solid material. The 4–8 harmonics together comprises a UV–vis–NIR supercontinuum white laser with conversion efficiency of 18%. In 2021, the team showed that in addition to ordinary second-NL like SHG ad SFG, CPPLN also exhibits significant third-NL effect like SPM so that a pump NIR fs pulse laser has its bandwidth expanding from 100 nm to 300 nm when passing through CPPLN, making UV–vis–NIR white laser readily available via SHG and THG [30]. This first demonstration of synergic action of second-NL and third-NL in nonlinear optics has shined a new light on the route toward all-spectrum white-laser. In 2022 the team realized intense two-octave UV–vis-IR supercontinuum laser via high-efficiency one-octave SHG via a cascaded silica plate and CPPLN module against 0.5 mJ Ti:Sapphire pulse laser, with the former greatly expanding the spectral width around 800 nm due to third-NL effect and the latter further pushing the spectral band deep into UV and vis [31]. Very recently, a Ti:Sapphire fs laser with 3 mJ pulse energy was used to pump the silica plate-CPPLN crystal module, creating a brilliant white-laser with 1 mJ per pulse and 700 nm 3 dB bandwidth (385–1080 nm). All these studies confirm the power of synergic action of second-NL and third-NL in expanding the spectral width of pump fs laser into an unprecedented level.

Concluding remarks

Construction of all-spectrum white laser remains a great challenge in terms of physics and optics (nonlinear optics, ultrafast optics), laser sciences, and material sciences. Without the collaborative effort of expertise from these research fields, the great dream to build a UV–vis-IR all-spectrum white laser with simultaneous merits of high power, large pulse energy, extremely large bandwidth, superflat spectral profile, and high coherence, cannot become a reality. From the fundamental physics point of view, this dream is closely related with the ultra-broadband nonlinear optics, whose theoretical basis should be the following nonlinear Maxwell's equation describing various NL interactions of femtosecond laser with nonlinear crystals and materials.

$$\nabla^2 \mathbf{E}(\mathbf{r},t) = \mu_0 \varepsilon_0 \frac{\partial^2 \mathbf{E}(\mathbf{r},t)}{\partial t^2} + \mu_0 \frac{\partial^2 \mathbf{P}^{(1)}(\mathbf{r},t)}{\partial t^2} + \mu_0 \frac{\partial^2 \mathbf{P}^{(2)}(\mathbf{r},t)}{\partial t^2} + \mu_0 \frac{\partial^2 \mathbf{P}^{(3)}(\mathbf{r},t)}{\partial t^2}.$$

Here $\mathbf{E}(\mathbf{r},t)$, $\mathbf{P}^{(1)}(\mathbf{r},t)$, $\mathbf{P}^{(2)}(\mathbf{r},t)$, and $\mathbf{P}^{(3)}(\mathbf{r},t)$ are the electric field, linear polarization, second-order and third-order nonlinear polarizations, respectively. This nonlinear equation, seemingly simple at first glance, is subject to huge challenge and difficulty of solution as it involves complicated spatial-temporal evolution of electric field and wave under the influence of field-induced linear and nonlinear polarizations. This equation should be the physical basis for ultrabroadband nonlinear optics investigating various NL interactions of high-peak-power fs laser with nonlinear crystals and materials. Solution of this equation should teach us many things about the route toward all-spectrum white laser.

Acknowledgments

3. Stimulated Brillouin scattering for high power laser applications

Yulei Wang[1,2], *Zhenxu Bai*[1,2] *and Zhiwei Lv*[1,2]
[1] Center for Advanced Laser Technology, Hebei University of Technology, Tianjin 300401, People's Republic of China
[2] Hebei Key Laboratory of Advanced Laser Technology and Equipment, Tianjin 300401, People's Republic of China

Status

As a third-order NLO process, SBS is generated by the interaction between light wave and acoustic wave in different kinds of media including solid, liquid, gas, and plasma [32]. The excited Stokes and pump are in opposite directions for unguided structures, as shown in figure 4. The parameters of SBS are mainly determined by the intrinsic properties of the gain medium and input wavelength. In general, the Brillouin frequency shift for most media is in the range of 0.1–100 GHz, and the gain linewidth is only 0.01–1 GHz, both of which are much smaller than that of SRS. Therefore, SBS can achieve a theoretical quantum loss of less than 0.1% and is of help to achieve a laser output with a very narrow linewidth. Therefore, the quantum defects during the SBS conversion are negligible, meanwhile, extremely narrow linewidth laser output can be generated. In addition, with the characteristics such as threshold, amplification, and phase conjugation, SBS has been widely applied in the fields of beam time-domain shaping, spectral narrowing, power scaling, sensing, etc.

In the past decades, high-energy and high-power laser technology has developed rapidly thanks to the introduction of SBS technology. Scientific researchers in China have performed well at this stage. As shown in figure 5(a), the SBS-based phase conjugation mirror (PCM) is used to compensate for the wavefront distortion caused by optical defects and thermal distortion, so as to obtain high-quality beam output [33]. In the process of opposite propagation between Stokes and pump, the self-amplification effect of SBS makes the pulse width of the Stokes significantly compressed compared with the pump, as shown in figure 5(b). For example, from several nanoseconds to hundreds of picoseconds, therefore, leads to the peak power of the laser increased by 1–2 orders of magnitude [34]. Brillouin amplification breaks through the bottleneck of traditional main oscillation power amplifier that is difficult to generate high-efficiency short-pulse amplification. It can realize the efficient energy transfer from the long-pulse directly to that of the short. At present, a 2.4 J, 200 ps laser pulse has been demonstrated via stimulated Brillouin amplification [35]. The serial beam combination technology which is also based on Brillouin amplification makes it possible to break the energy limit of a single laser beam while maintaining the operation repetition rate, as shown in figure 5(c). At present, 2.5 J nanosecond beam combined pulses at the repetition rate of 10 Hz have been obtained via non-collinear Brillouin amplification, which has shown great potential in the field of laser fusion drivers [36]. In addition, the Brillouin laser has been developed from the guided-wave structure to the free space with output power up to 20 W, which is 1–2 orders of magnitude higher than the guided-wave Brillouin lasers. It provides a new opportunity for realizing high-power narrow-linewidth lasers with a high signal-to-noise ratio [37].

Current and future challenges

Although SBS has made remarkable progress in the application and development of high-power laser technology, it still faces many challenges and outstanding problems. In order to realize the long-term stable operation of the SBS with a high-efficiency conversion efficiency, a gain medium with a high Brillouin gain coefficient, high damage threshold, high thermal conductivity, and high physical and chemical stability are usually required [32]. However, it is difficult to find a medium that takes into account all the above advantages, so it is necessary to make a choice according to the specific application scenarios. At present, the liquid medium that represented by heavy fluorocarbon is the most widely used SBS gain media, whose damage threshold is inversely proportional to the impurity content of the media. However, how to realize the production, filling and preservation of high-purity media is still a problem in engineering. Due to the narrow Brillouin linewidth of SBS gain media (viz. only a few tens of MHz for crystalline media), it is necessary to use a narrow linewidth (single-longitudinal-mode) laser as the pump source to excite the Stokes effectively [38]. This also means that in the process of non-collinear Brillouin amplification, the interaction angle between the pump and Stokes needs to be limited to a small range to avoid the reduction of energy conversion efficiency [36, 39]. In addition, how to generate controllable Stokes outputs in space, time domain and frequency domain, and how to develop compact SBS generators, amplifiers, and oscillators, are also the focus of attention in realizing the transformation of high-power SBS technology into the industry [40, 41].

Figure 4. Working principle of SBS. (a) Energy level diagram, and (b) conservation of momentum.

Figure 5. Typical applications of SBS in high-power lasers. (a) SBS-PCM, (b) SBS pulse compression, (c) SBS serial beam combination.
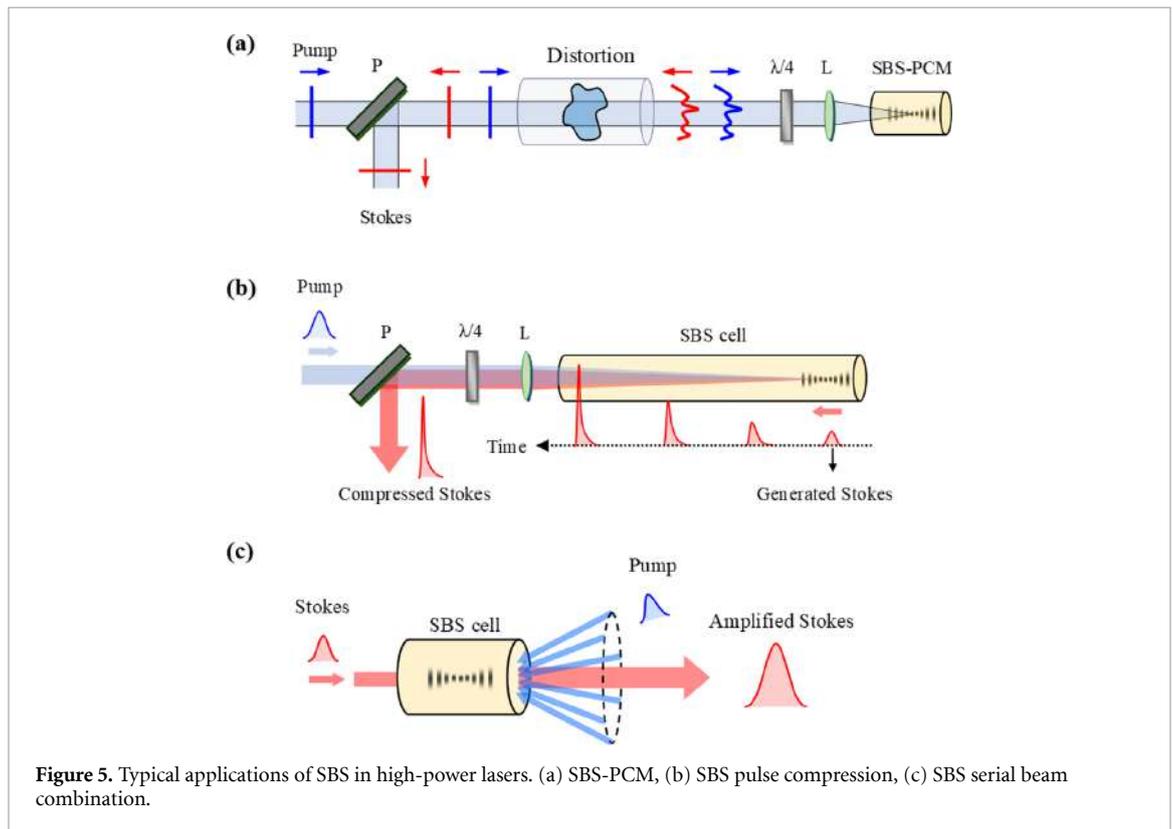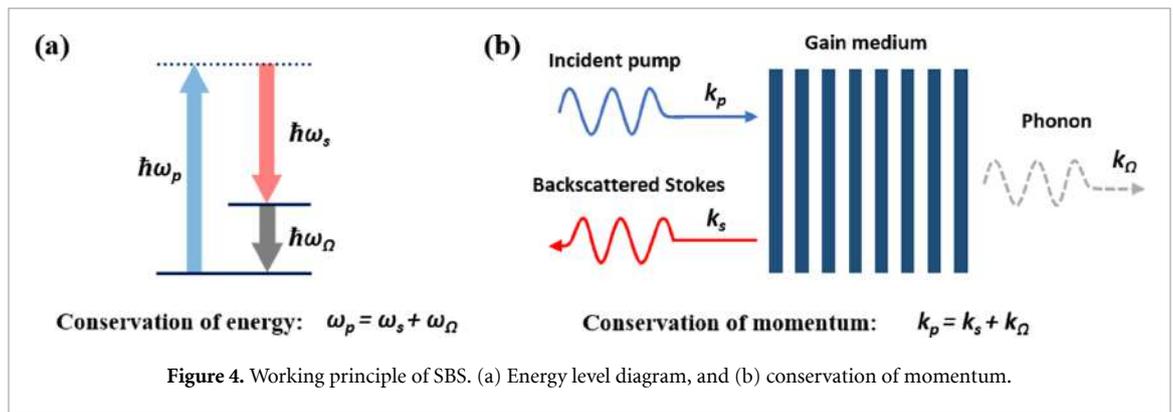
Advances in science and technology to meet challenges

In order to expand the application of SBS technology in the field of high energy and high power, there is still room for improvement in theory, technology, and engineering. For the theory, it is critical to establish a multidimensional dynamic model which includes pump parameters, SBS medium parameters, focusing parameters and medium heat distribution, so as to provide an overall explanation of the process of SBS generation, amplification and beam propagation. For the technology, on the one hand, the influence of the characteristics of SBS gain medium on the performance of SBS needs to be further studied, and the performance of SBS medium should be investigated and optimized (viz. improving the purity, increasing damage threshold, reducing absorption loss, etc). On the other hand, active modulation in both time- and frequency-domain should be further explored to optimize the conversion efficiency and realize adjustable output parameters of SBS. For engineering, attention should be paid to increasing the power load of SBS media, as well as breaking through the output power and repetition rate limits. Potential paths include optimizing the SBS structure and adopting thermal management technology. In addition, the combination of SBS and other NLO effects deserves further study, which is an important step to expand its application field.

Concluding remarks

As an important physical technology to generate laser beams with specific spatial/time/frequency domain and power characteristics, SBS has played an irreplaceable role in the fields of high-energy high repetition

rate PCM, high-energy beam combination laser, high-power Brillouin laser and optical frequency comb (OFC) generation at present. It is expected that in the next decade, with the progress of material science and the breakthrough of key technologies, more exciting new applications in high-power lasers are expected to be achieved for SBS. Meanwhile, SBS-based lasers are being developed for 'plug and play' portable devices.

Acknowledgments

4. Nonlinear optics based quantum light sources and their applications

Zhi-Yuan Zhou and Bao-Sen Shi

CAS Key Laboratory of Quantum Information, University of Science and Technology of China, Hefei 230026, People's Republic of China

Status

Quantum light sources are indispensable for applications in quantum information science and technology (QIST), typical applications include: quantum computations, communications, metrology, imaging and revealing basic principles of quantum mechanics [42, 43]. Therefore to prepare and control the properties quantum light sources on demand determines the developing level of QIST. Generally, two rather different methods are invented for preparing quantum light sources, one is based on excitation-reemission of photon in semiconductor quantum dot, single defect in color centers or single atom; another common used method is based on spontaneous emission based on nonlinear processes [42, 43]. Here, we describe and discuss quantum light sources generated based on nonlinear processes. Typically, two nonlinear processes are mostly used for preparing quantum light sources: spontaneous parametric down conversion (SPDC) and spontaneous four wave mixing (SFWM), which are based on second and third order nonlinear processes, respectively (see figures 6(a) and (b)). In both nonlinear processes, conservation laws of energy, linear momentum and angular momentum should be hold. In combining these conservation laws and making possible eigenstate of the system indistinguishable by quantum interference, entangled states in various degrees of freedoms can be prepared (figure 6(c)), some mostly prepared and studied entangled states are polarization, energy-time, orbital angular momentum, position-linear momentum, angular momentum and photon number and path [42]. For certain application scenarios in QIST, a specific quantum light sources can be used.

In SPDC, a pump photon of laser beam with higher frequency has the probability to split into two daughter photons with lower frequencies, which are usually called signal and idler photons [44]. While in SFWM, the annihilation of two pump photons creates signal and idler photons [45]. To generate frequency degenerate photon pairs, it is better to use SPDC process instead of SFWM. While for nondegenerate photon pair preparation, both SPDC and SFWM can be used. The most advantage for SFWM is photon pair generation in waveguide platform, which can greatly reduce the volume of the setups. For quantum light sources generated in SPDC and SFWM, the vacuum state is obtained most of the time for weak pump, while the photon pair state of interest is created with a low probability. A moderate pump intensity should be used to eliminate higher photon number states, this is a basic constrain for photon pair generated in nonlinear processes. As for the materials used for photon pair preparation, the mostly used materials in SPDC can be divided into two kinds depend on phase matching types: birefringent phase matching materials, such as LBO, BBO; QPM crystals such as periodically-poled potassium tit-anyl phosphate (PPKTP) and PPLN. For SFWM, the commonly used materials include: gas ensembles, guided-wave materials such as different kinds of fibers, silicon-on-insulator (SOI) waveguide [46]. Therefore, entangled photon sources can be prepared in various materials with different optical configurations and some basic measurement tool kits are developed to characterize the quality of the sources.

Current and future challenges

For quantum light sources, there are some parameters to evaluate the quality of the prepared sources, some typical parameters that of concerns are: spectral brightness, total photon flux, coincidence to accidental coincidence count ratio, single photon second order correlation function, heralded efficiency and single photon purity. To demonstrate entanglement between two photons, various available and faithful methods are devised for different entangled states in two-dimension and high dimension Hilbert space, these methods include: two-photon interference fringes, Bell CHSH inequality and quantum state tomography (QST). Two-photon interference fringe is much easier to measure, the quality of an entangled source can be evaluated by calculate the interference visibility. To fully know the content of a quantum state, QST for the measured quantum state should be performed. Bell inequality is another parameter to indicate that the prepared quantum state has non-classical properties and contains Bell nonlocality. Only a few parameters are of great concern for specific applications, for example, single photon purity is of great importance for interference of independent photons; the heralded efficiency is of important for measurement or communication with heralded single photon; for applications based on entanglement, a high entanglement quality and total photon flux is preferred.

The trend for preparing quantum light sources based on nonlinear optics is to engineer photon parameters on demand in a compact platform and simple configuration [47]. Following this trend, QPM guided wave platform based on nano-film LN and complementary metal-oxide-semiconductor

Figure 6. Basic principles for spontaneous emission. (a) The simplified diagram for spontaneous parametric down conversion; (b) the simplified diagram for spontaneous four wave mixing; (c) a diagram for generation and applications of quantum light sources.
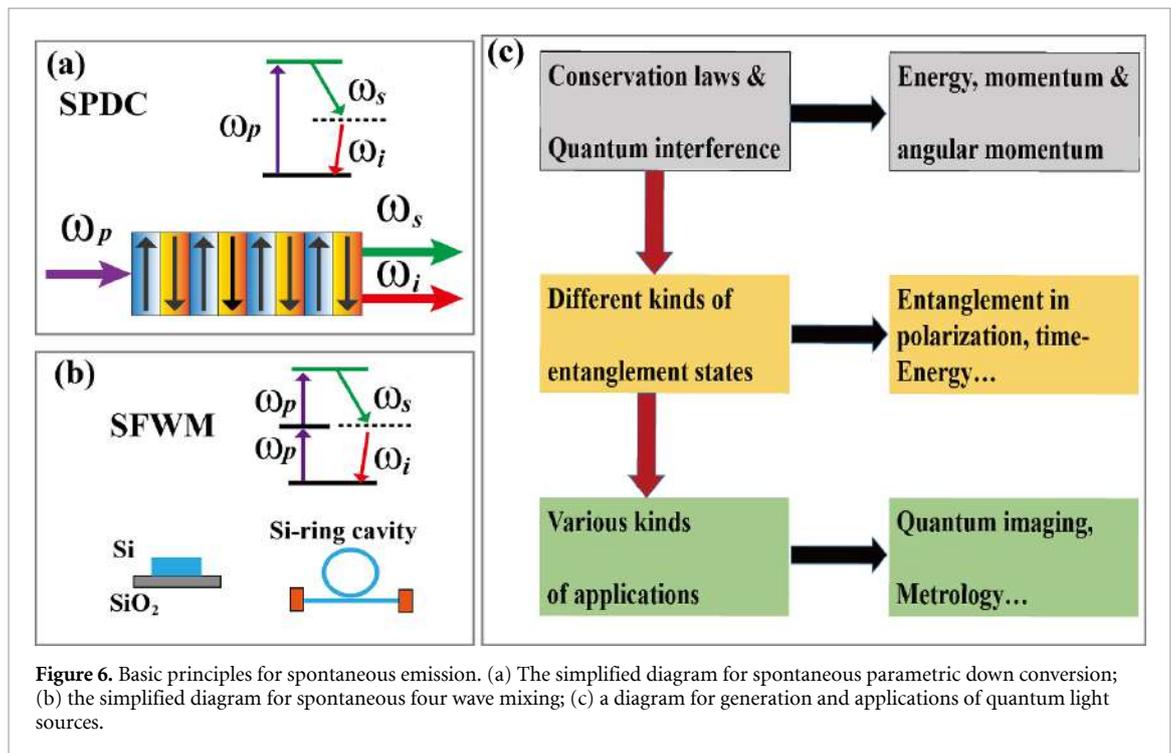
(CMOS)-compatible integrated platform like SOI and silicon-nitride are developed for QIST. QPM crystals have the advantages of high spectral brightness, narrow bandwidth, which are frequently used in photon pair preparation in quantum optics [44]. Wave-guided PPLN or PPKTP can further enhance the conversion efficiency in SPDC, which can greatly reduce the pump power by comparing with bulk QPM crystals. CMOS-compatible integrated platform also has high nonlinear conversion efficiency, and the most promising aspect for guided platform is the ability to construct small footprint devices with versatile functions by integrated other optical component in the same chip. Some common challenge for quantum light sources prepared based on nonlinear optics are: to overcome the probability feature of the photon pair preparation in spontaneous emission processes; to prepare high quality multi-photon or high dimensional quantum state in a scalable manner aims in realizing more important applications; to greatly reduce insertion losses for guided-wave platform in order to extract quantum light from the chip much more efficiently; to find new kinds of phase matching configurations for entanglement preparation; to devise much more application scenarios that can take advantage of the quantum nature of the light sources.

Advances in science and technology to meet challenges

For the challenges described in the above section, some advances in science and technology should be achieved to meet these challenges. For pulsed heralded single photon source, the heralded efficiency and total photon count are important parameters, but the probability of single photon prepared per pulse is very low, which is a limitation of high flux photon pair preparation. This defect can be overcome by using time, frequency and OAM multiplexing to enhance the photon generation probability per pulse and total count rate [48]. When optical elements for multiplexing device have low losses, the heralded efficiency and rate can be increasing substantially after a few number of multiplexing (see figure 7(b)). For generating multi-photon and high dimensional states, advances in fabricating of low loss integrated optical elements is required. The single photon detector should have near unity detection efficiency. Moreover, some more efficient methods should be developed to measure high dimensional and multi-photon states. Currently, the measurement time increasing exponentially with photon number and dimension. To extract photon from chip more efficiently, optimal output coupling structure designs and high resolution fabrication processing process are indispensable. Recently, backwards QPM is developed, in this special phase matching condition, photon pair prepared based on SPDC are propagating in opposite directions, this will open new opportunity for preparing high quality photon pairs (see figure 7(a)), the bandwidth of photon pair prepared in back-QPM crystal is much narrower than traditional QPM crystals, also the photon pair prepared with the same polarization can be separated, which is not possible for traditional QPM crystal [49]. Though back-wards QPM crystal is promising, the challenge is to fabricate ultra-short poling period with high quality. To date, most demonstrations are based on third order backwards QPM waveguide, the advances in fabricating high

Figure 7. (a) The diagram for backward quasi-phase matching; (b) simplified schematic for quasi-deterministic heralded single photon source based on frequency multiplexing and frequency conversion.
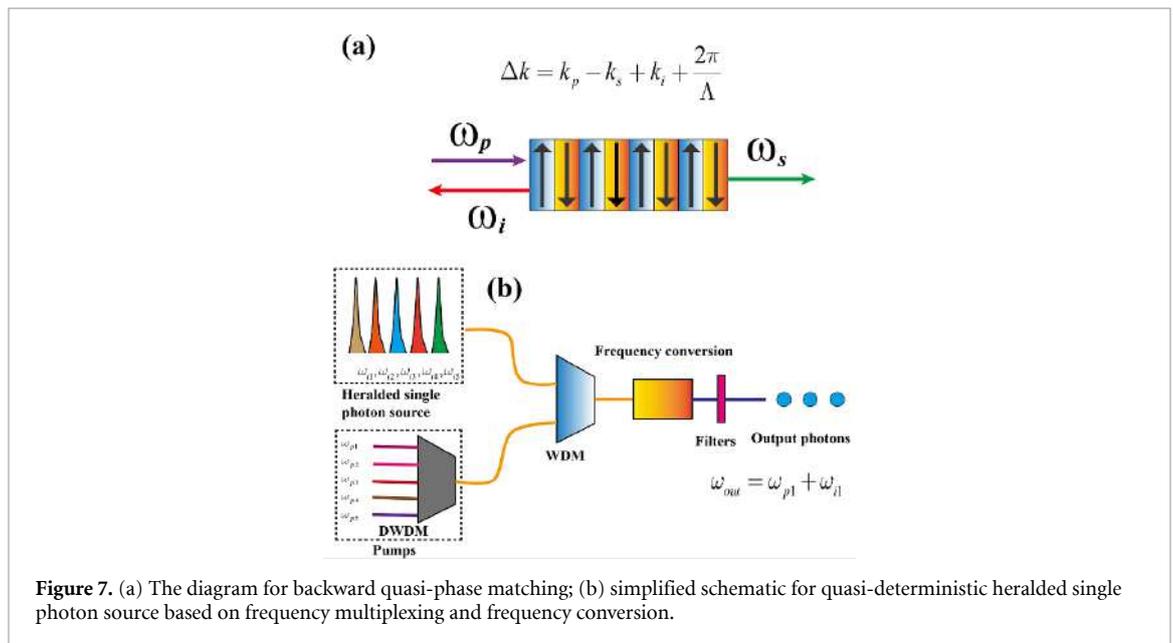
quality devices with shorter poling period for first order QPM is very urgent. Currently, high quality quantum light sources can be prepared based different materials with different configurations, an important task in QIST is to apply these sources in different application scenarios, which can show its advantages over traditional methods. A few promising applications include: entanglement based quantum light spectroscopy, which will show different properties by comparing with laser spectroscopy [50]; to develop new measurement methods for measuring physical quantities that can not be achieved with laser sources; cross with other disciplines such as biology, chemistry and material science for various measurement tasks which can show distinct features of both fields [51].

Concluding remarks

In conclusion, most of the advances and progresses for preparation and manipulation quantum light sources in nonlinear processes are briefly reviewed, this chapter provides a glance at the current status and challenges remains to be solved in this field. We also give some discussions on possible advances in science and technology in order to meet these challenges. Another important task in this field is to explore and expand new applications based on quantum light sources by utilizing its unique properties that can not be achieved by using laser light sources. With the developing of micro-fabrication technology, high compact high quality chip scale quantum light sources and some special chip aims at certain applications will be realized. In the near future, we will see significant progresses in integrated nonlinear optics based quantum light sources and view various scenarios that make use of high quality quantum light sources.

Acknowledgments

5. Nonlinear optics in 3D $\chi^{(2)}$ structures

Yong Zhang[1]*, Shining Zhu*[1] *and Min Xiao*[1,2]
[1] National Laboratory of Solid-State Microstructures, College of Engineering and Applied Sciences, Nanjing University, Nanjing 210093, People's Republic of China
[2] Department of Physics, University of Arkansas, Fayetteville, Arkansas 72701, United States of America

Status

The conversion efficiency of a NLO process strongly depends on the phase mismatch between the interacting waves. Let us consider a SHG process as an example. The material dispersion results in different phase velocities at the fundamental and second-harmonic (SH) waves, leading to the energy oscillation between them. To solve this problem, one useful way is to utilize the crystal birefringence to achieve phase matching (i.e. BPM), in which the fundamental and SH waves have the same refractive indices but different polarizations. Generally, the BPM configuration cannot use the maximal nonlinear coefficient and the BPM condition can be satisfied within partial transparent band. In 1962, Armstrong *et al* [26] proposed the concept of QPM to enhance the conversion efficiency of a NLO process. The sign of $\chi^{(2)}$ is periodically inverted under QPM configuration, which is equivalent to a reciprocal vector to compensate the phase mismatch. The reciprocal vector is determined by the period of $\chi^{(2)}$ structure. This technique provides a powerful solution to overcome the limitation of natural material dispersion with artificial micro-structures.

In 1980, Feng *et al* [52] successfully developed a growth striation technique to prepare PPLN crystals (also called optical superlattice) for the experimental demonstration of QPM. Since then, PPLN crystals have become one of the most important materials for the applications of nonlinear and quantum optics. Many domain poling techniques, such as electric field poling, chemical indiffusion, scanning force microscopic poling, electron-beam poling, and light-induced domain inversion, have been developed to fabricate $\chi^{(2)}$ structures in LN, lithium tantalite, KTP, and other NLO crystals.

In 1998, Berger [53] introduced the idea of nonlinear photonic crystal (NPC), conceptually extending the $\chi^{(2)}$ structures from one-dimension (1D) to two-dimension (2D) and three-dimension (3D). The functions of high-dimensional $\chi^{(2)}$ structures can be significantly expanded from the traditional laser frequency conversion to nonlinear beam shaping, nonlinear holography and high-dimensional quantum entanglement. Two years later, 2D $\chi^{(2)}$ structures were experimentally realized by using the popular electrical poling technique. However, these traditional poling techniques cannot fabricate 3D $\chi^{(2)}$ structures.

On 2018 (i.e. 20 years after its first proposal), the experimental demonstrations of 3D $\chi^{(2)}$ structures (figure 8(a)) were achieved by using two different femtosecond laser writing mechanisms (i.e. laser-induced $\chi^{(2)}$ erasing [54] and laser-induced domain poling [55], see figure 8(b)), which pave the way to investigate nonlinear optics in 3D space.

Current and future challenges

The 3D $\chi^{(2)}$ erasing approach was demonstrated by Wei *et al* in 2018. Its mechanism is quite different from the traditional domain poling techniques. Instead of trying to invert the sign of $\chi^{(2)}$, a focused femtosecond laser beam is used to selectively erase $\chi^{(2)}$. The fabrication strategy is to promote strong light–matter interaction to reduce the crystallinity as well as $\chi^{(2)}$. Correspondingly, the laser parameters feature low repetition rate ($\sim$1 kHz) and high pulse energy ($\sim$100 nJ). It is relatively easy to obtain $\chi^{(2)}$ erasing in experiment. For example, the QPM SH process can be observed when the pulse energy of laser writing ranges from 50 nJ to 300 nJ in LN crystal [54]. In experiment, Wei *et al* successfully fabricated 3D $\chi^{(2)}$-amplitude-modulated structures in LN crystals. Particularly, this technique is suitable for almost all the nonlinear crystals including ferroelectric and non-ferroelectric ones. For instance, it has been recently utilized to fabricate $\chi^{(2)}$ structures in a quartz for QPM SH generation in deep-ultraviolet band [56]. The main challenge of such $\chi^{(2)}$ erasing approach is how to reduce the value of $\chi^{(2)}$ into 0 in an effective and controllable way. Also, $\chi^{(1)}$ change is generally non-negligible under such strong laser illumination, which may cause extra scattering loss.

The laser-induced 3D domain poling [55] was realized by Xu *et al* in an x-cut barium calcium titanate (BCT) crystal. In this approach, nonlinear absorption of light produces a high temperature field, leading to the appearance of an electric field for domain creation. The experimental parameters differ from the $\chi^{(2)}$ erasing approach. Typically, it requires a high repetition rate ($\sim$80 MHz) and low pulse energy ($\sim$3 nJ) for the poling laser. Such laser poling technique is applicable to ferroelectric crystals. In comparison to the above $\chi^{(2)}$ erasing approach, the modulation depth of $\chi^{(2)}$ in laser poling (from $\chi^{(2)}$ to $-\chi^{(2)}$) is doubled, so the conversion efficiency is quadrupled correspondingly. Besides, the $\chi^{(1)}$ change can basically be neglected. Currently, 3D domain poling has been successfully demonstrated in ferroelectric crystals featuring low

Figure 8. (a) The concept of 3D $\chi^{(2)}$ structure. (b) Light-induced $\chi^{(2)}$ modulation.

Figure 9. Potential applications of 3D $\chi^{(2)}$ structures.
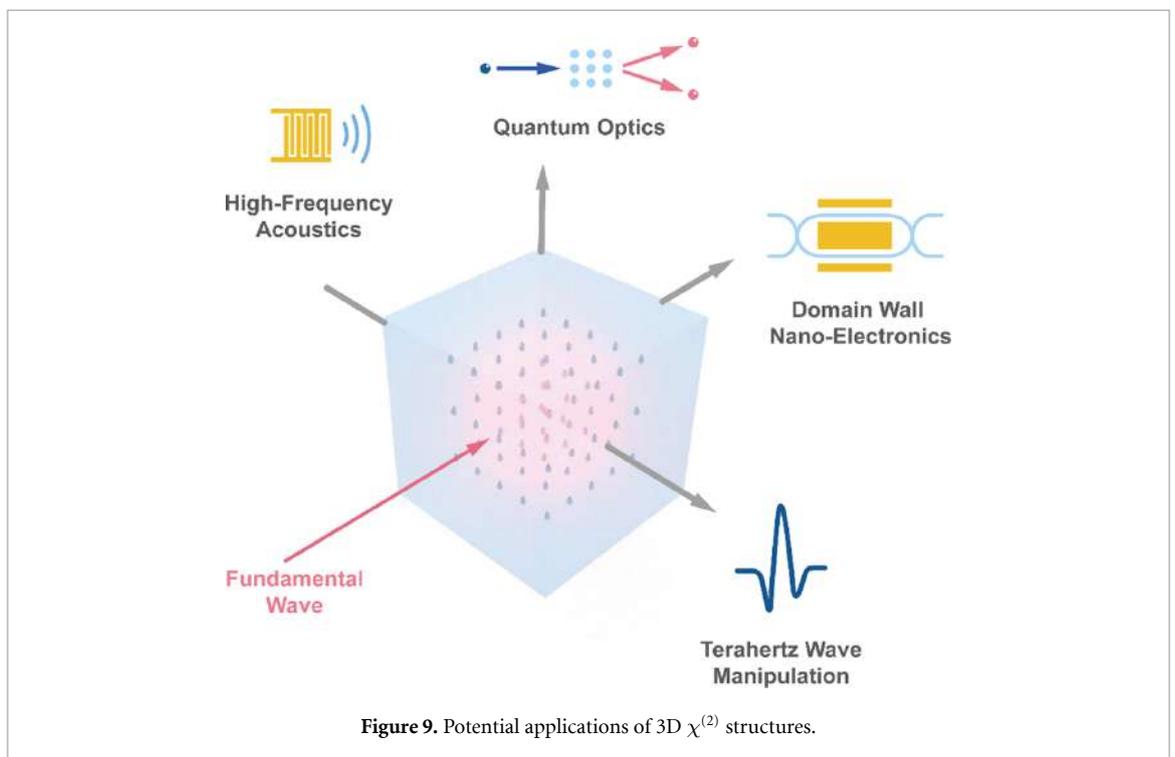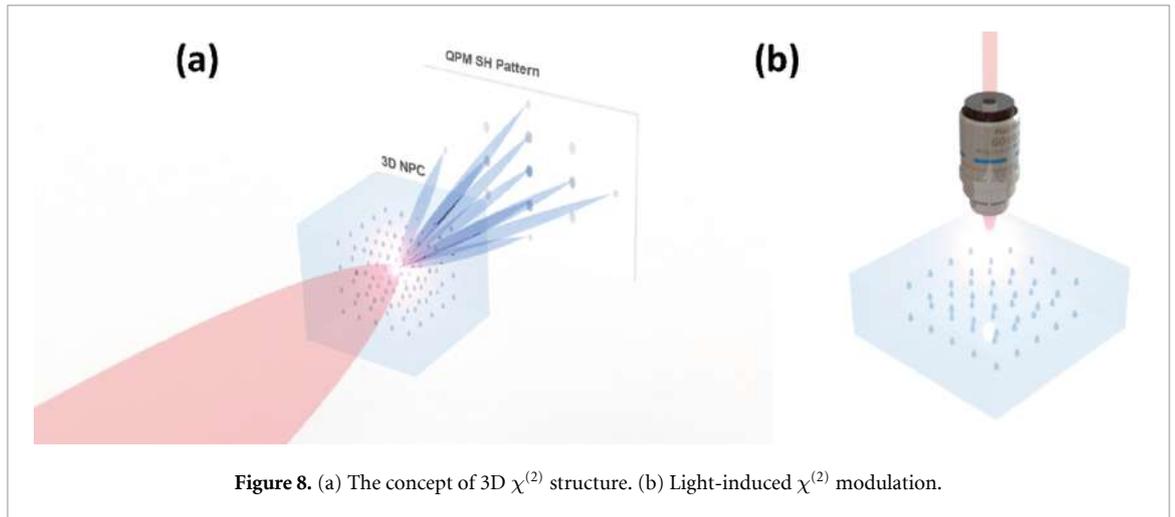
coercive fields including BCT and calcium barium niobate crystals. However, it is still a great challenge to expand its application to ferroelectric crystals with high coercive fields such as LN crystal.

Advances in science and technology to meet challenges

Many novel and important applications in nonlinear optics such as nonlinear beam shaping and nonlinear holography have been realized in 3D $\chi^{(2)}$ structures. For example, through full 3D QPM configuration, vortex beams and Hermite–Gaussian beams at SH wavelengths have been efficiently generated in 3D laser-induced $\chi^{(2)}$ structures [57, 58]. Multi-channel nonlinear holography is achieved under QPM-division multiplexing scheme, which significantly enhances the capacity as well as the efficiency [59]. It also has been theoretically predicted that high-dimensional entanglement states can be realized through SPDC processes in 3D $\chi^{(2)}$ structures [60].

To meet the increasing requirements of these advanced optical applications, the major challenge is how to fabricate large-scale 3D $\chi^{(2)}$ structures with high precision, good repeatability and high stability. Currently, the typical dimensions of 3D $\chi^{(2)}$ structures are limited within $\sim$200 μm. It is necessary to significantly expand the sample size for many practical applications. For example, it requires a sample length of at least 1 cm (along the light propagation direction) to improve the conversion efficiency to 10% and above. High-resolution and high-capacity nonlinear holography requires a large transverse area ($\sim$1 mm^2).

The present laser writing of 3D $\chi^{(2)}$ structures relies on a point-to-point fabrication strategy. Clearly, when the sample length is increased to 1 cm, the fabrication time will be increased to a level beyond the system stability. It is critical to develop parallel processing techniques such as multi-focal laser writing system for fast fabrication of 3D $\chi^{(2)}$ structures at large scale. Another technical issue is the non-uniform structure along the depth direction. NLO crystals generally have large refractive indices (for example, 2.2 for LN crystal). When a laser-writing beam is focused from air into the crystal, the refractive index mismatch will induce strong spherical aberration and then distort the focal intensity distribution. For example, the focal spot will be elongated along the fabrication depth, leading to a considerable decrease in peak intensity. One may modify the pulse energies at different depths to partially compensate the effect of spherical aberration. Also, pre-shaping the laser writing beam can be an important way to correct the intensity profile at the focal point.

Concluding remarks

In comparison to 1D and 2D $\chi^{(2)}$ structures, 3D structure has an additional $\chi^{(2)}$ modulation dimension. This advantage makes it naturally capable of performing those complicated tasks that require high capacity, high coding rate, and high processing efficiency. Currently, the fabrication resolution of laser writing system is typically $\sim 1\,\mu$m, which is manly limited by the diffraction limit of light. In future techniques, it is possible to reduce the resolution of 3D $\chi^{(2)}$ engineering down to 100 nm, which can be used in the generation of ultra-narrow-bandwidth quantum entangled light (matching the linewidth of quantum storage). Besides, the potential applications of 3D $\chi^{(2)}$ structures can be further extended from nonlinear and quantum optics to terahertz wave manipulation, high-frequency acoustics and domain wall nano-electronics (figure 9). After 60 years of scientific research, $\chi^{(2)}$ structures have been conceptually and experimentally extended from 1D and 2D to 3D. The researchers interested in $\chi^{(2)}$ structures have expanded from nonlinear optics society to quantum optics, integrated photonics, and microwave/terahertz-wave photonics. 3D $\chi^{(2)}$ structures provide a novel and powerful platform to perform fundamental research and develop practical devices.

Acknowledgments

6. Emerging nonlinear optical phenomena enabled by ferroelectric fluids

Satoshi Aya[1,2] *and Yan-qing Lu*[3,4]
[1] South China Advanced Institute for Soft Matter Science and Technology (AISMST), School of Emergent Soft Matter, South China University of Technology, Guangzhou 510640, People's Republic of China
[2] Guangdong Provincial Key Laboratory of Functional and Intelligent Hybrid Materials and Devices, South China University of Technology, Guangzhou 510640, People's Republic of China
[3] National Laboratory of Solid-State Microstructures, College of Engineering and Applied Sciences, Nanjing University, Nanjing 210093, People's Republic of China
[4] Key Laboratory of Intelligent Optical Sensing and Manipulation, Nanjing University, Nanjing 210093, People's Republic of China

Status

As seen in the other sections of this Roadmap, diverse NLO effects arise in many different systems. Among them, SHG, as a special case of three-wave mixing mechanisms, is the most classic and important nonlinear phenomenon that brought the beginning of the field of nonlinear optics in 1961 [61]. SHG is the lowest-order NLO effect with the second-order nonlinear susceptibility $\chi^{(2)}$ and an inherent up-conversion process, producing a doubled-frequency photon at $2f$ from two input photons at a fundamental frequency of f. The response is at least over ten orders stronger than the other higher-order NLO effects characterized by susceptibilities, $\chi^{(n)}$ ($n \geqslant 3$) (figure 10) [62]. Such high-efficient wavelength convertibility has not only offered a technological solution for generating short-wavelength light that cannot be obtained from normal light sources, but also made it possible to probe symmetry-broken nano- to macro-structures [63].

Generally, SHG process becomes active when the inversion symmetry is broken. This condition puts a considerable limitation on the material space one can use for wavelength-conversion applications. In the past years of SHG development history, low-symmetry polar crystalline materials were the main candidates. To obtain strong nonlinear light from these materials, the fabrication of periodic poling structures is essential to satisfy the classic QPM condition [63–65] (figure 11). However, the limited processability and manipulability of domain engineering restrict the diversity of the polarization orders, hindering one from exploring the correlation of NLO phenomena with polarization structures and optimizing device performance.

These difficulties would be overcome by using soft matter systems. The self-organization capability makes them useful candidates for generating NLO structures spontaneously. However, the intrinsically high symmetry generally exists in soft matter, contradictory to the incidence of polar order and strong SHG property. Very recently, we have witnessed a game-changer: the liquid-like ferroelectric matter states, the variants of ferroelectric nematic LCs (N_F and HN* LCs) (figure 11) [66–68]. These fluids exhibit spontaneous polarization with the local electric polarity coupled to the orientation of molecules. Unlike crystalline materials, their three-dimensional orientational structures can be easily 'assembled' and modulated by traditional LC alignment techniques and ultra-low electric field (E-field; $\sim$1 mV μm^{-1}) [66]. This situation brings us to a new era in the quest of producing and manipulating various nonlinear light states on-demand through diverse designable polarization structures.

Current and future challenges

Conceptually, the emerging ferroelectric LCs add substantial richness and complexity to accessible structure and property spaces. Thanks to the sensitive electric-field response of ferroelectric LC structures, the material group offers an unprecedented playground for developing switchable and programmable NLO elements. The inherent fluidity further benefits fabricating flexible nonlinear devices. However, practically, neither the polarization structures nor the resultant nonlinear property is explored and developed. Especially, we have only aware that polarization LC states have a large pool of nontrivial topological structures distinct from those in traditional LC phases, which have even never been addressed in other polar systems such as spintronics and magnetic systems. The want of the relevant knowledge inevitably avoids one from studying the NLO effects in detail. In response to these circumstances, three fundamental challenges arise as follows.

(1) Understanding the polarization topology of ferroelectric LCs

This challenge consists of two tasks: experimental and theory. Scanning probe microscopy techniques such as Kelvin probe force and piezoelectric force microscopies are known as the most popular methods for characterizing polarization topology in crystalline polymers and inorganics. However, the scanning probe microscopy does not apply to ferroelectric LC systems, since their fluidity necessitates alternative mechanically contactless measurement approaches. From the theoretical viewpoint, it is urgent to establish mean-field free-energy formalism to describe possible topological species and their structural stability.

$$P(t) \propto \chi^{(1)}E(t) + \boxed{\chi^{(2)}E(t)^2} + \chi^{(3)}E(t)^3 + \cdots$$

Wavelength conversion

SHG, SFG, DFG, …
High-yield approach: QPM

Symmetry & structure probe

Mirror symmetry, surface, …
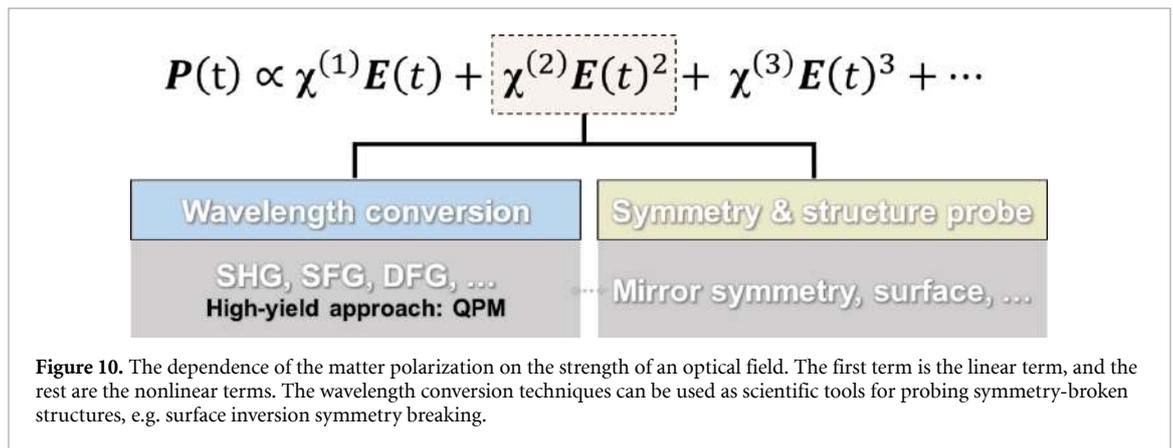
Figure 10. The dependence of the matter polarization on the strength of an optical field. The first term is the linear term, and the rest are the nonlinear terms. The wavelength conversion techniques can be used as scientific tools for probing symmetry-broken structures, e.g. surface inversion symmetry breaking.

	Apolar nematic	Ferroelectric nematic	Helielectric nematic	Periodic poling structure
SHG process	SHG inactive	Phase-mismatched	Phase-matched by polar helices	Quasi-Phase-matched by poling structure
SHG active?	No	Yes	Yes	Yes
Chirality selectivity	No	No	Yes	No
E-field tunability	Yes	Yes	Yes	Difficult
SH amp.	No	No	Yes	Yes
Polarization processing	Apolar (dielectric) even under E-field	Spontaneous	Spontaneous	Need high-E-field Pre-poling

Figure 11. Apolar *vs* emerging polar orientational states. Relationships between the distinct nematic LC states and the SHG properties. The color coding in the polarization states indicates the difference in the azimuthal angle of the orientation. SH amp. is the abbreviation of SH amplification.

(2) Understanding polarization structure *vs* light interaction relationships

Given that the fabricated polarization topology is determined as in (1), revealing the coupling between the polarization topology and NLO output is the next task. While experimentally investigating NLO effects by designing various polarization topologies through ferroelectric fluids is intriguing, developing a generalized theory that captures SHG processes in arbitrary polarization structures remains challenging.

(3) Extending from SHG to general second-order NLO effects

SHG process is the starting point for extending applications of ferroelectric fluids to other second-order NLO effects, e.g. SFG, DFG, and optical parametric oscillator (figure 10). The essential step in bringing the SHG process to them is to systematically understand how phase-matching (PM) condition depends on polarization structure, and polarization, wavelength, and wave-vector directions of interacting lights. This dedicates the amplification rate and polarization state of generated NLO fields.

Advances in science and technology to meet challenges

To tackle the challenges listed above, interdisciplinary approaches must be taken to address both the fundamental and engineering issues. The essential bottleneck to clarifying polarization topologies in fluids is the deficiency of the observation method due to the powerlessness of traditional scanning probe microscopy tools. A feasible and potential alternative would be microscopy methodology based on SHG process, i.e. SHG microscopies. Since SH signal itself arises as a product of symmetry breaking of systems, the microscopy techniques probe the spatial distribution of the symmetry-broken structures like polarization topology. Yet, much remains to be understood concerning the analysis of 3D topological structures. Unlike traditional confocal microscopy techniques, the SH signal in a 3D volume depends on not only the orientation of polarity but also the optical phase between fundamental and SHG lights. The optical simulation and data fitting methodologies should be established and further improved [69]. Moreover, there is a limit of structural size above nearly-micron-scale dominated by the diffraction limit. Developing nonlinear microscopies with resolution down to tens of nanometers, similar to super-resolution microscopy technologies in the linear optical regime, would be a big challenge in this emerging field.

Going to identifying novel NLO phenomena, a long-term challenge would be the establishment of a database that correlates polarization structures to NLO properties. This can be linked with the machine-learning method, effectively predicting potentially-possible NLO effects. The experimental realization of polarization structures would be made by employing traditional LC fabrication techniques such as anchoring engineering, spatial confinement, structural template, and so on [70]. Yet, how to precisely control the polarization vector in 3D space remains elusive, and polarization engineering based on LC nature should be developed. The main difficulty arises because orientational engineering is optimized for only the so-called nonpolar director field, where the head-to-tail equivalence is present. Another obstacle is the limitation of traditional NLO theories. Since they assume linear polarization for fundamental optical wave and non-birefringent nature in most cases, the polarity-orientation-dependent effects like tensor of nonlinearity and optical retardation are ignored. This results in the incorrectness of calculation of NLO properties in birefringent NLO mediums, thus necessitating generalized theories for the effects. These combined efforts will push toward more exotic NLO phenomena.

Concluding remarks

Beyond the traditional solid NLO elements, the recent discovery of highly-fluid ferroelectric LCs, as the first class of liquid nonlinear materials, has generated considerable scientific interest and technological value in electronics and photonics. Particularly, the gift of desirability, controllability, and manipulability of polarization structures demonstrates a great potential for exploring many unknown NLO effects. In the next years, the community will be at the urgent stage of understanding the principle of how 3D polarization fields modify NLO fields and establishing the relevant database guided by both the theories and experiments. The facile polarization engineering in the ferroelectric LCs provides unique opportunities for amplifying nonlinear light through specifically-designed polarization structure and topology, and tuning nonlinear light actively by external fields. These approaches, on one hand, will keep offering new and exciting branches of fundamental science in nonlinear optics. On the other hand, they provide important implications for future NLO devices with compactness, flexibility, as well as fast and low-external-field responsivity.

Acknowledgments

7. Structural design in nonlinear optical crystal

Huixin Fan[1], Min Luo[1] and Ning Ye[2],*
[1] Fujian Institute of Research on the Structure of Matter, Chinese Academy of Sciences, Fuzhou 350002, People's Republic of China
[2] Institute of Functional Crystals, Tianjin University of Technology, Tianjin 300384, People's Republic of China

*Email: nye@email.tjut.edu.cn

Status

Over the past decades, the invention of the laser greatly promoted the development of modern science and technology. NLO materials as a crucial part of the laser science have attracted increasing attentions from researchers because of their widely applications in information storages and precise micro-manufacturing *et al.* An ultraviolet (UV) or DUV NLO crystal with excellent performances needs to fulfil three key properties: strong SHG responses, sufficient birefringence, and the UV cut-off edge as short as possible. Therefore, it is important to study the relationship between these three key properties and structures of materials.

Academician Chen Chuangtian proposed the anionic group theory [71, 72] in the 1980s for the first time to study the structure-property relationship of these NLO crystals. According to the anionic group theory, BO_3, B_3O_6 and B_3O_7 groups are considered to be the most core functional building blocks (FBBs) to construct UV NLO borates due to their π-conjugated structures and wide band gaps. Since then, borates as NLO materials [73] have received amounts of attentions and vigorous developments. Some famous UV NLO borates, such as $KBe_2BO_3F_2$ and $SrBe_2BO_7$ with BO_3 groups, β-BaB_2O_4 (β-BBO) with B_3O_6 groups, and LiB_3O_5 (LBO), CsB_3O_5 (CBO) and $CsLiB_6O_{10}$ (CLBO) with B_3O_7 groups, have been synthesized and utilized. The unremitting pursuits of new NLO materials with excellent performances not only are the urgent demands for more advanced applications, but also ease the difficulties to discover new borate NLO crystals. Based on these considerations, expanding the materials with planar π-conjugated groups would be the key point to exploring the new UV NLO crystal materials.

Inspired by triangular π-conjugated structural BO_3 group, carbonates (CO_3) [74], nitrates (NO_3) [75], guanidine compounds ($C(NH_2)_3$) [76] and other compounds with planar triangular π-conjugated structures have been proposed to study as NLO materials. Moreover, the B_3O_6-typed structures enlighten the researches on the six-membered ring planar π-conjugated structures as NLO crystals, such as cyanurate ($C_3N_3O_3$) [77] and its derivative units ($HC_3N_3O_3$) [78] and ($H_2C_3N_3O_3$) [79]. Amounts of NLO materials with these π-conjugated structures have been designed and exhibited excellent properties (figure 12). Therefore, exploring new NLO materials by expanding the π-conjugated structures is not only one of the most effective ways, but also the state-of-the-art research hotpot.

Current and future challenges

Over the past decade, the UV/DUV NLO materials have been developed prosperously. Amounts of famous NLO crystals have been developed to fulfil the applications in many civil and military fields. However, several issues are still under investigations. The three key properties which affect the applications of UV/DUV NLO crystals are large SHG responses, sufficient birefringence, and wide band gap. According to the structure-property relationships, these three key properties restrict each other, and it is difficult for them to be optimal in one crystal. Therefore, how to regulate these three key properties is a significant issue and huge challenge in the design of UV/DUV NLO crystals with excellent comprehensive properties.

Based on the anionic group theory, the π-conjugated structures are more conducive to having strong SHG responses due to their large hyperpolarizability. Furthermore, strong anisotropy of the FBBs in crystals is beneficial to improve the birefringence. If the birefringence is too small, that will make the NLO crystals unable to achieve the PM. Therefore, lots of efforts on expanding the π-conjugated FBBs with large hyperpolarizability and strong anisotropy have been spent. Furthermore, a wide band gap will help to
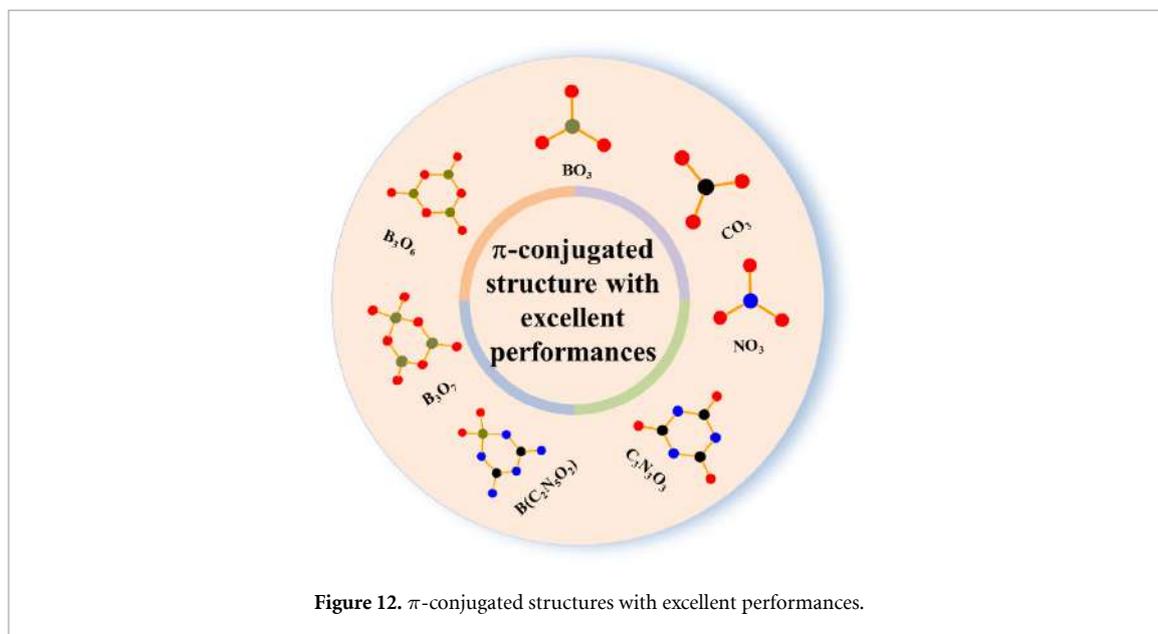
Figure 12. π-conjugated structures with excellent performances.

expand the transmission range of crystal. Theoretical calculations exhibit that the band gap of a NLO crystal is determined by the range between the top of the valence band and the bottom of the conduction band. Therefore, the width of the band gap is related to the elements which make up to the NLO-active units. The large electronegativity difference is beneficial for broadening the band gaps of the NLO materials. In addition, according to the structure-property relationships, the dangling bonds in the structures have large influences on the band gap. Currently, the relationships among the three key properties of NLO materials have received a lot of attentions and continuous researches have been carried out on them. In-depth study of structure-property relationships of NLO crystals, and making use of the π-conjugated units to regulate the three key properties are still huge challenges.

Advances in science and technology to meet challenges
The wide applications of NLO materials bring huge challenges to the structural design of materials. Structural modification by molecular engineering is an important approach to design and synthesize novel structures. In the next decades, utilizing of structural design to regulate the three key properties of UV/DUV NLO crystals is still a huge challenge. What's more, the use of counter ions to regulate the arrangements of new FBBs could be benefit to acquire UV/DUV NLO crystals with excellent comprehensive properties (figure 13). Based on the deeper study of the structure-property relationship, the larger hyperpolarizability and stronger anisotropy with π-conjugated structures will beneficial to increase the SHG responses and birefringence. These π-conjugated structures are no longer limited to the inorganic units, but would have been extended to some organic units. Expanding inorganic NLO-active units with π-conjugated structures and designing the new organic π-conjugated NLO-active units have become the new approach and directions for the development of this field. These organic units often have stronger p_π–p_π connections, which will increase the hyperpolarizability and anisotropy of the units. Based on these considerations, it could be inferred that the stronger p_π–p_π connections may benefit to the stronger SHG responses in the organic FBBs. However, when organic units absorb UV radiation, their outer electrons will transition from the ground state to the excited state. Excessively large p_π–p_π connections will narrow the width of the band gap and further cause the red shift of the UV cutoff edge of the compound. Therefore, by introducing the terminal group, such as F^- or OH^- groups, the dangling bonds in the structure are effectively reduced, thereby increasing the energy band width, which is beneficial to the extension of the ultraviolet transmission range to the short wavelength direction.
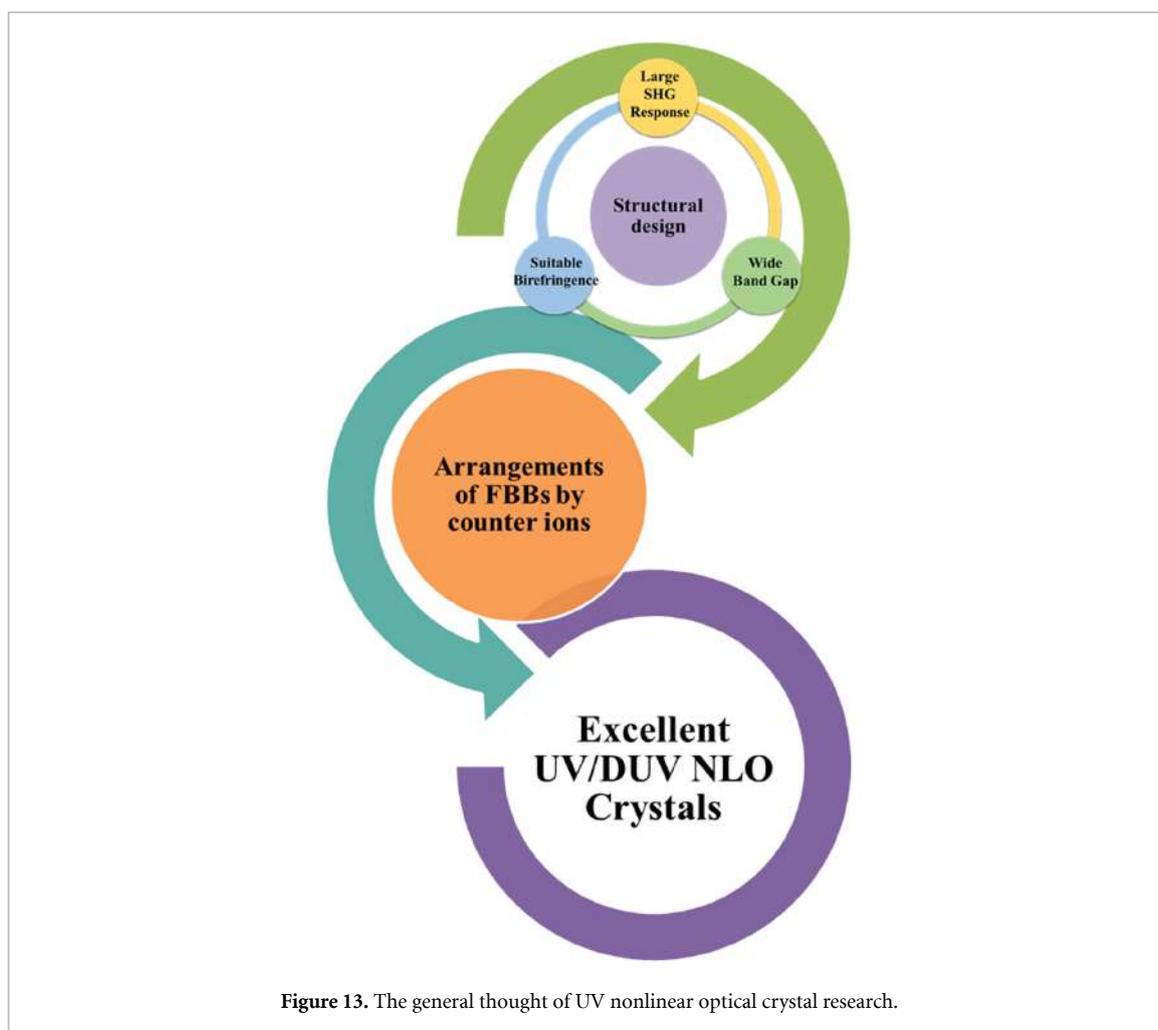
Figure 13. The general thought of UV nonlinear optical crystal research.

Concluding remarks

The field of UV/DUV NLO material has aroused great interest in the scientific community over the past few decades. As a key component of laser frequency doubling technology, UV/DUV NLO materials lay the foundations for the applications of lasers in many civil and military sciences. With the continuous increase of UV/DUV laser applications, it is a necessary and state-of-the-art development direction to expand UV/DUV NLO materials with excellent performances. To balance the three key properties of the UV/DUV NLO crystals is a crucial challenge based on the in-depth study of the structure-activity relationship. Molecular engineering with organic FBBs on the ionic organic compound is an effective approach to developing new generation UV/DUV NLO crystals. With these considerations, we anticipate researches in the field of NLO materials would provide significant developments for both fundamental science and practical applications.

Acknowledgments

8. Nonlinear optics in two-dimensional materials

Zeyuan Sun, Wei-Tao Liu and Shiwei Wu
State Key Laboratory of Surface Physics, Key Laboratory of Micro and Nano Photonic Structures (MOE), and Department of Physics, Fudan University, Shanghai 200433, People's Republic of China

Status

Ever since the discovery of graphene in 2004, a growing number of van der Waals (vdW) two-dimensional materials have been observed and studied. As key member of low-dimensional materials, the atomically thin two-dimensional materials exhibit many intriguing and sometimes exotic properties and phenomena, driving quite a few important developments in fundamental science and technological applications in the past 18 years. The emergence of novel materials and properties also provide a new playground for the investigation of new NLO phenomena and potentially functional applications.

Because the light–matter interaction in vdW 2D materials is confined to the atomic thin layer, many NLO responses such as SHG, THG, sum-frequency or difference-frequency wave mixing, and even HHGs are extraordinarily enhanced, as we have witnessed in graphene [80–82], monolayer transition metal dichalcogenides [83–85] or monochalcogenides [86]. Moreover, some often negligible nonlinear processes become prominent. For example, SHG in centrosymmetric graphene, arising from electro-quadrupole contribution, was revealed [81]. For another example, giant nonreciprocal SHG in CrI_3 bilayer from interlayer antiferromagnetism was discovered [87], whose second-order nonlinear susceptibility was found about three orders of magnitude larger than that in bulk antiferromagnet.

With the expansion of 2D materials family, 2D materials exhibit various crystal structures and symmetries. More intriguingly, depending on how one monolayer sheet is stacked on top of the other, the crystallographic symmetry can be varied [82, 84–86]. Because of the weak van der Waals interaction between layers, such symmetry variations can be artificially engineered, without the restriction of lattice match for conventional materials. Nonlinear optics such as SHG is known for its extreme sensitivity to symmetry. Therefore, 2D materials host rich layer- and stacking-dependent NLO responses.

Perhaps the most fascinating part of 2D materials is the susceptibility to external controls such as carrier doping [80, 81], electric and magnetic fields [87], strain [88] and pressure [89] (figure 14). The NLO responses of 2D materials thus can be readily controlled. By tuning the chemical potential to switch on or off the interband transitions in gated monolayer graphene, the second- and third-order NLO coefficients were varied by several orders of magnitude [80, 81]. By controlling the magnetic states in two-dimensional magnets with external magnetic field, the time-noninvariant SHG was turned on or off [87]. The tuning of NLO responses in 2D materials not only demonstrates the power of nonlinear optics for studying novel quantum materials, but also illustrates the potential of 2D materials for developing NLO devices, such as mode-locked fiber laser [90, 91].

Current and future challenges

The emergence of novel NLO responses in 2D materials brings the excitement but also poses quite a few challenges.

Firstly, 2D materials exhibit intriguing physical properties and novel quantum phases, so that various NLO processes could appear. Furthermore, they are thinned down to the atomic scale and all of their atoms are exposed to the surface or interface, so it is challenging to identify the origin of NLO responses. It is known that the second-order nonlinear processes such as SHG are sensitive to the inversion symmetry breaking under the electric-dipole approximation. At a surface or interface, the inversion symmetry is intrinsically broken, and the SHG is electric-dipole allowed. If the 2D materials is noncentrosymmetric in view of a bulk, these surface vs bulk mechanisms of SHG would be both electric-dipole allowed. Even if the crystallographic structure of 2D materials is centrosymmetric, SHG could be produced under the stimulus of electric field, magnetic field, strain, or pressure. In particular, nonreciprocal SHG in magnetic materials with time-reversal symmetry breaking could appear. Therefore, the pinpoint of NLO processes requires special attention.

Secondly, the flatland of 2D materials is enriched by the moiré superlattices that are artificially created in the form of hetero- or homo-structures. Depending on the twisting angle and lattice mismatch, the period of these moiré superlattices is often in the range of 1–100 nm. This length scale is much larger than the lattice constant, but smaller than the diffraction limited laser spot in the visible or near-infrared wavelength for NLO measurements. Within the moiré period, the interface may undergo the atomic reconstruction, particularly when the twisting angle is small. The atomic reconstruction, along with the distortion of moiré superlattice inevitably induced by strain and disorders, further complicates the understanding of NLO phenomena that are measured on an ensemble of moirés. The study of nonlinear optics in 2D moiré superlattices urgently calls for ultrahigh spatial resolution.
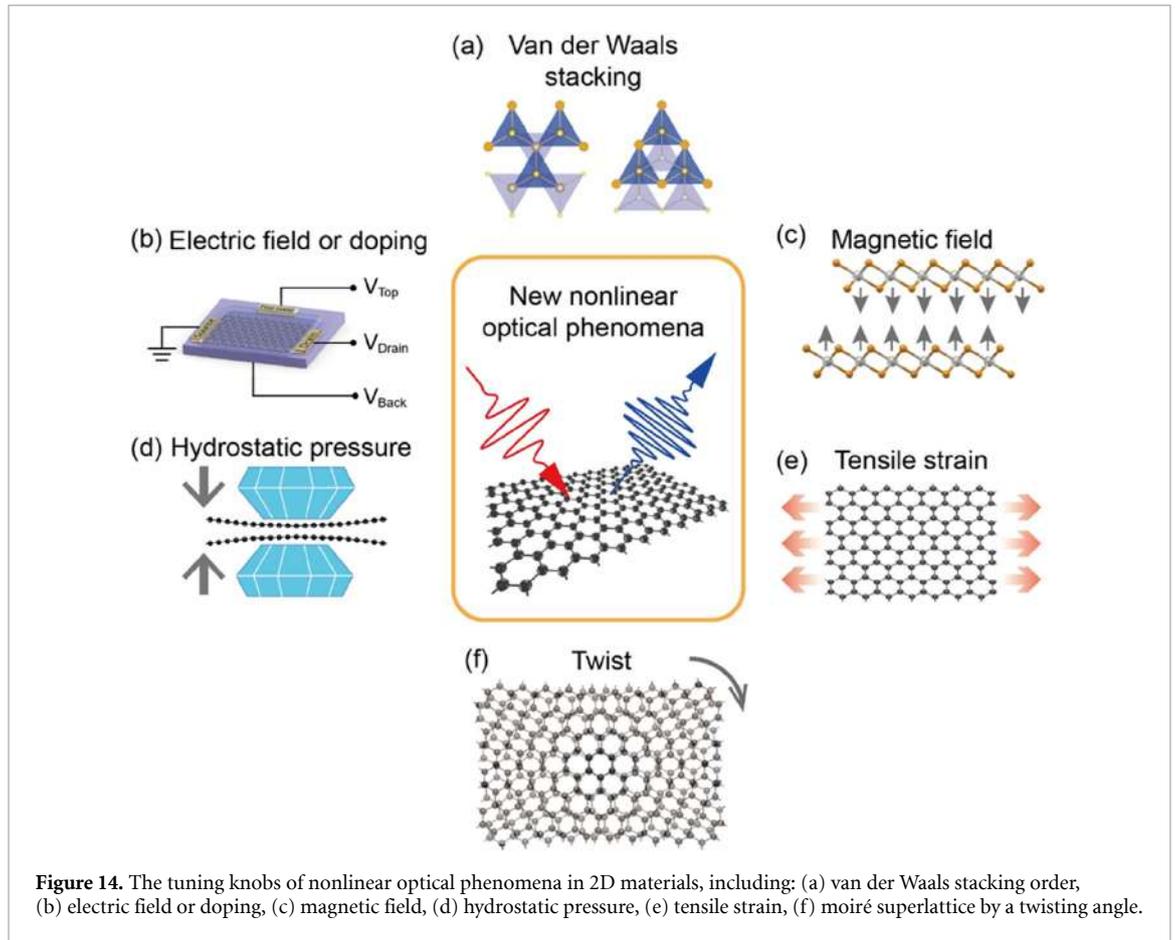
Figure 14. The tuning knobs of nonlinear optical phenomena in 2D materials, including: (a) van der Waals stacking order, (b) electric field or doping, (c) magnetic field, (d) hydrostatic pressure, (e) tensile strain, (f) moiré superlattice by a twisting angle.

Last but not least, the limited sample volume and electronic states of 2D materials permit the possibility of nonperturbative NLO processes such as HHGs driven by readily available femtosecond pulsed lasers, although the damage threshold of 2D materials is relatively low. Such processes are not only subject to the symmetry restrictions but also the many-body coherent dynamic interactions. Unlike the three-step model applied for gas-phase high harmonic generations, new physical picture and theoretical framework are demanded to understand the nonperturbative ultrafast coherent process in ultrathin materials.

Advances in science and technology to meet challenges

To understand the emergent NLO phenomena in 2D materials, one can conversely utilize the tunability of their structures and properties. Therefore, the corresponding NLO measurements shall be compatible with various tuning techniques, such as cryogenic temperature, electric transport, superconducting magnet, hydrostatic pressure, and strain engineering. If so, the rich nonlinear optics of 2D materials can be deciphered in a neat way. The symmetry-sensitive NLO experiments would become a powerful tool to help resolve a series of important problems in condensed matter physics and materials science, such as pairing mechanism in unconventional superconductivity, exotic quantum phases in intrinsic multiferroics, topological materials and so on.

The advances of nonlinear optics in 2D materials have been greatly benefitted from the diffraction limited optical microscopic technique. To achieve higher spatial resolution for imaging the interior of moiré superlattices or various domains, tip-enhanced NLO microscopy is a better choice. This near-field technique collects the inelastic NLO signals such as SHG and THG. Because of the local electric field enhancement at the tip apex, the NLO signals could be enhanced by orders of magnitude so that spatial resolution can reach to nm or even sub-nm scale. So far such tip-enhanced NLO microscopy has been demonstrated at room temperature. The combination with low temperature, magnetic field and ultrahigh vacuum would largely extend its applications in revealing the NLO processes in nanomaterials.

The development and applications of nonlinear optics heavily rely on the pulsed laser sources. For the study of atomically thin 2D materials, the average laser power is around 1 mW or so with a diffracted limited focusing, otherwise the sample will be damaged. The ideal lasers are the wavelength tuneable femtosecond pulses with a repetition rate of 1–10 MHz. To push the applications of NLO effects in 2D materials, fiber-based portable lasers are also desirable.

Concluding remarks

The fascinating properties of van der Waals 2D materials provide a unique opportunity to explore various NLO phenomena in a neat manner. Likewise, the NLO technique has become an indispensable and powerful method for revealing symmetry and physics in 2D materials. By incorporating the various tuning knobs, device fabrication and scanning probe techniques used in condensed matter physics and material science, the understanding and development of nonlinear optics in 2D materials and related systems would be advanced to an unprecedented level. The real applications based on these novel NLO effects will emerge in a foreseeable future.

Acknowledgments

9. Lithium niobate single-crystal thin films: status and perspectives

Qingyun Li and Hui Hu
School of Physics, Shandong University, Jinan 250100, People's Republic of China

Status

LN crystal has been widely used in photonics due to its wide transparent window, large electro-optic (EO) effect, and high second- and third-order nonlinear-optical coefficients. Classical optical waveguides (proton exchange and titanium diffusion) on LN bulk materials generally have a subtle refractive index contrast, resulting in large bending radius of the waveguide, which hampers miniaturization of devices and the further development of LN in integrated optics. LNTF (LN on insulator, [LNOI], or thin film LN) has a large refractive index contrast, which results in a tight bending radius of tens of microns and a waveguide cross-section of sub-microns, allowing high density photonic integration and strong optical confinement to enhance light–matter interactions. In 1998, single-crystal LNTF was obtained by the combination of ion implantation and lateral etching [92]. With the improvement of preparation technology, high-quality and wafer-size LNOIs have become commercially available, which facilitates the development of integrated LN photonics. One LNOI fabrication method uses a series of processes such as ion implantation, direct bonding, and thermal annealing, to physically peel the LNTF from the LN bulk material and transfer it to the substrate [93]. The lapping and polishing method can also produce high-quality LNOIs. This method has a smaller influence on crystal quality but puts strict requirements on thickness uniformity control. The LNOI not only retains the original physical properties of LN bulk material, but also has a single-crystal lattice structure, which benefits low light transmission loss.

Compared to other integrated optical material platforms (such as SOI, InP, and SiN_x), LNOI has low optical absorption, fast optical modulation, and efficient all-optical nonlinearities. Optical waveguide is one of the fundamental components in integrated photonics. LNOI waveguides achieved a propagation loss of 0.027 dB cm^{-1} [94], which was a milestone advancement implying large-scale photonic integration and single-photon level processing. Numerous photonic functions have been realized, such as high-bandwidth EO modulation, high-efficiency nonlinear conversion, and EO controllable OFC generation [95]. A series of LNOI materials have also been developed, such as rare-earth-doped LNOI for amplifiers and lasers, MgO-doped LNOI for high optical power applications, and double LNOI layers for nonlinear-optical processes [96]. Currently, 4 and 6 inch LNOIs have become routinely available, and have important applications in optical communications, microwave photonics, and quantum photonics.

Current and future challenges

LNOIs have become a promising material platform for integrated photonics, but several challenges remain.

1. *Large-size LNOIs*. Photonics device fabrication generally requires a photolithography resolution of tens of nanometers. A lithography system for large-size substrate (8 or even 12 inch substrate, for example) has a much better accuracy and resolution than those of small-size substrate (4 or 6 inch substrate, for example), and can be used to fabricate photonic devices with fine structures and good repeatability. In addition, large-size LNOIs can reduce the average cost of device fabrication. Hence, large-size (8 or 12 inch) LNOIs are preferred for better device performance and industry production. Depending on the fabrication process, the LNOI diameter is determined by the LN bulk wafer, which is limited by the crystal boule growth process.

2. *Uniform-thickness LNOIs*. To achieve a high efficiency nonlinear-optical process using $\chi^{(2)}$, a careful design and strict control of the waveguide geometry are needed to meet the phase matching conditions. A thickness variation of several nanometers may have a distinct effect on the joint spectral intensity of SPDC [97].

3. *Local rare-earth doping on LNOIs*. Many important photonic devices (such as lasers, amplifiers, and optical quantum memories) are enabled by various rare-earth ions. Significant progresses in the developments of lasers and amplifiers have been made owing, for example, to Er^{3+}-doped LNOIs [98]. However, light transmission absorption manifests in the rare-earth-doped areas of LNOIs. Therefore, local rare-earth doping on LNOI platforms is preferred for integrated photonic circuits.

4. *Heterogeneous integration*. Heterogeneous integration of materials (such as Si or III–V semiconductors) on LNOIs, which enables complementary material properties, is an area of interest. The heterogeneous integration can also provide light sources and detectors for LNOI photonics. Furthermore, LNTFs are usually supported by SiO_2/Si substrate, which can survive a maximum annealing temperature of about 600 °C. Substrate materials such as sapphire, quartz, and SiC are sometimes preferred due to such features as MIR transparency, low radio frequency loss, high acoustic velocity, and high thermal conductivity. One challenge in heterogeneous integration is to overcome thermal mismatch of materials.
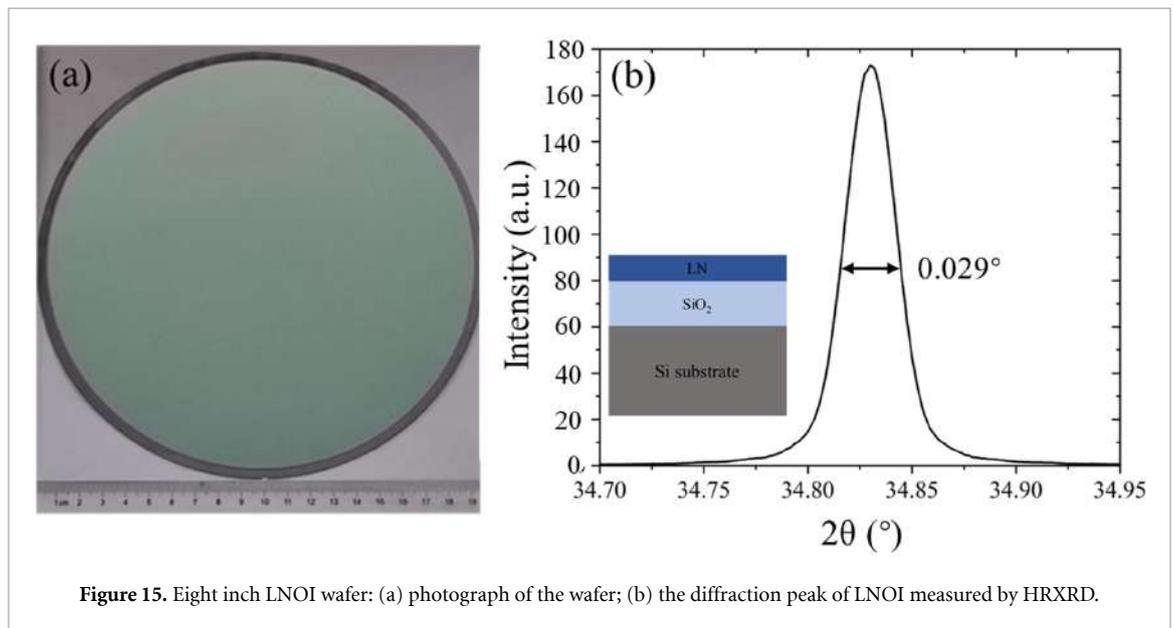
Figure 15. Eight inch LNOI wafer: (a) photograph of the wafer; (b) the diffraction peak of LNOI measured by HRXRD.

Advances in science and technology to meet challenges

The fabrication steps in semiconductor processing, e.g. direct wafer bonding, ion implantation, and chemical mechanical polishing, are mature technologies that can support large-size LNOI fabrication. LNOI size and physical properties are primarily decided by LN bulk crystal (LN wafer). Currently, the maximum size of commonly available optical-grade LN wafers is 6 inches. Such LN wafers have low optical absorption and uniform physical properties (such as refractive indices) across the wafer. MgO-doped and rare-earth-doped LN wafer can have diameters of 4 and 3 inches, respectively. They can all be X-cut, or Z-cut. The development of large-size LN bulk crystal is driven by market demands, and 8 inch LN and LNOI wafers are being developed. Figure 15(a) shows an 8 inch LNOI wafer. The LNTF is X-cut with a thickness of 400 nm. Figure 15(b) shows the diffraction peaks of the LNOI as measured by high resolution x-ray diffraction. The FWHM of the LNTF is 0.029°, showing that the LNTF is mono-crystalline. The insert shows the schematic of the cross-section. The systematic optimization of the LNOI production process is aimed at improving the thickness uniformity of LNOIs and solving the thermal mismatch between LNTF and various substrate materials. LNOIs are expected to achieve a thickness uniformity of 1 nm and strong bonding strength with substrate. Meanwhile, physical property studies, such as photorefractive, dielectric relaxation, and loss mechanisms of LNOIs, are essential for many applications.

For nonlinear-optical processes, using the concept of optical superlattice, periodic polarization structures are realized on LNOI by several poling techniques to fulfill the QPM condition. A periodic poling period of sub-microns was achieved on an MgO-doped LNOI using multiple bipolar preconditioning pulses [99]. For industrial application, the techniques and mechanisms of poling must be further explored to improve yield and domain uniformity. Local doping of rare-earth metal on LNOI has been achieved by selective ion implantation and annealing [100]. Heterogeneous integration was also developed on LNOIs to obtain charge-injection lasers and detectors with excellent performance [101]. All of these processes require optimization of the heterogeneous integration process to overcome the complexity of fabrication and improve yield. Stoichiometric LNTFs are sometimes needed due to their low coercive field and high EO coefficient.

Concluding remarks

Benefitting from its excellent physical properties, large refractive index contrast, and low optical loss, LNOI comprises a promising material platform for the development of integrated photonics. Furthermore, LN is an industry-proven material with an annual usage of millions of wafers. Gradually industrialized LNOI devices will strongly guide and support LNOI material development. In the future, multifunctional integrated photonic systems with more diverse types and more complex structures are expected to be realized on the LNOI platform. With further improvement of the fabrication technology, LNOIs will be developed with large size, high uniformity, and heterogeneous integration to meet the needs of academic and industrial applications.

Acknowledgments

10. Classical and quantum nonlinear frequency conversion in lithium niobate thin film

Yuanlin Zheng and Xianfeng Chen
State Key Laboratory of Advanced Optical Communication Systems and Networks, School of Physics and Astronomy, Shanghai Jiao Tong University, Shanghai 200240, People's Republic of China

Status

LNTF is only in its teenage phase but has been considered as a revolutionary platform for integrated photonics. Multifunctional dense integrated photonics is directly accessible on LNTF thanks to the exceptional properties of LN and a high refractive index contrast of LN to buffering silica. Photonics integrated circuits (PICs) on LNTF, consisted of nanowaveguides, resonators and cavities for strong light–matter interaction, have shown unprecedented conversion efficiency and superior performance in terms of nonlinear wave mixing. The advancement has rejuvenated LN-based photonics in a plethora of science and applications in EO, nonlinear and quantum regimes [95, 102, 103]. Nonlinear frequency conversion processes based on second-order nonlinearity, such as SHG, SFG/DFG, OPA/OPO, SPDC and third-order nonlinearity, like FWM, supercontinuum generation and Kerr OFC have been successfully demonstrated. These progresses have significantly expanded opportunities to flexibly tailor, manipulate or convert light in a nonlinear manner with high efficiency. It has thus been straightforward to explore how to further enhance the light–matter interaction in the fundamental physics aspect and develop high-performance (nonlinear) photonic devices in the technological aspect.

Focusing on the domestic research, the experimental advancement has been developed in parallel with the international community. In the past few years, several seminal works regarding nonlinear frequency conversion on the platform have been reported. As shown in figure 16(a), efficient quadratic wave mixing by exploring novel broadband QPM mechanism in x-cut LNTF microdisks (Q factor $\sim 10^7$) has resulted in simultaneous second-harmonic and cascaded THG with normalized conversion efficiencies as high as $9.9\%\mathrm{mW}^{-1}$ and, respectively [104]. Later, the Q factor has reached a record high of 10^8, close to the theoretical prediction. It further paves the way for cavity enhanced nonlinearity for weak light. By designing an ultra-broadband edge coupler and high-performance PPLN nanowaveguides, efficient SHG with a fiber-to-fiber normalized efficiency of $1027\%\mathrm{W}^{-1}\mathrm{cm}^{-2}$, has recently been demonstrated [105], which is ready for user application (figure 16(b)). A heterostructure cavity composed of a guided-mode resonance (GMR) resonator and distributed Bragg reflectors (figure 16(c)) showcases strongly enhanced electromagnetic field localization to boost SHG by three orders of magnitude [106]. LNTF metasurfaces in figure 16(d) have been shown to selectively boost SHG at different wavelengths via Mie resonances [107]. All these works and others have shown excitement in this field, suggesting the current research focus in China.

Current and future challenges

Applications of classical and quantum PICs on LNTF calls for full manipulation of light on all properties. Yet, challenges are still to be addressed to achieve the ultimate goal. These challenges include theoretical and experimental aspects. For the theoretical aspect, current coupled mode theory models could solve most problems in classical parametric processes. Kerr OFC with OFC exploiting quadratic cascading processes is anticipated to be more efficient yet more sophisticated, which requires detailed systematic investigation. When the interaction enters the few-photon or single-photon level, full quantum modelling is needed. Besides, new concepts in related research areas are to be adopted or considered when such type of nonlinearity is presented, such as twisted photonics, topological photonics, non-Hermitian photonics, and synthetic dimension. For the experimental aspect, efficient nonlinear wave mixings in LNTF requires perfect phase matching and QPM is still the best solution, where the condition is more stringent as dispersion gets stronger in the nanowaveguides. On one hand, strong waveguide dispersion provides more engineering flexibility in terms of dispersion management for wide bandwidth phase matching. On the other hand, although the electrical poling voltage for LNTF domain reversal is dramatically reduced to less than 1 kV, the required QPM period is also reduced and high uniformity is needed. This also makes the fabrication of QPM gratings in the LNTF nanowaveguides technically difficult, especially nano QPM gratings for backward SHG, mirrorless OPO or counter-propagating photon pair generation.

Further improving the conversion efficiency toward single-photon nonlinearity to manifest quantum effect would open new avenues for the fundamental research of light–matter interaction. Accessing single-photon nonlinear interaction is also a key step toward quantum photonic circuits for the flying qubit. It is in need to achieve high absolute frequency conversion efficiency, because not only single-photon nonlinearity is extremely weak, but also quantum optics is less tolerant to loss. Besides, to be integrated with superconduct nanowire single-photon detectors, working in cryogenic environment is also important.
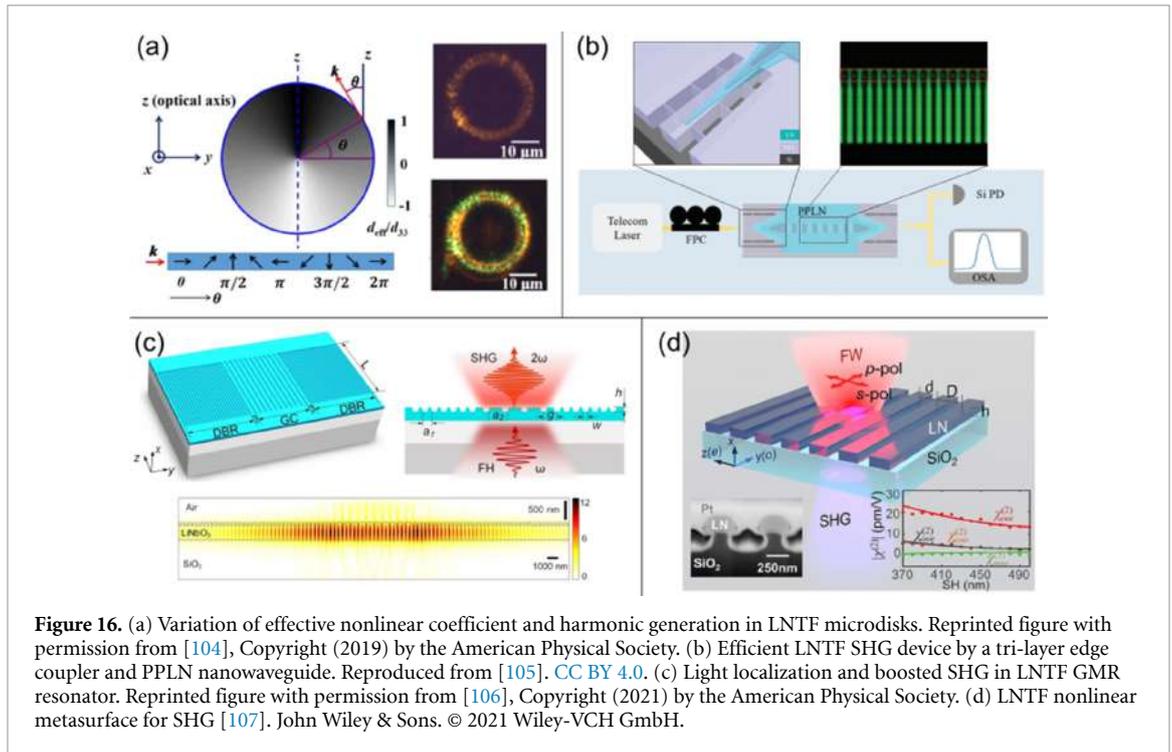
Figure 16. (a) Variation of effective nonlinear coefficient and harmonic generation in LNTF microdisks. Reprinted figure with permission from [104], Copyright (2019) by the American Physical Society. (b) Efficient LNTF SHG device by a tri-layer edge coupler and PPLN nanowaveguide. Reproduced from [105]. CC BY 4.0. (c) Light localization and boosted SHG in LNTF GMR resonator. Reprinted figure with permission from [106], Copyright (2021) by the American Physical Society. (d) LNTF nonlinear metasurface for SHG [107]. John Wiley & Sons. © 2021 Wiley-VCH GmbH.

Reaching single-photon nonlinearity for upconverted detection to work at room temperature is also highly desired for quantum applications.

For LNTF nonlinear metasurface, the nanostructure requires higher precision etching demanding advances in LNTF nanofabrication. Simultaneous multidimensional manipulation with fast response and high efficiency is still a challenge, although novel mechanisms based on GMR resonators, Mie resonance and bound state in the continuum (BIC) [108] have been successfully realized. The nonlinear efficiency and tunability by the LNTF metasurface is far from satisfied.

Advances in science and technology to meet challenges

The development of photonics on LNTF relies on science and technology advancement on the platform, where the core techniques mainly involve high-precision LNTF fabrication, domain engineering and heterogeneous integration.

High-precision nanofabrication is important for dispersion management. The dry etching of LNTF is more favored and adopted among most research groups. But the sidewall loss should be mitigated by optimized plasma etching, with improved surface roughness or reduced material redeposition. Developing wet chemical corrosion method to remove the redeposition and smooth the sidewalls is also a good solution. Other than the plasma etching technology, the photolithography assisted chemo-mechanical etching has been proven to be a good method for fabrication of meter-long nanowaveguides or scalable high-quality PICs on LNTF, where surface roughness can be easily minimized via chemomechanical polishing.

Domain engineering is important for QPM frequency conversion. Generally, the poling technique on LNTF is less demanding than that on bulk LN. One way of direct electric poling the LNTF can achieve micrometer scale QPM periods as defined by ultraviolet or E-beam lithography. Experimentally, the SHG conversion efficient, over 20 folds of that in proton-exchanged PPLN waveguides, has approached the theoretical prediction, suggesting a high-quality matching. Direct electric poling of LNTF with sub-micrometer periods is still difficult. With the assistance of piezo force microscopy, a poling period down to 200 nm has been demonstrated [109], which is feasible for backward QPM in nanocavities or microresonators. Other novel configurations to achieve enhanced nonlinear wave mixing while avoiding domain reversal involves nontrivial mode matching in ultrahigh-Q resonators, GMR resonances and (quasi-)BIC conditions. These efforts have showcased giant enhancement by orders of magnitude improvement in experiments.

For system on a chip, integration is important yet cannot be achieve with pure LNTF. To realize on-chip classical light source, rare-earth ion doped LNTF has been developed, with successful demonstration of lasing and optical amplification. Double doping has also been realized to improve the energy transfer efficiency. Heterogeneous integration of LNTF with silicon, Si_3N_4, InP, GaN, etc, to form hybrid systems not

only provides laser sources and detectors but also compatible operation with other platforms. The implementation will provide full functionalities for disruptive photonics, microwave photonics and quantum optics applications.

Concluding remarks

The past few years has witnessed an exponential growth in integrated photonics on the LNTF platform. The current trend is to improve the interaction efficiency from the physical and technical points of view, which is a natural direction in the nonlinear optics. The motivation to fully incorporate laser sources (both classical and quantum), optical devices (including frequency converters) and photodetectors (by heterogeneous integration) on the monolithic chip to tailor, manipulate or convert light at will for all-optical processing propels the research and technological progress in this field. In the future, new concepts, such as twisted photonics, topological photonics, non-Hermitian photonics, and synthetic dimension, can be incorporated with nonlinearity to explore new physics, new technology and new applications on LNTF. Challenges still exist on both physical and technological basis, where there are new opportunities in the same time. Research on integrated photonics on LNTF is anticipated to grow even more rapidly to provide opportunities for both optical physics and applications.

Acknowledgments

11. Ultrafast and low-power nanoscale photonic devices

Xiaoyong Hu
State Key Laboratory for Mesoscopic Physics and Frontiers Science Center for Nano-Optoelectronics, School of Physics, Peking University, Beijing 100871, People's Republic of China

Status
Along with the rapid development of information technology, the need for ultrahigh-speed and low-energy-consumption information processing chip is becoming increasingly urgent. Using photon as information carrier is a very promising way to reach ultrahigh-speed and low-energy-consumption information processing. Nanoscale photonic devices are essential basis for constructing integrated photonic chips. Two key indexes for nanoscale photonic devices are ultrahigh-speed of over 10 Tbit s^{-1} and low energy consumption of less than 10 fJ/bit [110]. Unfortunately, ultrafast response and giant third-order optical nonlinear coefficient are difficult to obtain for conventional optical materials and microstructures. This makes it a great challenge to reach weak light induced ultrafast and giant third-order optical nonlinearity [111]. This has greatly restricted the realization of ultrafast and low-power nanoscale photonic devices. More often than not, nanoscale photonic devices with high energy consumption and high speed (ultrafast time response of several femtoseconds order and large energy consumption of several nJ/bit order), or low energy consumption and low speed (slow time response of several microseconds and low energy consumption of several fJ/bit order) are relatively easy to reach. Recently, great breakthrough has been achieved in ultrafast and low-power nanoscale photonic devices, as shown in figure 17. In 2020, NTT company reported a nanoscale all-optical modulator based on plasmonic slot waveguide covered with single-layer graphene flake, with an energy consumption of 30/fJ bit and modulation speed of 1 Tbit s^{-1} [111]. However, great efforts are still needed to reach the target of nanoscale photonic devices with ultrahigh-speed of over 10 Tbit s^{-1} and low energy consumption of less than 10 fJ/bit [112].

Current and future challenges
High-speed and low energy consumption photon information processing is established on the method of light-control-light based on third-order optical nonlinearity. For example, based on the third-order NLO Kerr effect,

$$n = n_0 + n_2 I \tag{1}$$

where n, n_0, and n_2 are the refractive index, linear refractive index, and nonlinear refractive index of nonlinear material, I is the pump light intensity, the refractive index of nonlinear material changes with the external pump light intensity. This makes it possible to reach that the propagation state of signal light could be controlled by the pump light based on the pump-light-intensity dependent refractive index change of nonlinear materials and nanostructures. For the conventional semiconductor and organic materials, nonresonant-excitation will result in small third-order nonlinear coefficient and ultrafast response time of several femtoseconds order, while resonant-excitation will lead to large third-order nonlinear coefficient and slow response time. Plasmonic microstructures could be used to enhance third-order optical nonlinearity response by using strong light confinement of plasmonic mode. Relatively large intrinsic Ohmic losses has limited the large-scale integration application of plasmonic microstructures in integrated photonic chips [113]. Therefore, this material bottleneck has greatly restricted the realization of ultrafast and low-power nanoscale photonic devices. Great efforts are needed to overcome this material bottleneck difficulty in the future.

Advances in science and technology to meet challenges
Various approaches have been proposed to obtain weak light induced ultrafast and giant third-order optical nonlinearity in the near-infrared and optical communication range. In the wavelength range from visible to around 800 nm, constructing organic composites and adopting excited-state charge transfer (or energy transfer) is an effective method to reach nonlinear refractive index of order of 10^{-9}–10^{-7} esu and fast response time of the order of several picoseconds [114]. On-chip triggered all-optical switch with a speed of 60 Gbit s^{-1} and energy consumption of 100 fJ/bit has been achieved [114]. In the optical communication range, constructing nanocomposite materials and adopting compound reinforcement of nonlinearity is an effective method to enhance third-order optical nonlinearity response [115]. Not only local-field enhancement effect and quantum size effect of nanoscale crystal grain could be used to enhance the third-order nonlinear coefficient, but also fast response time of dozens of picoseconds order could be

Figure 17. Development status of nanoscale photonic devices.

Figure 18. Comparation of nonlinear photonic microstructure materials in the optical communication range.
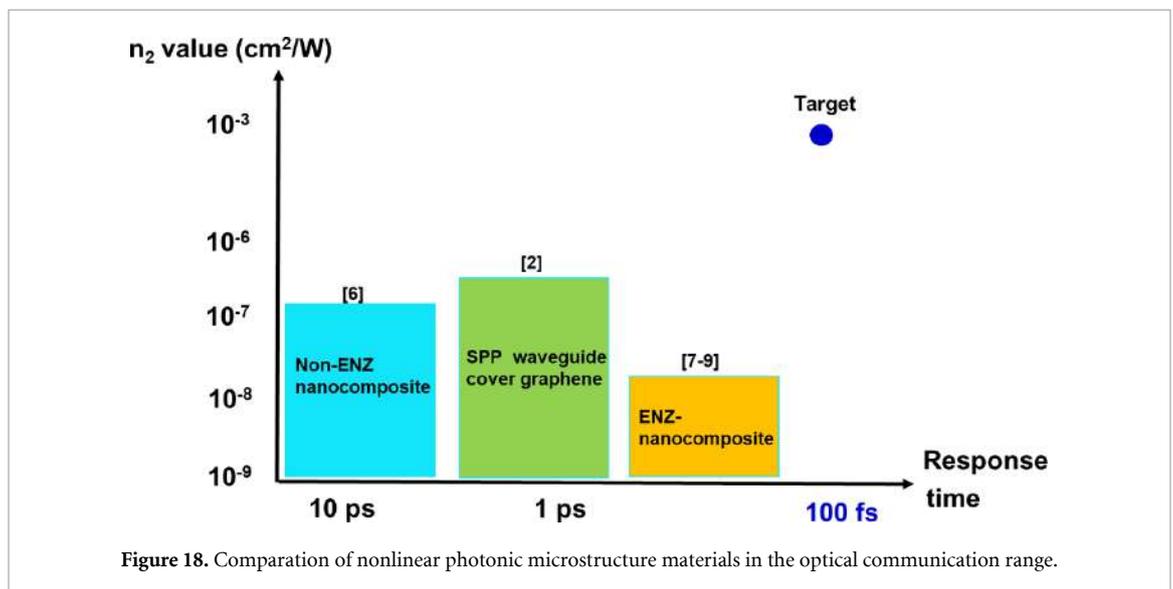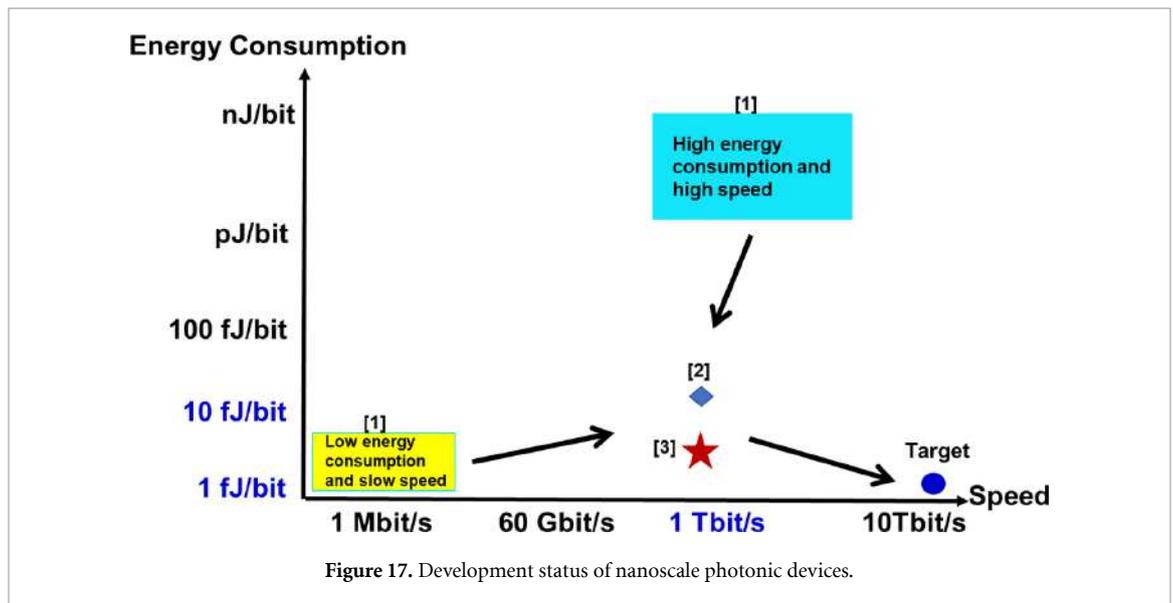
achieved due to fast recombination of carriers induced by the lattice defects in the interfaces of nanoscale crystal grains. The value of nonlinear refractive index could reach the order of 10^{-10}–10^{-7} cm^2 W^{-1}. On-chip triggered all-optical modulator with a speed of 50 Gbit s^{-1} and energy consumption of 80 fJ/bit has been achieved [115]. Constructing nanocomposites based on epsilon-near-zero material is also an excellent method to obtain large nonlinear refractive index of the order of 10^{-10}–10^{-8} cm^2 W^{-1} and ultrafast response time of the order of hundreds of femtoseconds [116–118], as shown in figure 18. Recently, the method of signal light modulating imaginary part of refractive index induced parity-time symmetry broken (or inverse parity-time symmetry broken) was proposed and used to realize an all-optical modulator with a speed of 1 Tbit s^{-1} and low energy consumption of less than 10 fJ/bit [112]. New methods of enhancing ultrafast and giant third-order nonlinearity are still urgently needed to obtain the target of nanoscale photonic devices with ultrahigh-speed of over 10 Tbit s^{-1} and low energy consumption of less than 10 fJ/bit [119].

Concluding remarks

The realization of ultrahigh-speed and ultralow-energy-consumption photon information processing chips is a long-term goal full of challenges. Ultrafast and low-power nanoscale photonic devices, as a core of the photon information processing chips, still requires novel physics and effects to improve their performances, response time and energy consumption. Since great efforts have been put in this field, continuous breakthroughs could be expected in the near future.

12. Surface nonlinear optical spectroscopy

Chuanshan Tian

State Key Laboratory of Surface Physics, Key Laboratory of Micro and Nano Photonic Structures (MOE), and Department of Physics, Fudan University, Shanghai 200433, People's Republic of China

Status

The trend of surface science has been directed more toward complex systems in recent years [120], in which the microscopic structures are in close relation to electrochemistry, catalytic chemistry, biology, and many other disciplines. However, experimental study of such interfaces is challenging, because most surface-specific analytic tools that found successful applications in vacuum encounter various difficulties in ambient/liquid conditions. At an interface between two adjacent media, the second-order NLO process is allowed because the inversion symmetry is necessarily broken. Thus, SHG and sum-frequency spectroscopy (SFS) are highly surface-specific [121]. These spectroscopic techniques have been used widely to probe surfaces and interfaces of many materials in various disciplines since their demonstration in 1981 for SHG and in 1987 for SFS, respectively. In comparison to other surface analytical tools, SHG/SFS allows *in situ*, remote and non-destructive probe of surfaces in real environments with sub-monolayer sensitivity.

Benefiting from the continuous advances in laser techniques, SFS/SHG has been improved significantly regarding its sensitivity, spectral range, spatial and time resolution, etc. One notable progress is the development of phase-sensitive SFS [122–124]. It can provide both the real and imaginary spectra of interfacial resonances, avoiding ambiguity in the spectral analysis. The first viable phase-sensitive SFS was developed in the Shen group in 2007 using a green beam and a tunable MIR beam as the pump derived from a narrow-band picosecond laser [123]. As depicted in figure 19(a), the pump beams propagate collinearly passing through the sample and a reference nonlinear crystal. Their relative phase is modulated through continuous rotation of a phase plate inserted in between. Alternatively, the phase information can also be measured using the multiplex scheme shown in figure 19(b) as demonstrated by the Benderskii group and the Tahara group based on broadband femtosecond laser system [125, 126]. With the acquired complex spectra, one may not only obtain the complete spectral information of an interface, including the absolute orientation of a moiety, but the decomposition of different contributions is feasible in the experiment.

Current and future challenges

In the past 15 years, phase-sensitive SFS has provided new opportunities for surface and interface studies, arousing researchers' interest to revisit the structure interpretation of some solid and/or liquid interfaces. In particular, our understanding of a charged interface has been greatly advanced with the help of phase-sensitive SFS. Charged interfaces are ubiquitous, e.g. lipid membrane, photocatalysis, electrochemical interface, etc. Following the Stern–Gouy–Chapman model, a charged interface is composed of two sub-layers, as depicted in figure 20(a): an atomically thin Stern layer in which orientation and arrangement of molecules are directly influenced by bonding to the charged plane, and a diffuse layer away from the charged plane in which molecules can be reoriented by the dc electric field set by the surface charge and screening ions. It is the Stern layer that plays the most important role in controlling interfacial properties and functionality. Despite extensive studies in the past, little is known about the molecular structure of the Stern layer. The difficulty lies in the fact that the Stern layer spectrum is overwhelmed by and the large background from the diffuse layer. In 2016, we devised a viable experimental scheme that can obtain separately the vibrational spectra of the two sublayers using phase-sensitive SFS [127]. The method utilized the physical properties of the two sublayers that bear different response sensitivity with respect to variation of surface charge, ion concentration, and other factors. With the help of the Stern–Gouy–Chapman model (or modified Gouy–Chapman model taking into account the ion size effect) [128], the vibrational spectra of the two sublayers can be separately deduced for a charged interface with known surface charge density. Accordingly, the microscopic structure in the Stern layer can be deduced (figure 20(b)). Alternatively, given the SF susceptibility of molecules in the diffused layer (polarized by the dc electric field within), one can obtain quantitatively the surface charge density of specific ions emerging at the interface, as shown in figure 20(c).

The technical progress of SFS sheds more light on the chemical reactions at various interfaces that are relevant to many environmental and energy issues. As mentioned above, it is highly desired to learn the microscopic reaction pathways and the intermediate products at the interface. However, probing the reaction radicals is much more difficult than detecting the average interfacial physical structure. It is because only very few portions of the surface moieties are chemically active, which demands the sensitivity of SFS to be better than at least 1%–0.1% of a monolayer, while the current sensitivity reaches around 3% of a monolayer. This
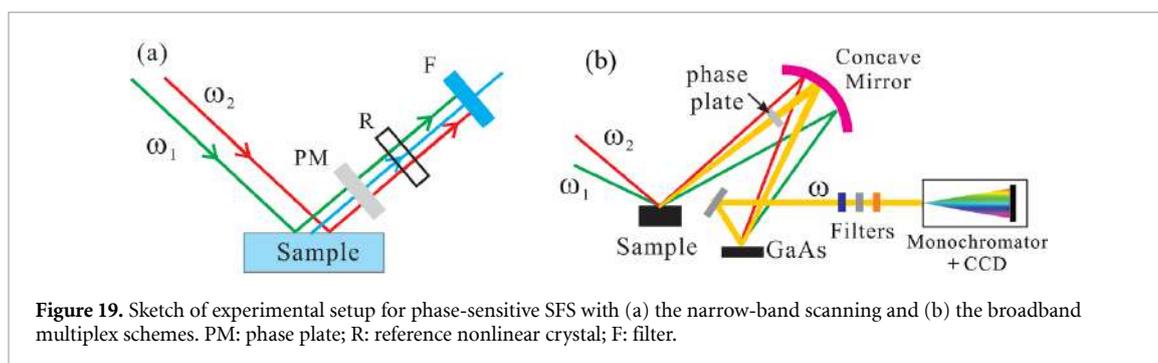
Figure 19. Sketch of experimental setup for phase-sensitive SFS with (a) the narrow-band scanning and (b) the broadband multiplex schemes. PM: phase plate; R: reference nonlinear crystal; F: filter.
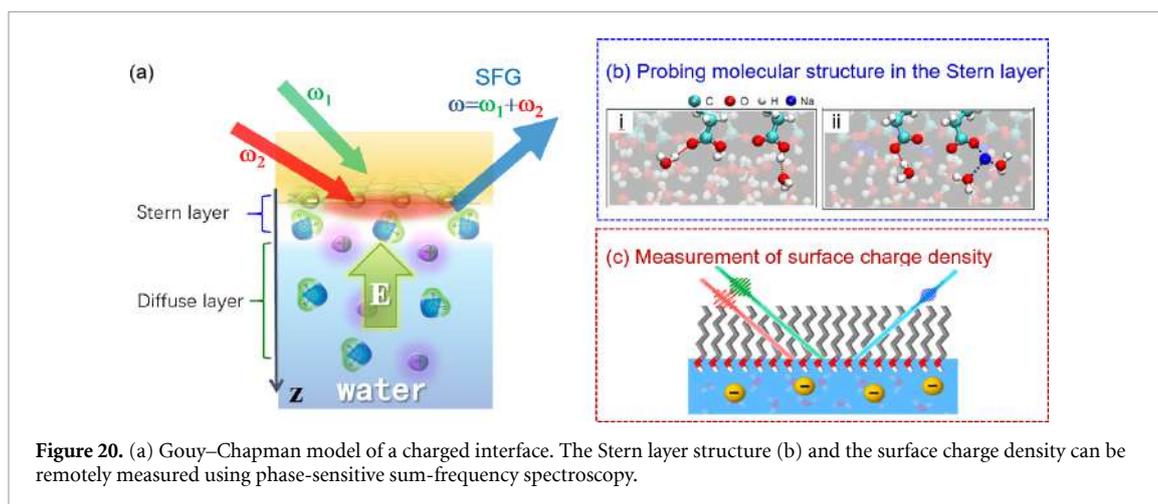
Figure 20. (a) Gouy–Chapman model of a charged interface. The Stern layer structure (b) and the surface charge density can be remotely measured using phase-sensitive sum-frequency spectroscopy.

calls for a revolutionary promotion of the SFS detection sensitivity in order to unravel the microscopic chemical processes at the interface of, e.g. photo-catalysis for water-splitting in fuel cells.

Another challenge is the extension of the spectral range of SFS. Limited by serious absorption of most nonlinear crystals for frequency conversion in the infrared, the generation of an intense infrared beam with a wavelength longer than 16 μm is difficult. Without the intense long wavelength pulse, the applications of SFS were mainly limited to the system composed of light elements, for instance, H, C, N, O, Si, etc, the vibrational resonances of which lie in the MIR. Many fundamental excitations at the interface of complex oxides that play a pivotal role in catalytic reactions and emergent physics are hardly touched thus far. Thus, there is an urgent need for a surface-specific NLO spectroscopic technique operating in the wavelength range beyond 16 μm. Such a technique is expected to benefit the studies of chiral vibrations of biomolecules and collective motions of hydrogen-bonding networks at interfaces as well.

Advances in science and technology to meet challenges

The detection sensitivity of SFS is mainly limited by the damage threshold intensity of the pump laser pulses. The pump beams derived from a high-power picosecond or femtosecond laser usually carry plenty of pulse energy. However, their intensities must be lowered to the values such that the properties of the target sample are not affected. Considering that the threshold intensity becomes higher for a shorter laser pulse, using an ultrashort pulse as the pump source, e.g. single- or few-cycle pulse, would allow stronger intensity shining on the sample. On the other hand, further promotion of the optical field in the interfacial region can be realized through proper design of the meta structure to enhance the local field.

The family of second-order optical crystals used in DFG to produce infrared light is not so large. The obvious advantage of the second-order process is its high conversion efficiency. But their phonon resonances often appear in the long-wavelength infrared range, causing severe absorption of the infrared. The third-order optical process is generally considered inefficient in comparison to DFG. However, given femtosecond pump pulses with strong intensities, the third-order frequency mixing can also be appreciable, especially when a Raman resonance involves in the process [129]. Moreover, the choice of third-order optical materials is essentially unlimited. Thus, depending on the desired infrared wavelength, one can readily find a

transparent material without infrared attenuation. For example, liquid nitrogen could be a good candidate for the generation of the mid- and far-infrared beam.

Concluding remarks

We have outlined here some recent progress and challenges of SFS. Due to the limited length of this letter, some other advances are not covered, such as sum-frequency scattering spectroscopy [130, 131], SHG/SFG microscopy [132], ultrafast dynamics at the interface [133], etc. Recent state-of-the-art laser technology and novel spectroscopic techniques can be harnessed to improve the capability of NLO spectroscopy and to broaden the scope of SFS applications. With continuous efforts, the field of surface-specific NLO spectroscopy may enter a new era. More and more detailed information regarding the physical structure and chemical reaction at an interface can be revealed in spatial, spectral, and time domains.

Acknowledgment

13. Controlling the angular momentum of harmonic waves with metasurfaces

*Zixian Hu and Guixin Li**
Department of Materials Science and Engineering, Southern University of Science and Technology, Shenzhen 518 055, People's Republic of China

*Email: ligx@sustech.edu.cn

Status

The angular momentum is an important intrinsic property of light, which contains two degrees of freedom: spin and orbital component (SAM and OAM). SAM is associated with the circular polarizations of light and is represented by σ, where $\sigma = \pm 1$ corresponds to the left- and right- circular polarization. In comparison, OAM is manifested by the helical wavefront of light. The electric field of the OAM beam carries a factor of $\exp(il\varphi)$, in which l is the topological charge and φ is the azimuthal angle. Light with OAM is a special kind of structured light, the generation, manipulation, and detection of which have been attracting growing interests. In the regime of linear optics, metasurfaces have been utilized to control the angular momentum of light based on several phase manipulation mechanisms, such as propagation phase, resonant phase, and geometric phase. Recently, there are plenty of metasurface-based devices for practical applications having been reported. They realize various optical functions while manipulate the OAM of light, such as the fork grating [134], Cassegrain system [135] and holography [136]. Owing to the ability for localizing the incident light, metasurface has been proved to be a promising platform for nonlinear optics. Hence, as being extended to the regime of nonlinear optics, metasurfaces have also been used to control the angular momentum of the harmonic waves generated in NLO processes.

In 2015, the plasmonic metasurfaces were used for the generation of the second harmonic waves (SHWs), during which a nonlinear geometric phase related to the SAM of light is introduced [137]. Based on the mechanism of nonlinear geometric phase, we are able to control the OAM of the harmonic waves. As shown in figure 21(a), by judiciously arranging the meta-atoms with three-fold (C3) rotational symmetry, nonlinear phase singularities with predesigned topological charges were introduced [138]. Under the pumping of circularly polarized fundamental waves (FWs), SHWs with controllable OAM values were generated as a result of the spin–orbit interaction in the NLO processes. Moreover, if the circularly polarized FWs also carry OAMs, the analysis of the angular momentum of harmonic waves can be extended to a generalized situation [139]. The angular momentum state of light is expressed as $(\sigma, l)_\omega$, where $\sigma = \pm 1$ and l represent the SAM and OAM states, and the subscript ω is the angular frequency of FWs or SHWs. For a plasmonic metasurface designed as a q-plate, which obeys the conservation law of the OAM during the NLO process, the angular momentum states of FW and SHW are $(\sigma, l)_\omega$ and $(-\sigma, 2l + 3\sigma q)_{2\omega}$, respectively, where q is the topological charge of the metasurface (figure 21(b)). Apart from plasmonic metasurfaces, which consist of meta-atoms whose materials are noble metals, dielectric metasurfaces have also been applied to control the angular momentum of harmonic waves. By decorating traditional nonlinear crystals with dielectric metasurfaces, the on-chip wavefront engineering of the generated harmonic waves can be realized [140]. As shown in figure 22, the metasurface-decorated quartz crystal was first pumped by circularly polarized FWs, the SHWs were generated during the nonlinear process in the crystal. Then, the generated SHWs were manipulated by the metasurface fabricated on the one side of the crystal, which is a linear optical process. Such a hybrid system represents an alternative method to control the angular momentum of harmonic waves in an ultra-compact way.

Current and future challenges

Due to the various phase manipulation mechanisms and the ability for the localization of light, metasurfaces represent promising platforms for generating and controlling the angular momentum of the harmonic waves. As for the plasmonic metasurfaces, however, the ultrathin layer characteristic limits the length of the light–matter interaction, resulting in relatively lower nonlinear conversion efficiencies compared with that in nonlinear crystals. The low damage thresholds of plasmonic meta-atoms also restrict the potentials to improve the nonlinear conversion efficiencies by increasing the pumping power.

Advances in science and technology to meet challenges

There are several solutions to overcome the aforementioned challenges. The first solution is to increase the area of the plasmonic metasurfaces. Under the same pumping density limited by the damage thresholds, plasmonic metasurfaces with a larger area are able to endure higher pumping power. Therefore, the nonlinear conversion efficiencies are able to be improved. The second solution is to replace metals with other

Figure 21. Controlling the angular momentum of the generated harmonic waves by using plasmonic metasurfaces. The plasmonic metasurfaces are composed of gold meta-atoms with three-fold rotational symmetry. (a) Schematic of the spin-controlled generation of the OAM beams during the second harmonic generation (SHG) process. By encoding phase singularities into the metasurfaces, the generated SHWs carry OAMs with designed topological charges [138]. (b) A generalized principle to predict the angular momentum state of the SHWs generated during the SHG process on the q-plate plasmonic metasurfaces [139].

Figure 22. Schematic of the crystal-metasurface hybrid platform. The wavefront of the harmonic wave generated in the nonlinear crystal can be artificially engineered by the dielectric metasurface [140].

materials, which have higher NLO susceptibilities or damage thresholds. Such as semiconductors or dielectric materials. The last solution is to employ the crystal-metasurface hybrid platform. The harmonic waves are generated in the nonlinear crystals rather than the layer of metasurfaces, providing a longer length for the light–matter interaction. The higher damage thresholds of the crystals and dielectric metasurfaces ensure that a higher nonlinear conversion efficiency can be obtained.

Concluding remarks

By using the concepts of geometric phase in the NLO regime, we are able to locally control the phase, amplitude, and polarization of harmonic waves from the plasmonic metasurfaces. Therefore, the geometric phase controlled plasmonic metasurfaces are versatile platforms to control the angular momentum of the generated harmonic waves. Recently, by combining conventional optical crystals and the linear optical metasurfaces, one can efficiently generate and manipulate the angular momentum of harmonic waves with higher efficiency and versatilities.

Acknowledgments

14. Nonlinear self-accelerating effect of light

*Yi Hu and Jingjun Xu**

The Key Laboratory of Weak-Light Nonlinear Photonics, Ministry of Education, School of Physics and TEDA Applied Physics Institute, Nankai University, Tianjin 300071, People's Republic of China

*Email: jjxu@nankai.edu.cn

Status

Self-accelerating effect of wave packets was initially proposed in quantum mechanics [141]. It describes that a quantum particle can self-accelerate without any external field. Such effect was later introduced into optics, resulting in the pioneering self-accelerating optical beams, namely Airy beams [142], which brought about many fancy applications [143]. The acceleration is sustained by transforming the energy from a part of the beam to the other part that carries the peak intensity. Indeed, the center of mass of the beam still evolves along a straight line. People attempted to generate beams of true self-acceleration by means of nonlinearity [144], which was yet limited to the non-conservative type [145]. During the rapid development of Airy-like self-accelerating beams, a nonlinear effect, namely diametric drive self-acceleration was proposed [146, 147]. Two optical pulses were designed to undergo an acceleration merely by means of their interaction in optical fibers. The center of mass of the paired pulses followed in this case a parabolic path in space-time space. This is attributed to the counterintuitive dynamics of effective negative mass, rather than to a non-conservative nonlinearity. The interaction of the two pulses, subject to inverted dispersion, is in analogy to the interplay between two objects having opposite mass signs (figure 23(a)). Such a diametric drive self-acceleration was also observed in spatial domain [148], offering new ways for beam steering.

The Airy-like self-acceleration and the diametric drive self-acceleration received lots of attention, yet they were investigated independently. Quite recently, the two mechanisms were linked together [149]. Using this linkage, self-accelerating optical pulses with tunable number of peaks were demonstrated, featuring a more precise control of the acceleration. Such structured pulse complexes may be used to encode information beyond the binary coding limit.

By using the nonlinear interaction of optical fields, another scheme was proposed to induce self-accelerating effect. The basic idea was to break the Newton's third law in the beam interaction (figure 23(b)), allowing the two involved optical fields to experience forces of the same direction [150]. Theoretically, this nonlinear effect was demonstrated in a LC.

The self-accelerating effect stemming from the light interaction is analogous to the self-propel effect or non-reciprocal interaction in active or living matters. Regarding that the self-propulsion motion is the key to various intriguing collective dynamics in active systems. The nonlinear self-accelerating effect of light is foreseen to bring about novel phenomena to many body physics in optics.

Current and future challenges

In most studies, the two optical fields forming a pair of diametric drive self-acceleration are incoherent to each other. They are designed well using the developed theoretical tools. Once the mutual coherence of them is considered, these theories become invalid for precise designs. As a result of the beating effect of the two involved beams, it is difficult to transform the associated dynamics into a static problem as done in the incoherent case. The brute-force way is to scan the beam parameters in simulations, which is time-consuming, and even unachievable for solutions with unknown shapes.

The concept of negative mass brings about new ways to realize localized NLO structures. These nonlinearly binding effect is reminiscent of soliton molecules that commonly appear in optical cavities or resonators. It is difficult to realize these soliton molecules in transmission fibers as the soliton interactions are not balanced well. Using negative effective mass of optical pulses may offer opportunities to tackle this problem. Future work will focus on how to design nonlinear localized states beyond the two-body model describing the diametric drive self-acceleration.

Diametric drive self-acceleration is mainly discussed in two dimensions, one of which is for light evolution. Extending it into three dimensions (for instance, two transverse plus one longitudinal dimensions) may bring about more novel phenomena that do not have counterparts in lower dimensions. But in this configuration, it is challenge to make the beam localized in both transverse directions. While the light spreading is suppressed by the mechanism of diametric drive self-acceleration in one dimension, the beam tends to broaden as a result of a self-defocusing nonlinearity in the orthogonal direction.

By combining the methods for generating Airy-like self-acceleration and diametric drive self-acceleration, localized structured pulses with tunable number of peaks can be designed. With the increase of the peak numbers, the difficulty in their experimental realization goes up. Thus far, the common

Figure 23. Two mechanisms to realize self-accelerating effect of light via nonlinear interactions. (a) Diametric drive self-acceleration for two optical fields having opposite signs of effective mass; (b) breaking of the Newton's third law.
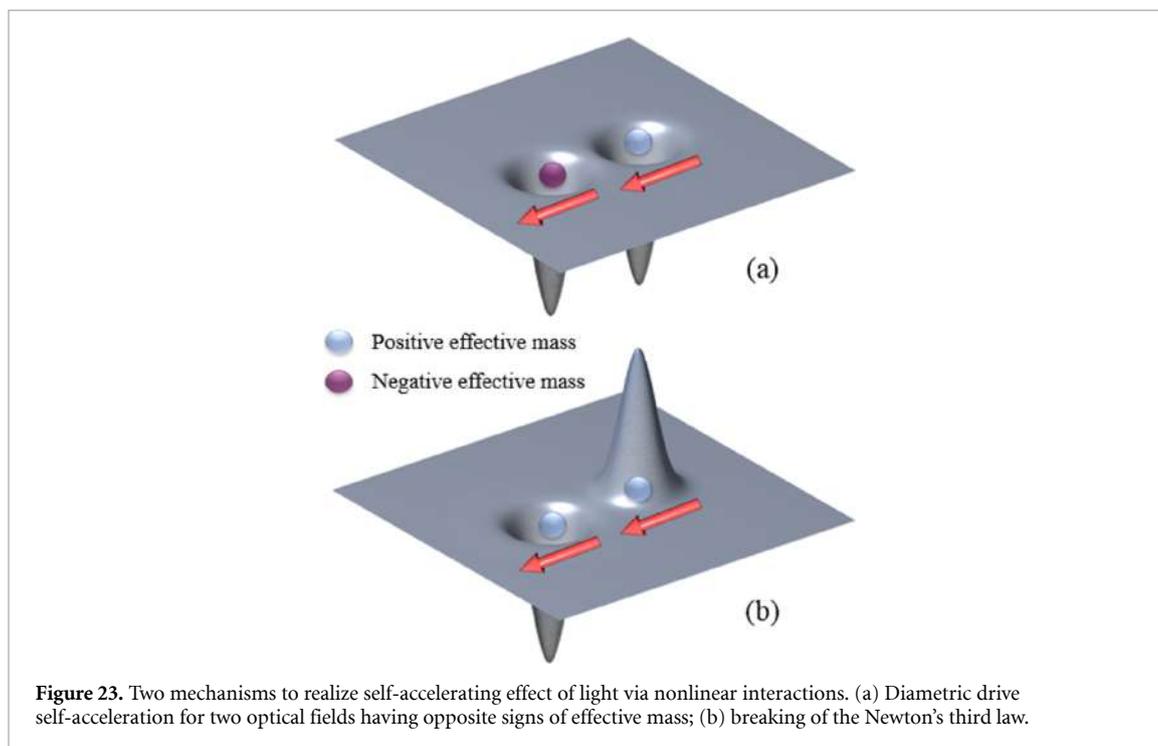
method to produce ultra-short shaped pulses is to encode the spectrum information of a target pulse in a spatial light modulator (SLM). The modulator, generally made of LC, faces resolution limit to generate pulses having more complex shapes. Thus a device featured with high resolution modulation is on demand.

The proposed breaking of the Newton's third law during light interactions relies on special nonlinearities in LCs. It will be meaningful to put forward a general way of non-reciprocal interaction that is applicable to different nonlinear materials.

Advances in science and technology to meet challenges

In nonlinear light propagation, there exist many solutions that change their shapes during evolution, such as rogue waves in fibers or Floquet solitons in periodically driven photonic structures. The developed theories in these areas may be referred for finding new tools to design coherent diametric drive self-acceleration.

It is possible to construct nonlinear localized optical fields by involving more waves having both positive and negative effective masses. For instance, in optical fibers, three waves may bind in the following picture: the repulsion of two out-of-phase solitons is balanced by the attraction of a dispersive pulse experiencing normal dispersion, while the paired solitons offer a potential well to confine the dispersive pulse. The method to design diametric drive self-acceleration and the approach to solve soliton solutions may be combined for realizing nonlinear binding of multi-waves with signed effective masses. In order to overcome the resolution limit of the pulse shaper to generate these complex pulse structures, the LC may be replaced by metasurface.

In the design of three dimensional diametric drive self-acceleration, the light localization in both transverse dimensions may be achieved by using some special diffraction regions in optical structures. For instance, relying on the co-existence of normal and anomalous diffraction, an optical field is able to experience self-focusing and -defocusing nonlinearities in two orthogonal directions. While its self-defocusing spreading is suppressed by the mechanism of diametric drive self-acceleration, it is possibly localized in the orthogonal dimension via the self-focusing effect.

To break the Newton's third law in beam interactions, one may simply let the refractive index potentials induced by two beams are inverted. For this purpose, self-focusing and -defocusing effects are imparted to each beam. In this framework, the forces experienced by the two beams point to the same direction during their interaction. There are various materials where the two nonlinear effects co-exist. For instance, some photorefractive crystals exhibit self-focusing/-defocusing nonlinearity for positive/negative biased electric field, respectively. Applying an alternative field, the beams injecting into the crystal at different half-period of time experience inverted nonlinearities, and they can interact relying on the storage property of photorefractive effect. Atomic vaper is another candidate, in which two optical beams with a positive/negative detuning to the resonance line exhibit self-focusing/-defocusing nonlinearity, respectively. Both materials can offer a considerable nonlinear effect at a low power level, which is beneficial to studying optical many-body physics mediated by the self-accelerating effect.

Concluding remarks

The nonlinear self-accelerating effect of light discussed here is associated with the one that truly changes the center of mass of optical beams. It stems from light interactions, yet in two unconventional configurations. One is based on counterintuitive dynamics of negative mass, and the other one is in the framework of violating the Newton's third law. In both cases, two optical waves are able to show a synchronized acceleration merely via their nonlinear interplay. More unexpected phenomena are about to appear when this kind of interactions is extended into high dimensions and many-body interactions. In particular, the self-accelerating effect can intrinsically alter the interacting scenarios of a multi-wave system by making the photons 'active' and may bring about novel collective dynamics in nonlinear optics as inspired by the crucial role played by self-propulsion motion in active materials.

Acknowledgments

15. Mid-infrared frequency upconversion imaging

Kun Huang[1,2] *and Heping Zeng*[1,2]
[1] State Key Laboratory of Precision Spectroscopy, East China Normal University, Shanghai 200062, People's Republic of China
[2] Chongqing Key Laboratory of Precision Optics, Chongqing Institute of East China Normal University, Chongqing 401121, People's Republic of China

Status

The MIR spectral region is pertaining to favorable features to support molecular fingerprint analysis and cover the Earth's atmosphere transparent window, which attracts intensive attention in various fundamental and applied fields. Nowadays, MIR imagers based on narrow-band gap semiconductors with indium antimonide (InSb) and mercury cadmium telluride usually require high-cost fabrication process and stringent cryogenic operation, thus severely limiting the wider application and promotion. Recently, breakthroughs in using emerging low-dimensional materials have been achieved to implement sensitive MIR detectors at room temperature, albeit that the currently attainable noise equivalent power is still many orders of magnitude from the single-photon level. Besides of the sensitivity enhancement at elevated operation temperatures, parallel challenges for the MIR focal plane arrays lie in further improving the pixel number and the response time to realize high-resolution imaging at high-speed frame rates.

In this context, frequency upconversion imaging has been recognized as a promising alternative to the MIR imaging, where the infrared light is nonlinearly converted to the visible regime while maintaining coherent properties including the spatial modes and photon statistics. The resulting upconverted photons can be registered by low-cost and high-performance silicon-based cameras with desirable features of high quantum efficiency, low dark noise, megapixel sensor matrix, and high readout rate [151]. Consequently, the performance of the indirect infrared imaging is essentially determined by the conversion unit and silicon imager. Although the seminal implementation of upconversion imaging can be traced back to 1960s, yet rapid progresses have only been witnessed in the last decades thanks to the technological advances and fabrication maturation for high-efficiency nonlinear crystals, high-power pump lasers, and high-sensitivity silicon cameras. Specifically, the combination with ingenious designs of upconversion system has enabled to demonstrate passive and active MIR single-photon imaging based on cavity-enhanced continuous-wave pump and mode-locked ultrafast-pulse pump, respectively [152, 153]. The unprecedented imaging sensitivity opens new possibilities for low-light-level applications. Moreover, the intrinsic PM requirement makes it possible to engineer the nonlinear conversion process to access the unique imaging capability in resolving information encoded in wavelength, phase, polarization, and time domains. Therefore, the superior imaging performances and novel imaging modalities render the upconversion imager a powerful tool in expanding interdisciplinary fields.

Current and future challenges

The core of the upconversion imaging system is the conversion unit, which typically involves a second-order nonlinear crystal and a high-intensity pump source as depicted in figure 24(a). Ideally, the conversion process is expected to have a unitary conversion efficiency for all spectral components, add no noisy photons under intensive pumping, and preserve imaging information with all spatial frequencies. Practically, these parameters are never perfect, thus imposing limitations in the achieved imaging performance. First, the efficient nonlinear conversion usually requires at least 100 W pump power even using efficient QPM crystals [152]. The required pump power would be much higher to attain a broadband operation with a shorter crystal, which particularly imposes a great challenge to prepare such a high-power continuous-wave light source. The situation is more severe for the upconversion of longer MIR wavelengths owing to limited options for suitable nonlinear materials. Second, the intensive pump field would inevitably induce severe background noises from the parametric fluorescence and Raman scattering. To identify the single-photon-level signal from the large dark noise, it is thus imperative to develop a high-efficiency filtering system with a high rejection ratio. Furthermore, some noise may locate within the spectral band of the upconverted signal, which merits the development of novel filtering techniques beyond the typical spectral domain. Third, the conversion process acts as a soft aperture for the upconversion imaging, which results in the loss of high-frequency spatial components. Additionally, the stringent PM requirement imposes a constraint on the monochromatic field of view (FOV) of the imaging system. Therefore, it remains another major challenge to simultaneously enlarge the FOV and enhance the spatial resolution. Generally, there needs a global optimization on various available parameters to maximize the imaging performance relevant to a specific application. For instance, a larger pump beam within the crystal favors a higher resolution, but

Figure 24. (a) Conceptual illustration of the frequency upconversion imaging, where the infrared object is nonlinearly converted into the visible replica before being captured by a high-performance silicon-based camera. (b) Various degrees of freedom for the optical field can possibly be used to realize different imaging modalities with the help of set-up modification and pump-mode engineering. Reported applications for the mid-infrared upconversion imaging include non-invasive identification of embedded chips (c) Reproduced from [156]. CC BY 4.0, volume visualizations of ceramic stacks (d) Reproduced from [160]. CC BY 4.0, and histopathological inspection of biomedical samples (e). Reproduced from [159]. CC BY 4.0.

the reduced pump intensity leads to a lower conversion efficiency. A longer crystal helps to increase the efficiency, yet at the expense of a reduced operation bandwidth and a smaller acceptance angle.

Advances in science and technology to meet challenges

The cavity enhancement configuration is introduced to realize the sufficient pump power in the passive MIR upconversion imaging. The optical cavity confines an enhanced field within a resonant Gaussian spatial mode, leading to substantial improvement on the conversion efficiency [152]. Alternatively, the coincidence-pumping scheme is suitable for active MIR imaging, where the pulsed excitation provides a high peak power and a short temporal duration, thus favoring to increase the conversion efficiency and reduce the background noise [154]. In combination with a chirped-poling nonlinear crystal, a broadband MIR imaging is feasible based on the efficient adiabatic conversion [155]. The resultant large PM bandwidth also enables to access a wide FOV [156]. Moreover, the optical pump gating can be used to implement a high-resolution depth imaging by temporally selecting the reflected photons [156]. To reach longer working wavelengths above 5 μm, possible candidates can resort to nonlinear crystals based on $BaGa_4Se_7$, $AgGaS_2$, GaAs, and GaP [157]. The last two optical materials are possible to be fabricated in orientation-patterned configurations for QPM, which hence hold great potential to achieve efficient conversion up to 12 μm. As an interesting trend for upconversion imaging, the involved nonlinear conversion process allows to manipulate the incident fields by engineering the pump properties in the spectral, temporal, and spatial domains. This unique feature has recently been exploited to implement the MIR edge-enhanced imaging [158]. Notably, as exemplified in figures 24(c)–(e), immediate applications are rapidly driven by the enhanced MIR imaging performance, such as label-free histopathological diagnosis by high-speed hyperspectral imaging [159] and non-destructive defect inspection based on real-time optical coherence tomography [160].

Concluding remarks

The upconversion imager inherits the superior performance of cutting-edge silicon cameras, and thus provides an effective solution to achieve favorable MIR imaging features of single-photon sensitivity, MHz-level frame rate, and massive resolvable elements. However, there is still much room for improvement especially in increasing the spectral bandwidth, reaching longer wavelengths, enlarging the acceptance angle, and enhancing the spatial resolution. Furthermore, the inherent nonlinear process can be engineered to implement multi-dimensional upconversion imaging with the resolving power for the wavelength, phase,

polarization, and time, as illustrated in figure 24(b). In the future, integration and miniaturization are also expected to facilitate a field-deployable device for widespread use in practical scenarios.

Acknowledgments

16. Ultrafast laser nonlinear manufacturing

Zhen-Ze Li[1] and Hong-Bo Sun[2]
[1] State Key Laboratory of Integrated Optoelectronics, College of Electronic Science and Engineering, Jilin University, Changchun 130012, People's Republic of China
[2] State Key Laboratory of Precision Measurement Technology and Instruments, Department of Precision Instrument, Tsinghua University, Beijing 100084, People's Republic of China

Status

Over the past decades, ultrafast laser manufacturing has attracted extensive attentions in various fields benefiting from its intrinsic three-dimensional (3D) processing capability and broad material applicability. The advantages of ultrafast laser origin from the extremely nonlinear laser-matter interaction which is far beyond linear optics. By the strong nonlinear threshold effect of multiphoton ionization or Zener ionization, laser energy deposition can be confined to a sub-diffraction range of the focal spot without causing any redundant damage/modification in the light propagation path before the focus. Therefore, as shown in figure 25(a), the laser-processed voxel can penetrate deep into the material and enable free-form shaping of 3D structures with a precision of hundreds of nanometers [161]. To date, based on two-photon 3D nanoprinting and femtosecond laser refractive index modification of transparent materials, a large number of prototype functional devices have been successfully prepared, which exhibits strong application potential in various fields including smart micro-robots, optical storage (figure 25(d)), fiber sensing and integrated diffractive optics elements (figure 25(g)).

In addition, the transient electrons excited by intense laser irradiation perturbate the atomic potential energy surface [162] and inject a large amount of energy into the lattice system through the electron–phonon coupling, driving a pronounced collective atomic displacement within tens of picoseconds (figure 25(c)), which provides a unique technique for precise phase engineering of materials at nanoscale (e.g. ablation, evaporation, melting, crystallization, amorphization or defect center generation). For example, 3D NPCs [54] can be realized by femtosecond lasers selectively erasing of the second-order NLO coefficients in crystals (figure 25(b)). Another interesting and important scheme is the NV color centers in diamond. By femtosecond laser irradiation, single diamond NV center can be directly introduced with impressive yields and 3D positioning accuracy [163], which is promising for applications such as quantum sensing and distributed quantum computing.

Meanwhile, since the pulse duration of ultrafast laser is much smaller than the characteristic time of energy exchange between electrons and phonons (several picoseconds), the thermal damage during laser processing can be effectively suppressed, which is very suitable for modern high-accuracy industrial processing of hard (or brittle) material, such as dicing, grooving and drilling of silica glass, sapphire or transparent ceramics. Combined with the current booming spatial/temporal light modulation technologies, the efficiency and accuracy of ultrafast laser processing can be further improved. Therefore, it is expected to build a cross-scale universal processing platform based on ultrafast laser technology.

However, despite these achievements, there are still some tricky problems to be solved for further promoting the application of ultrafast laser processing in science and industry. This roadmap aims to identify current scientific and technical issues and the necessary methods to be developed to address these challenges.

Current and future challenges

Mechanisms of laser-matter interaction

Exploring the interaction of ultrafast lasers and matter is not only of great significance in physics, but can also promote the improvement of laser processing technology. However, until now, these mechanisms have not been fully understood. The fundamental difficulty lies in that ultrafast laser processing is a complex multiphysics process spanning multiple spatio/temporal scales, covering the interdisciplinary knowledge from quantum theory, nonlinear optics, elastic mechanics, thermology and hydromechanics. It is a formidable challenge for both experimental observations and numerical simulations to record/resolve the complex physical and chemical processes at a nanoscale spatial scale while maintaining a femtosecond temporal resolution, which further hinders the establishment of the systematic theoretical model. A well-known case is the phenomenon so-called laser-induced periodic structures [164]. Although they were first observed decades ago and have been found important applications in surface texturing (figure 25(h)) and optical storage, its formation mechanism is still debated. The confusion of the theory leads to the lack of methodologies for high-quality structure preparation.

Figure 25. Applications of ultrafast laser nonlinear fabrication. (a) The famous nano-bull fabricated by two-photon polymerization, which powerfully demonstrates the 3D capabilities and precision of this technology. Reproduced from [161], with permission from Springer Nature. (b) 3D nonlinear photonics crystal by laser erase of the second-order nonlinear susceptibility. Reproduced from [54], with permission from Springer Nature. (c) Perturbation of the atomic potential energy surface (PEC) by the electron excitation and the subsequent coherent motion of lattice. Reprinted figure with permission from [162], Copyright (2018) by the American Physical Society. (d) Optical storage recorded by femtosecond laser irradiation. Reproduced from [165], with permission from Springer Nature. (e) Far-field-induced near-field fabrication. The far-field beam was converted to near-field components which facilitates dynamical high-resolution direct laser writing. Reproduced from [166]. CC BY 4.0. (f) 3D non-Abelian photonic chip fabricated by femtosecond laser direct writing of waveguides in glass. Reproduced from [167], with permission from Springer Nature. (g) Diffractive elements integrated with the opto-fluidic components. Reproduced from Hu *et al* [170]. John Wiley & Sons. © 2021 Wiley-VCH GmbH. (h) Large-area, rapid surface nanotexturing by surface plasma imprinting technology. The surface plasmon standing wave forms due to the metallization of the fabricated material under the femtosecond laser excitation. Reproduced from [164]. CC BY 4.0.

Fabrication resolution

Another important question is the ultimate fabrication resolution that can be stably achieved by laser processing. Technically, the precision of laser processing directly determines the allowable complexity of the fabricated devices. Typically, the accuracy of current ultrafast laser processing is limited to hundreds of nanometers. Most of optical meta surfaces/materials or high-dimensional optical storage [165] working at visible wavelength consist of meta atoms/bytes with feature size around 100 nm, which accordingly cannot be directly fabricated by standard ultrafast laser processing technologies. Various techniques such as stimulated emission depletion (STED) can significantly improve the processing accuracy of two-photon polymerization, but these methods are not applicable to dielectrics or semiconductors. For solid materials, a recent proposed O-FIB technology [166] indicated that the polarization-controlled near-field optical components emerging from boundary conditions can play a key role to realize nanoscale free-form direct laser writing (figure 25(e)). Further, can we use ultrafast lasers to excite specific electronic states to drive coherent phonon modes for atomic-level processing or manipulation? Therefore, chasing the ultimate precision of ultrafast laser processing is a still topic of great significance both in physics and technology.

Processing efficiency

Typically, ultrafast laser processing adopts a point-by-point scanning strategy, therefore the processing time increases cubically with the device volume and processing resolution. It often takes several hours or even

dozens of hours to complete the processing, which hinders the practical applications of ultrafast laser processing in scientific research, medicine or industrial production. Conventional approaches to overcome this trade-off including spatial light modulation, multi-focus parallel scanning or projection optics, are limited by the current state-of-the-art capability of phase/amplitude modulation and the basic principle of diffractive optics, sacrificing part of the processing accuracy and making it difficult to realize complex device structures.

Tunable/reconfigurable devices and heterogeneous integration

The three-dimensional in-volume integrated devices directly written by the ultrafast laser is protected from the disturbance of the external environment and therefore can work well under high temperature or high humidity conditions. However, this also makes it difficult to tune or reconfigure these devices. For example, in-volume optical waveguides fabricated by femtosecond lasers [167] play a crucial role in three-dimensional integrated photonic quantum chips (figure 25(f)). However, limited by the physical properties of glass, only the thermo-optic effect can be used for phase modulation, the modulation speed is still unsatisfactory and the waveguides deep in the body also cannot be modulated. For materials whose optical properties are easy to be electrically modulated, such as lithium niobite, however, these crystals are tricky to fabricate, and till now their ultrafast laser-based processing technique still needs to be further improved to realize high performance devices.

Another solution may circumvent this challenge is the heterogeneous integration. Thanks to the flexibility of two-photon polymerization, it can fabricate structures on optical fibers and electronic chips for direct integration. However, for most of the inorganic solid materials, the related bout solutions/methods are still lacking.

Advances in science and technology to meet challenges

To address the significant challenges to establish a universal, multiscale, efficient fabrication platform based on ultrafast laser, the following advances are required.

Ultrafast pump-probe techniques specific to laser processing should be further improved to reach higher spatio/temporal resolution for direct observation of the physical processes during the laser fabrication. At the same time, simulation techniques covering from the atomic scale to the mesoscopic scale should be established to better understand the laser-matter interaction, for example, the recently flourished time-dependent density-functional theory and multiphysics simulation based on nonlinear Maxwell equations, Navier–Stokes equations and thermo-elasto-plastic equations, which can cover from the energy absorption at the atomic level to the structural evolution at the micrometer scale.

Accordingly, advanced processing techniques which benefit both accuracy and efficiency are worth expecting. On the one hand, such advances could be attributed to a deeper understanding of the mechanism of laser-matter interaction. They may originate from cutting-edge concepts in nanophotonics, such as the STED technique or optical near field mentioned above, or from laser-induced multiphysics effects, such as heat (typical heat accumulation or ablation-cooling material removal), liquid, gas or plasma-assisted laser processing techniques. For example, a recent work has shown that the laser-induced micro-jet in a liquid environment can effectively improve the quality of laser processing, bringing off micro-optical elements with nanoscale roughness on the surface of normally difficult-to-process crystalline materials, such as sapphire, yttrium aluminum garnet, etc [168]. On the other hand, the technological advances of processing equipment/algorithm matter as well. For example, the development of more stable ultrafast lasers with higher repetition rates, SLMs with higher pixel density and faster refresh rates or light shaping algorithms with higher degrees of freedom.

Notably, the recent rise of scientific machine learning is promising to play an important role in ultrafast laser processing in the future, as it dominates various areas of science and engineering such as image recognition, automation, structure prediction. Based on artificial intelligence, automatic processing and *in-situ* inspection are expected to be realized in the future, which can greatly improve the efficiency and yield of processing. At the same time, machine learning has recently been proven to be applied to optical field modulation, inverse device design and even physical field reconstruction [169], that is, research on ultrafast laser processing mechanisms may also benefit from advances in artificial intelligence.

Concluding remarks

We expect that a universal processing platform based on ultrafast lasers will be established once these challenges are well resolved and contributes to the future 3D integration of next-generation functional devices. Correspondingly, industrialization of ultrafast lasers will be further boosted in the next decade. However, the advances to reach this goal require efforts across the photonics community, including laser, nonlinear optics, and the associate precision instrument technologies.

Acknowledgments

17. Quartz-enhanced photoacoustic spectroscopy

Lei Dong

State Key Laboratory of Quantum Optics and Quantum Optics Devices, Institute of Laser Spectroscopy, Shanxi University, Taiyuan 030006, People's Republic of China

Status

The PA effect was initially discovered by Bell in 1881. However, the phenomenon was almost completely forgotten for over 50 years. Its revival started soon after the advent of laser light sources. In the 1970s and 1980s, photoacoustic spectroscopy (PAS), which is based on the PA effect, experienced a significant surge in popularity, primarily through its combination with gas lasers. PAS offers two significant advantages: first, it is excitation wavelength-independent, allowing for the same PAS-based detector to be used with any type of laser and at any wavelength, ranging from ultraviolet to terahertz, with identical performance. As a result, a single instrument can realize a multi-gas PA sensor that is based on a different wavelength. Second, the sensitivity of PAS is proportional to the incident laser power. This feature enables PAS-based detectors to benefit from the development of high-power semiconductor lasers with high wall plug efficiency or from the enhanced excitation.

Quartz-enhanced photoacoustic spectroscopy (QEPAS) is a variant of PAS that has been shown to be a sensitive spectroscopic technique for the chemical analysis of gases since its initial demonstration in 2002 [171]. In QEPAS, a quartz tuning fork (QTF), as depicted in figure 26(a), is employed as a resonant acoustic transducer, replacing the conventional broadband microphone. Consequently, QEPAS unites the main characteristics of PAS with the advantages of using a QTF, providing an ultra-compact, cost-effective, robust acoustic detection module [172].

The fundamental principle behind QEPAS is quite straightforward. When optical radiation interacts with a trace gas, it generates a weak acoustic pressure wave that excites a resonant vibration of a QTF. The vibration is subsequently converted into an electric signal by the piezoelectric effect. The electric signal, which is proportional to the gas concentration, is then measured by a transimpedance amplifier. Compared to conventional resonant PA spectroscopy, QEPAS has several advantages, such as the sensor's immunity to environmental acoustic noise, a straightforward design for the absorption detection module, and its ability to analyze trace gas samples of $\sim$1 mm^3 in volume.

To-date, the QEPAS technique has been employed to measure numerous molecules with well resolved rotational-vibrational lines in the near-infrared spectral range (e.g. NH_3, CO_2, CO, HCN, HCl, H_2O, H_2S, CH_4, C_2H_2, C_2H_4) as well as in the MIR spectral region (e.g. NO, N_2O, CO, NH_3, C_2H_6, and CH_2O). QEPAS has also been demonstrated with larger molecules with broad, unresolved absorption spectra, such as ethanol, acetone and Freon. These results were shown in figure 26(b) [173].

Current and future challenges

Conventionally, the QEPAS technique assumes a linear relationship between the amplitude of PA signal and the excitation power, as well as between the amplitude of PA signal and absorption coefficient. However, it has been found that these linear dependences may not be universally applicable. Under certain conditions, the linear correlation no longer holds true and nonlinear dependence occurs. So far, several types of nonlinear mechanisms have been investigated and developed, including absorption saturation-based nonlinearity [174], thermal-based nonlinearity [175].

As mentioned earlier, one of the advantages of PAS is its proportionality of sensitivity to the incident optical intensity. However, this relationship is only applicable when the optical intensities are much lower than the saturation intensity. As the intensity approaches the saturation intensity, the absorption coefficient decreases to half of its original value, indicating a negative reciprocal function correlation with the incident intensity. With the continual development of the laser industry, the output power of commercial lasers is increasing. Fully utilizing these high-power lasers to achieve ultra-high detection sensitivity is now a significant challenge in the QEPAS technique.

In PAS, the temperature rise induced by the absorption of light generates thermal-elastic expansion. This expansion causes a pressure change and results in acoustic emission, which can be detected using a

Figure 26. (a) Two commercially available 32.768 kHz quartz tuning forks with and without the capsule. A Chinese dime is placed next to them as a size reference. (b) The detection sensitivity for different gases versus employed laser wavelength, in the UV–vis, near-IR, mind-IR and THz spectral ranges. NNEA: normalized noise equivalent absorption coefficient.
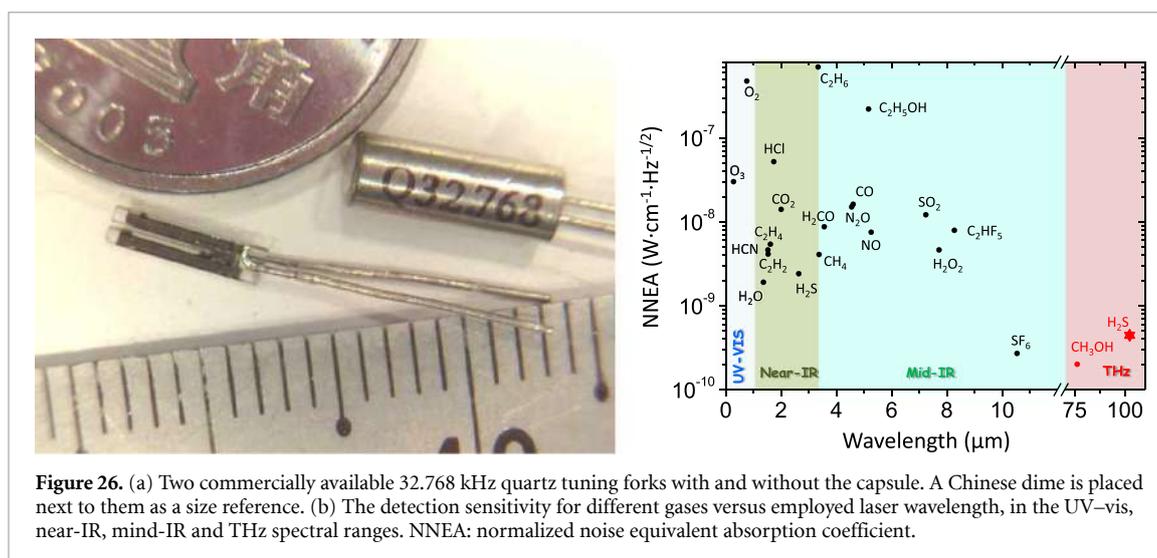
transducer. It is important to note that the thermal expansion coefficient exhibits the most notable dependence on temperature and needs to be considered when the temperature increase is significant. However, in most cases, the local temperature rise induced by excitation beam is often ignored by assuming that the thermodynamic parameters remain constant. This assumption is no longer valid when the temperature increase is significant and should be taken into consideration to ensure accurate measurements.

Advances in science and technology to meet challenges

To meet these challenges, it is necessary to provide new technological solutions on the one hand, and to improve the QTF performance to meet the requirement of nonlinear measurement on the other hand. In 2015, a power-boosted QEPAS sensor is developed for sub-ppm H_2S trace-gas detection in NIR region [176]. A 1.4 W distributed feedback laser was employed as its optical source. The linearity of the sensor response to the laser power and H_2S concentration confirms that the nonlinear effect did not occur since the 0.3 mm gap between the prongs of the commercially available QTF caused a larger background noise and limits the use of the higher optical power. Subsequently, a custom QTF with its two prongs spaced ∼0.8 mm apart was used to replace the commercial QTF [177]. Although the background noise was completely eliminated, the sensor system still worked in the linear region. In 2019, a PA sensor system for detecting ppb-levels of CO in sulphur hexafluoride decomposition was reported using a 10 W fiber-amplified NIR diode laser [178]. A saturated behavior of the PA signal was observed in this high-power system, indicating the further increases in optical excitation power would not benefit the PA signal. In order to increase the PA signal amplitude under high optical excitation power, more ground state molecules were supplemented into the PA cell. As a result, a portion of supplemented 'fresh' molecules were constantly excited to the excited state with strong optical excitation power. The PA amplitude was improved ∼3 times with the assistance of the gas flow. Therefore, the measurement of nonlinear effect requires a ∼10 W excitation optical power in PAS.

A QTF is easy to be broken in such a high optical power, especially when the prong gap is too narrow to accommodate the laser beam. These considerations determine the directions that should be followed for realizing QTFs optimized for nonlinear PAS. The prongs spacing should increase in order to minimize the noise signal due to fraction of the optical power that may hit the internal surface of the QTF; the quality factor must be kept as high as possible; a reduction of the QTF fundamental frequency down to a few kHz should be carried out in order to increase the QEPAS response in the slow-relaxing gases without adding any relaxation promoter. Some new QTF designs have been reported, as shown in figure 27 [179].

Figure 27. (a) Photograph of a T-shaped QTF; (b) photograph of a grooved QTF.
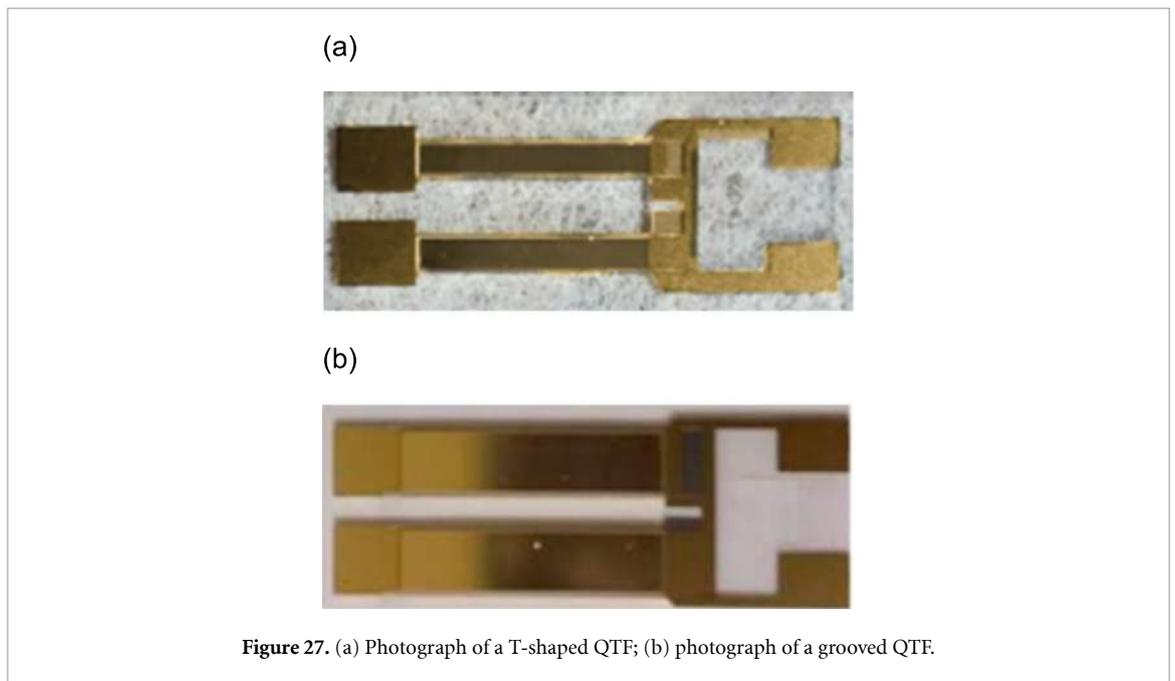
Concluding remarks

PAS can be considered as a linear spectroscopy technique with a low excitation optical power. However, some nonlinear effects occur with the increase of the excitation optical power. To date, the output power of a single laser diode can be up to watt level. In order to make use of the high power, the nonlinear effect can not be ignored in the QEPAS technique. In the near future, more and more important breakthroughs regarding the QEPAS technique are being made [180, 181].

Acknowledgments

18. Nonlinear optical imaging for bio-photonics

Runfeng Li, Wenkai Yang and Kebin Shi
State Key Laboratory for Mesoscopic Physics and Frontiers Science Center for Nano-Optoelectronics, School of Physics, Peking University, Beijing 100871, People's Republic of China

Status

Nonlinearly generated optical signal has been utilized as one of the most important contrast mechanisms for bio-photonic imaging. There have been increasing demands for higher spatiotemporal resolution, larger FOV, deeper imaging depth and better biochemical specificity in bio-imaging research field, where NLO microscopy has shown several advantages. As one of the most attracting features, strong laser intensity required by nonlinear signal generation enables highly localized excitation volume, leading to intrinsic optical sectioning capability. Nonlinearly enabled multiphoton excitation further allows the use of infrared laser sources and consequently the better three-dimensional imaging capability of thick bio-samples. Moreover, NLO response of bio-samples can probe diverse signal characteristics intrinsically and plays critical roles in label-free imaging modalities, as exemplified by optical harmonic microscopy for probing structural information and nonlinear wave mixing microscopy with electronic/vibrational resonance for biochemistry imaging.

Currently, multiphoton excited fluorescence microscopy has been widely employed in biomedical research. Large penetration depth and intrinsic three-dimension optical sectioning capability make multiphoton fluorescence microscopy a unique imaging modality for neuron science as well as thick fluorescence sample studies. In contrast to the fluorescent emission, signal generation originated from second or third order nonlinear polarization in light–matter interaction has been demonstrated to support various label-free microscopy modalities without fluorescent markers. Second or third order nonlinear parametric processes such as SHG, SFG, THG and FWM have been reported for bio-photonic imaging. Yet the nonlinear parametric-process-based imaging modalities are often limited to only provide morphological/structural information. Non-parametric nonlinear processes with vibrational or electronic resonance excitation further enable chemically selective imaging modalities such like coherent Raman microscopy and resonance-enhanced SFG microscopies.

Driven by emerging challenges such as *in-vivo* biomedical research, brain science and tissue-level study, optical imaging systems are expected continuously to achieve higher spatiotemporal resolution, better signal to noise ratio, deeper imaging depth and lower phototoxicity/photo-damage. To this end, the NLO imaging community will foresee on-going efforts enabled by new NLO physics mechanisms, novel optical technologies, and the interdisciplinary inspirations from other research fields.

Current and future challenges

NLO signal generation in bio-samples often requires high intensity thresholds to be produced by tightly focused beam with ultrafast pulses. Such excitation thresholds result in good performance in rejecting spatial background noise and consequently better optical sectioning capability. Yet, intense laser fields substantially lead to photo-damage, phototoxicity and physiological perturbations, which are particularly unwelcomed in live bio-sample studies. Label-free NLO imaging overcomes fluorescent phototoxicity by using intrinsically parametric or non-parametric NLO signals such as optical harmonics, nonlinear wave mixing without or with resonant excitations respectively. Despite the efforts in Raman/electronic enhanced nonlinear wave mixing microscopes, NLO signals are still limited in mapping diverse biochemical specificities in comparison to fluorescence imaging.

In short summary, the most challenging tasks in nonlinear bio-photonic imaging are centered to enhance photon efficiency and spatiotemporal resolution systemically while achieving less photo-damage and better biochemical specificity (as shown in figure 28), by developing novel excitation/illumination, nonlinear photon conversion, detection, and data analysis methodologies.

Advances in science and technology to meet challenges

NLO imaging community has made substantial progresses to tackle the challenges based on different technical approaches. Notable efforts have also been reported by Chinese scientists recently. For example, to optimize the nonlinear illumination efficiency, an adaptive excitation source (AES) was proposed for high-speed multiphoton microscopy in 2018. In this method, only the informative parts of the sample were illuminated by outputting pulses only with specified region-of-interest, which will significantly reduce the thermal damage to the brain tissue, resulting in a 30-fold reduction in the power requirement for two- or three-photon imaging of brain activity with an imaging depth of 680 μm, a field-of-view of 700 μm * 700 μm

Figure 28. The quest for ideal nonlinear bio-photonic imaging techniques.
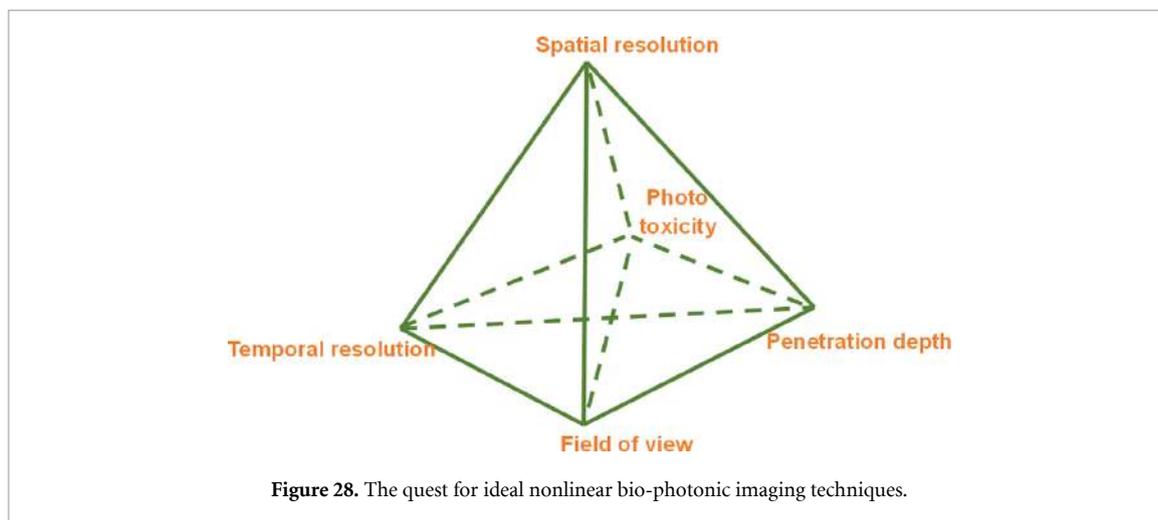
at 30 frames per second. Imaging of awake mouse brain at video rate was demonstrated. A high-pulse energy, wavelength-tunable (1600–2520 nm) femtosecond fiber laser was also used with the AES scheme to show the promising applications for *in vivo* deep-tissue multi-photon fluorescence imaging [182]. In 2017, improved multiphoton structured illumination microscopy using adaptive optics scheme was reported, where a nonlinear guide star was used to determine optical aberrations and a deformable mirror to correct them. The system offers better spatial resolution, optical sectioning, and easier sample preparation comparing with conventional microscopy [183]. A gradient excitation technique to accelerate three-dimensional two-photon excitation fluorescence imaging was also reported recently, where the axial positions of the fluorophores can be decoded from the intensity ratio of the paired images obtained by sequentially exciting the specimen with two axially elongated two-photon beams of complementary gradient intensities. Compared with traditional two-photon excitation fluorescence microscopy, the technique improves volumetric imaging speed (by at least six-fold), decreases photobleaching (less than $2.07 \pm 2.89\%$ in 25 min), and minimizes photodamages [184]. As an impressive progress toward *in vivo* multiphoton fluorescence imaging, miniature two-photon microscopy for fast high-resolution, multi-plane and long-term brain imaging was reported in 2017. In 2021, the same group developed the miniature FHIRM-TPM 2.0, which was equipped with an axial scanning mechanism and a long-working-distance miniature objective to enable fast volumetric and multi-plane imaging over a volume of 420 * 420 * 180 μm^3 at a lateral resolution of $\sim$1 μm.

As complementary signal modality to fluorescence, non-parametric NLO signal with molecular resonance excitation such as coherent anti-Stokes Raman scattering and SRS has emerged as an important label-free chemical imaging contrast mechanism. There have been inspiring works reported recently covering technology development and biomedical applications. To realize 3D coherent Raman scattering imaging of scattering samples, Yang *et al* adjusted spatial-temporal overlapping of pump and Stokes pulses so that the two counter-propagating pulses meet at different depths of the sample, and combined with galvanometer scanning to form a pulse sheet. This technique can be used to image highly scattering bone tissue with lateral resolution of 16.4 μm and axial resolution of 24.5 μm over a large FOV [185].

With engineered material design, probes suitable for coherent Raman imaging have attracted great interest recently. Yang *et al* synthesized a water-soluble and biocompatible Raman probe with 100-fold enhanced vibrational signals in cellular Raman-silent region (1800–2800 cm^{-1}) compared to conventional alkyne Raman probes. This ultra-strong probe enables functional SRS imaging of specific subcellular organelles [186]. Different from the above inert Raman probes, Ao *et al* developed a reversibly switchable vibrational probe. Based on an alkyne-labelled diarylethene, this probe undergoes reversible photoisomerization under ultraviolet or visible light irradiation, and the narrow Raman peak of the alkynyl group on the spectrum shifts accordingly, generating photoactive 'on' and 'off' SRS images [187], opening exciting pathway toward super-resolution Raman imaging.

Combined with information science, high-quality coherent Raman imaging can also provide valuable quantitative imaging analysis for precision biomedical applications. By utilizing the classification algorithm of support vector machine, it was achieved to analyze the spectral and morphological characteristics based on Raman images of calcified parts of breast tumors [188].

It can be concluded from the recent progresses that interdisciplinary technique/application integration will be a promising strategy to further develop advanced NLO microscopy and their applications.

Concluding remarks

The future development of NLO imaging for bio-photonic research can be a diverse and interdisciplinary research field involving optical physics, material, computing, and biomedical sciences. Multiple elements of optical techniques such as adaptive optics, holographic recording, tomographic detection, and computational imaging principles can serve as potential candidates to be integrated with NLO imaging systems. For instance, adaptive optical principle can be applied on laser source, excitation field engineering and detection optimization. Wide-field-based holography and tomography can be combined with nonlinearly generated signal to achieve high speed imaging [189, 190]. Rapid progresses in computation-based neuron network have enabled various machine learning tools, which will play promising roles for developing efficient NLO imaging techniques and big imaging data segmentation/analysis. More applications in clinical practices will be also possible for nonlinear imaging systems with the rapid advancing in small footprint nonlinear fiber laser sources and fiber optical systems.

Acknowledgments

Data availability statement

No new data were created or analyzed in this study.

ORCID iDs

Mengxin Ren ⓘ https://orcid.org/0000-0003-0322-8193
Bao-Sen Shi ⓘ https://orcid.org/0000-0002-5965-5365
Yong Zhang ⓘ https://orcid.org/0000-0003-1158-2248
Min Xiao ⓘ https://orcid.org/0000-0001-9207-0927
Shiwei Wu ⓘ https://orcid.org/0000-0001-9838-9066
Hui Hu ⓘ https://orcid.org/0000-0002-1194-5283
Xianfeng Chen ⓘ https://orcid.org/0000-0003-3025-9729
Xiaoyong Hu ⓘ https://orcid.org/0000-0002-1545-1491
Hong-Bo Sun ⓘ https://orcid.org/0000-0002-3797-9238

References

[1] Shen Y R 1976 Recent advances in nonlinear optics *Rev. Mod. Phys.* **48** 1–32
[2] New G 2011 Nonlinear optics: the first 50 years *Contemp. Phys.* **52** 281–92
[3] Ji Z and Qun L 1980 A 20 years' survey of laser science and technology in China (in Chinese) *Chin. J. Lasers* **7** 1–12
[4] Bloembergen N 1976 Contrasts in China's laser effort *Laser Focus* **2** 10–18
[5] Ye N, Tu C, Long X and Hong M 2010 Recent advances in crystal growth in China: laser, nonlinear optical, and ferroelectric crystals *Cryst. Growth Des.* **10** 4672–81
[6] Shen Y R 2012 50 years of nonlinear optics (in Chinese) *Physics* **41** 71–81
[7] Chen X, Zhang G, Zeng H, Guo Q and She W 2014 *Advances in Nonlinear Optics* (Berlin: de Gruyter & Co)
[8] Kong Y, Bo F, Wang W, Zheng D, Liu H, Zhang G, Rupp R and Xu J 2020 Recent progress in lithium niobate: optical damage, defect simulation, and on-chip devices *Adv. Mater.* **32** 1806452
[9] Gao B, Ren M, Zheng D, Wu W, Cai W, Sun J, Kong Y and Xu J 2021 Long-lived lithium niobate: history and progress *J. Synth. Cryst.* **50** 1183–99
[10] McPherson A, Gibson G, Jara H, Johann U, Luk T S, McIntyre I A, Boyer K and Rhodes C K 1987 Studies of multiphoton production of vacuum-ultraviolet radiation in the rare gases *J. Opt. Soc. Am.* B **4** 595
[11] Ferray M, L'Huillier A, Li X F, Lompre L A, Mainfray G and Manus C 1988 Multiple-harmonic conversion of 1064 nm radiation in rare gases *J. Phys.* B **21** L31
[12] Paul P M, Toma E S, Breger P, Mullot G, Auge F, Balcou P, Muller H G and Agostini P 2001 Observation of a train of attosecond pulses from high harmonic generation *Science* **292** 1689
[13] Hentschel M, Kienberger R, Spielmann C, Reider G A, Milosevic N, Brabec T, Corkum P, Heinzmann U, Drescher M and Krausz F 2001 Attosecond metrology *Nature* **414** 509–13
[14] Fu Y, Nishimura K, Shao R, Suda A, Midorikawa K, Lan P and Takahashi E 2020 High efficiency ultrafast water-window harmonic generation for single-shot soft X-ray spectroscopy *Commun. Phys.* **3** 92
[15] Takahashi E J, Lan P, Mücke O D, Nabekawa Y and Midorikawa K 2013 *Nat. Commun.* **4** 2691
[16] Corkum P B 1993 Plasma perspective on strong field multiphoton ionization *Phys. Rev. Lett.* **71** 1994
[17] Ghimire S, DiChiara A D, Sistrunk E, Agostini P, DiMauro L F and Reis D A 2011 Observation of high-order harmonic generation in a bulk crystal *Nat. Phys.* **7** 138
[18] Luu T T, Zhong Y, Jain A, Gaumnitz T, Pertot Y, Ma J and Wörner H J 2018 Extreme–ultraviolet high-harmonic generation in liquids *Nat. Commun.* **9** 3723
[19] Li L, Lan P F, Zhu X S, Huang T F, Zhang Q B, Lein M and Lu P X 2019 Reciprocal-space-trajectory perspective on high-harmonic generation in solids *Phys. Rev. Lett.* **122** 193901

[20] Furch F J, Witting T, Osolodkov M, Schell F, Schulz C P and Vrakking M J J 2022 High power, high repetition rate laser-based sources for attosecond science *J. Phys. Photon.* **4** 032001

[21] Fattahi H *et al* 2014 Third-generation femtosecond technology *Optica* **1** 45

[22] Russell P 2003 Photonic crystal fibers *Science* **299** 358–62

[23] Udem T, Holzwarth R and Hansch T W 2002 Optical frequency metrology *Nature* **416** 233

[24] Petersen C R, Møller U, Kubat I, Zhou B, Dupont S, Ramsay J and Bang O 2014 Mid-infrared supercontinuum covering the 1.4–13.3 μm molecular fingerprint region using ultra-high NA chalcogenide step-index fibre *Nat. Photon.* **8** 830

[25] He P, Liu Y Y, Zhao K, Teng H, He X K, Huang P and Wei Z Y 2017 High-efficiency supercontinuum generation in solid thin plates at 0.1 TW level *Opt. Lett.* **42** 474

[26] Armstrong J A, Bloembergen N, Ducuing J and Pershan P S 1962 Interactions between light waves in a nonlinear dielectric *Phys. Rev.* **127** 1918

[27] Zhu S-N, Zhu Y-Y and Ming N-B 1997 Quasi-phase-matched third-harmonic generation in a quasi-periodic optical superlattice *Science* **278** 843

[28] Chen B-Q, Ren M-L, Liu R-J, Zhang C, Sheng Y, Ma B-Q and Li Z-Y 2014 Simultaneous broadband generation of second and third harmonics from chirped nonlinear photonic crystals *Light Sci. Appl.* **3** e189

[29] Chen B-Q, Zhang C, Hu C-Y, Liu R-J and Li Z-Y 2015 High-efficiency broadband high-harmonic generation from a single quasi-phase-matching nonlinear crystal *Phys. Rev. Lett.* **115** 83902

[30] Chen B Q, Hong L H, Hu C Y and Li Z Y 2021 White laser realized via synergic second- and third-order nonlinearities *Research* **2021** 1539730

[31] Li M Z, Hong L H and Li Z-Y 2022 Intense two-octave ultraviolet-visible-infrared supercontinuum laser via high-efficiency one-octave second-harmonic generation *Research* **2022** 9871729

[32] Bai Z, Yuan H, Liu Z, Xu P, Gao Q, Williams R J, Kitzler O, Mildren R P, Wang Y and Lu Z 2018 Stimulated Brillouin scattering materials, experimental design and applications: a review *Opt. Mater.* **75** 626–45

[33] Kang Z, Fan Z, Huang Y, Zhang H, Ge W, Li M, Yan X and Zhang G 2018 High-repetition-rate, high-pulse-energy, and high-beam-quality laser system using an ultraclean closed-type SBS-PCM *Opt. Express* **26** 6560–71

[34] Cao C, Wang Y, Bai Z, Li Y, Yu Y and Lu Z 2021 Developments of picosecond lasers based on stimulated Brillouin scattering pulse compression *Front. Phys.* **9** 747272

[35] Yuan H, Wang Y, Lu Z and Zheng Z 2018 Active frequency matching in stimulated Brillouin amplification for production of a 2.4 J, 200 ps laser pulse *Opt. Lett.* **43** 511–4

[36] Cui C, Wang Y, Lu Z, Yuan H, Wang Y, Chen Y, Wang Q, Bai Z and Mildren R P 2018 Demonstration of 2.5 J, 10 Hz, nanosecond laser beam combination system based on non-collinear Brillouin amplification *Opt. Express* **26** 32717–27

[37] Chen H, Bai Z, Yang X, Ding J, Qi Y, Yan B, Wang Y, Lu Z and Mildren R P 2022 Enhanced stimulated Brillouin scattering utilizing Raman conversion in diamond *Appl. Phys. Lett.* **120** 181103

[38] Damzen M J, Vlad V, Mocofanescu A and Babin V 2003 *Stimulated Brillouin Scattering: Fundamentals and Applications* (Boca Raton, FL: CRC Press)

[39] Chen Y, Lu Z, Wang Y and He W 2014 Phase matching for noncollinear Brillouin amplification based on controlling of frequency shift of Stokes seed *Opt. Lett.* **39** 3047–9

[40] Zhu Z-H, Chen P, Sheng L-W, Wang Y-L, Hu W, Lu Y-Q and Gao W 2017 Generation of strong cylindrical vector pulses via stimulated Brillouin amplification *Appl. Phys. Lett.* **110** 141104

[41] Bai Z *et al* 2016 High compact, high quality single longitudinal mode hundred picoseconds laser based on stimulated Brillouin scattering pulse compression *Appl. Sci.* **6** 29

[42] Flamini F, Spagnolo N and Sciarrino F 2019 Photonic quantum information processing: a review *Rep. Prog. Phys.* **82** 016001

[43] Pan J, Chen Z, Lu C, Weinfurter H, Zeilinger A and Zukowski M 2012 Multiphoton entanglement and interferometry *Rev. Mod. Phys.* **84** 777–838

[44] Li Y, Zhou Z, Ding D and Shi B 2015 CW-pumped telecom band polarization entangled photon pair generation in a Sagnac interferometer *Opt. Express* **23** 28792–800

[45] Li Y, Zhou Z, Xu Z, Xu L, Shi B and Guo G 2016 Multiplexed entangled photon-pair sources for all-fiber quantum networks *Phys. Rev. A* **94** 043810

[46] Li Y *et al* 2017 On-chip multiplexed multiple entanglement sources in a single silicon nanowire *Phys. Rev. Appl.* **7** 064005

[47] Moody G *et al* 2022 2022 Roadmap on integrated quantum photonics *J. Phys. Photon.* **4** 012501

[48] Joshi C, Farsi A, Clemmen S, Ramelow S and Gaeta A 2018 Frequency multiplexing for quasi-deterministic heralded single-photon sources *Nat. Commun.* **9** 847

[49] Liu Y, Guo D, Yang R, Sun C, Duan J, Gong Y, Xie Z and Zhu S 2021 Narrowband photonic quantum entanglement with counter propagating domain engineering *Photon. Res.* **9** 1998

[50] Ndagano B, Defienne H, Branford D, Shah Y, Lyons A, Westerberg N, Gauger E and Faccio D 2022 Quantum microscopy based on Hong–Ou–Mandel interference *Nat. Photon.* **16** 384–9

[51] Zhou J, Liu S, Qian H, Li Y, Luo H, Wen S, Zhou Z, Guo G, Shi B and Liu Z 2020 Metasurface enabled quantum edge detection *Sci. Adv.* **6** eabc4385

[52] Feng D, Ming N-B, Hong J-F, Yang Y-S, Zhu J-S, Yang Z and Wang Y-N 1980 Enhancement of second-harmonic generation in LiNbO$_3$ crystals with periodic laminar ferroelectric domains *Appl. Phys. Lett.* **37** 607

[53] Berger V 1998 Nonlinear photonic crystals *Phys. Rev. Lett.* **81** 4136

[54] Wei D Z *et al* 2018 Experimental demonstration of a three-dimensional lithium niobate nonlinear photonic crystal *Nat. Photon.* **12** 596–600

[55] Xu T X, Switkowski K, Chen X, Liu S, Koynov K, Yu H, Zhang H, Wang J, Sheng Y and Krolikowski W 2018 Three-dimensional nonlinear photonic crystal in ferroelectric barium calcium titanate *Nat. Photon.* **12** 591

[56] Shao M, Liang F, Yu H and Zhang H 2020 Pushing periodic-disorder-induced phase matching into the deep-ultraviolet spectral region: theory and demonstration *Light Sci. Appl.* **9** 45

[57] Wei D *et al* 2019 Efficient nonlinear beam shaping in three-dimensional lithium niobate nonlinear photonic crystals *Nat. Commun.* **10** 4193

[58] Liu S, Switkowski K, Xu C, Tian J, Wang B, Lu P, Krolikowski W and Sheng Y 2019 Nonlinear wavefront shaping with optically induced three-dimensional nonlinear photonic crystals *Nat. Commun.* **10** 3208

[59] Chen P C *et al* 2021 Quasi-phase-matching-division multiplexing holography in a three-dimensional nonlinear photonic crystal *Light Sci. Appl.* **10** 146

[60] Xu C, Huang S T, Yu Q, Wei D Z, Chen P C, Nie S W, Zhang Y and Xiao M 2021 Manipulating the orbital-angular-momentum correlation of entangled two-photon states in three-dimensional nonlinear photonic crystals *Phys. Rev.* A **104** 063716

[61] Franken P A, Hill A E, Peters C W and Weinreich G 1961 Generation of optical harmonics *Phys. Rev. Lett.* **7** 118–9

[62] Royd R W 2008 *Nonlinear Optics* (New York: Academic)

[63] Fejer M M, Magel G A, Jundt D H and Byer R L 1992 Quasi-phase-matched second harmonic generation: tuning and tolerances *IEEE J. Quantum Electron.* **28** 2631–54

[64] Franken P A and Ward J F 1963 Optical harmonics and nonlinear phenomena *Rev. Mod. Phys.* **35** 23–39

[65] Lu Y, Zheng J, Lu Y, Ming N and Xu Z 1999 Frequency tuning of optical parametric generator in periodically poled optical superlattice LiNbO$_3$ by electro-optic effect *Appl. Phys. Lett.* **74** 123–5

[66] Chen X *et al* 2020 First-principles experimental demonstration of ferroelectricity in a thermotropic nematic liquid crystal: polar domains and striking electro-optics *Proc. Natl Acad. Sci.* **117** 14021–31

[67] Mertelj A *et al* 2018 Splay nematic phase *Phys. Rev.* X **8** 041025

[68] Zhao X, Zhou J, Li J, Kougo J, Wan Z, Huang M and Aya S 2021 Spontaneous helielectric nematic liquid crystals: electric analog to helimagnets *Proc. Natl Acad. Sci.* **118** e2111101118

[69] Zhao X, Long H, Xu H, Kougo J, Xia R, Li J, Huang M and Aya S 2022 Nontrivial phase matching in helielectric polarization-helices: universal phase matching theory, validation and electric switching *Proc. Natl Acad. Sci.* **119** e2205636119

[70] Li Z, Ruan Y-P, Chen P, Tang J, Hu W, Xia K-Y and Lu Y-Q 2021 Liquid crystal devices for vector vortex beams manipulation and quantum information applications *Chin. Opt. Lett.* **19** 112601

[71] Chen C T, Wu Y and Li R 1989 The anionic group theory of the non-linear optical effect and its applications in the development of new high-quality NLO crystals in the borate series *Int. Rev. Phys. Chem.* **8** 65–91

[72] Chen C-T and Liu G-Z 1986 Recent advances in nonlinear optical and electrooptical materials *Annu. Rev. Mater. Sci.* **16** 203–43

[73] Mutailipu M K, Poeppelmeier R and Pan S 2021 Borates: a rich source for optical materials *Chem. Rev.* **121** 1130–202

[74] Zou G, Ye N, Huang L and Lin X 2011 Alkaline-alkaline earth fluoride carbonate crystals ABCO$_3$F (A = K, Rb, Cs; B = Ca, Sr, Ba) as nonlinear optical materials *J. Am. Chem. Soc.* **133** 20001–7

[75] Liu X, Gong P, Yang Y, Song G and Lin Z 2019 Nitrate nonlinear optical crystals: a survey on structure-performance relationships *Coord. Chem. Rev.* **400** 213045–58

[76] Luo M, Lin C, Lin D and Ye N 2020 Rational design of the metal-free KBe$_2$BO$_3$F$_2$●(KBBF) family member C(NH$_2$)$_3$SO$_3$F with ultraviolet optical nonlinearity *Angew. Chem., Int. Ed.* **59** 15978–81

[77] Kalmutzki M, Ströbele M, Wackenhut F, Meixner A J and Meyer H-J 2014 Synthesis, structure, and frequency-doubling effect of calcium cyanurate *Angew. Chem., Int. Ed.* **53** 14260–3

[78] Lin D, Luo M, Lin C, Xu F and Ye N 2019 KLi(HC$_3$N$_3$O$_3$)●2H$_2$O: solvent-drop grinding method toward the hydro-isocyanurate nonlinear optical crystal *J. Am. Chem. Soc.* **141** 3390–4

[79] Lu J, Lian Y-K, Xiong L, Wu Q-R, Zhao M, Shi K-X, Chen L and Wu L-M 2019 How to maximize birefringence and nonlinearity of π-conjugated cyanurates *J. Am. Chem. Soc.* **141** 16151–9

[80] Jiang T *et al* 2018 Gate-tunable third-order nonlinear optical response of massless Dirac fermions in graphene *Nat. Photon.* **12** 430

[81] Zhang Y *et al* 2019 Doping-induced second-harmonic generation in centrosymmetric graphene from quadrupole response *Phys. Rev. Lett.* **122** 047401

[82] Shan Y, Li Y, Huang D, Tong Q, Yao W, Liu W-T and Wu S 2018 Stacking symmetry governed second harmonic generation in graphene trilayers *Sci. Adv.* **4** eaat0074

[83] Zeng H *et al* 2013 Optical signature of symmetry variations and spin-valley coupling in atomically thin tungsten dichalcogenides *Sci. Rep.* **3** 1608

[84] Hsu W-T, Zhao Z-A, Li L-J, Chen C-H, Chiu M-H, Chang P-S, Chou Y-C and Chang W-H 2014 Second harmonic generation from artificially stacked transition metal dichalcogenide twisted bilayers *ACS Nano* **8** 2951

[85] Jiang T, Liu H, Huang D, Zhang S, Li Y, Gong X, Shen Y-R, Liu W-T and Wu S 2014 Valley and band structure engineering of folded MoS$_2$ bilayers *Nat. Nanotechnol.* **9** 825

[86] Zhou X, Cheng J, Zhou Y, Cao T, Hong H, Liao Z, Wu S, Peng H, Liu K and Yu D 2015 Strong second-harmonic generation in atomic layered GaSe *J. Am. Chem. Soc.* **137** 7994

[87] Sun Z *et al* 2019 Giant nonreciprocal second-harmonic generation from antiferromagnetic bilayer CrI$_3$ *Nature* **572** 497

[88] Liang J *et al* 2017 Monitoring local strain vector in atomic-layered MoSe$_2$ by second-harmonic generation *Nano Lett.* **17** 7539

[89] Su H *et al* 2019 Pressure-controlled structural symmetry transition in layered InSe *Laser Photonics Rev.* **13** 1900012

[90] Qi Y, Yang S, Wang J, Li L, Bai Z, Wang Y and Lv Z 2022 Recent advance of emerging low-dimensional materials for vector soliton generation in fiber lasers *Mater. Today Phys.* **23** 100622

[91] Yang S, Zhang Q, Zhu Z, Qi Y, Yin P, Ge Y, Li L, Jin L, Zhang L and Zhang H 2022 Recent advances and challenges on dark solitons in fiber lasers *Opt. Laser Technol.* **152** 108116

[92] Levy M, Osgood R and Liu R 1998 Fabrication of single-crystal lithium niobate films by crystal ion slicing *Appl. Phys. Lett.* **73** 2293–5

[93] Jia Y, Wang L and Chen F 2021 Ion-cut lithium niobate on insulator technology: recent advances and perspectives *Appl. Phys. Rev.* **8** 011307

[94] Zhang M, Wang C, Cheng R, Shams-Ansari A and Lončar M 2017 Monolithic ultra-high-Q lithium niobate microring resonator *Optica* **4** 1536–7

[95] Zhu D *et al* 2021 Integrated photonics on thin-film lithium niobate *Adv. Opt. Photonics* **13** 242–352

[96] Zheng Y, Fang Z, Liu S, Cheng Y and Chen X 2019 High-Q exterior whispering-gallery modes in a double-layer crystalline microdisk resonator *Phys. Rev. Lett.* **122** 253902

[97] Xue G, Tian X, Zhang C, Xie Z, Xu P, Gong Y and Zhu S 2020 Effect of thickness variations of lithium niobate on insulator waveguide on the frequency spectrum of spontaneous parametric down-conversion *Chin. Phys.* B **30** 110313

[98] Luo Q, F. B, Kong Y, Zhang G and Xu J 2021 Research progresses of microcavity lasers based on lithium niobate on insulator *Infrared Laser Eng.* **50** 20210546

[99] Nagy J and Reano R 2020 Submicrometer periodic poling of lithium niobate thin films with bipolar preconditioning pulses *Opt. Mater. Express* **10** 1911

[100] Wang S, Yang L, Cheng R, Xu Y, Shen M, Cone R, Thiel C and Tang H 2020 Incorporation of erbium ions into thin-film lithium niobate integrated photonics *Appl. Phys. Lett.* **116** 151103

[101] Beeck C *et al* 2021 III/V-on-lithium niobate amplifiers and lasers *Optica* **8** 1288–9

[102] Gholipour Vazimali M and Fathpour S 2022 Applications of thin-film lithium niobate in nonlinear integrated photonics *Adv. Photonics* **4** 034001

[103] Zheng Y and Chen X 2021 Nonlinear wave mixing in lithium niobate thin film *Adv. Phys.* X **6** 1889402

[104] Lin J *et al* 2019 Broadband quasi-phase-matched harmonic generation in an on-chip monocrystalline lithium niobate microdisk resonator *Phys. Rev. Lett.* **122** 173903

[105] Liu X *et al* 2022 Ultra-broadband and low-loss edge coupler for highly efficient second harmonic generation in thin-film lithium niobate *Adv. Photonics Nexus* **1** 016001

[106] Yuan S, Yunkun W, Dang Z, Zeng C, Xiaozhuo Q, Guo G, Ren X and Xia J 2021 Strongly enhanced second harmonic generation in a thin film lithium niobate heterostructure cavity *Phys. Rev. Lett.* **127** 153901

[107] Junjun M, Xie F, Chen W, Chen J, Wei W, Liu W, Chen Y, Cai W, Ren M and Jingjun X 2021 Nonlinear lithium niobate metasurfaces for second harmonic generation *Laser Photonics Rev.* **15** 2000521

[108] Zhang X *et al* 2022 Quasi-bound states in the continuum enhanced second-harmonic generation in thin-film lithium niobate *Laser Photonics Rev.* **16** 2200031

[109] Hao Z, Zhang L, Mao W, Gao A, Gao X, Gao F, Bo F, Zhang G and Xu J 2020 Second-harmonic generation using d_{33} in periodically poled lithium niobate microdisk resonators *Photon. Res.* **8** 311–7

[110] Datta I *et al* 2020 Low-loss composite photonic platform based on 2D semiconductor monolayers *Nat. Photon.* **14** 256

[111] Ono M, Hata M, Tsunekawa M, Nozaki K, Sumikura H, Chiba H and Notomi M 2020 Ultrafast and energy-efficient all-optical switching with graphene-loaded deep-subwavelength plasmonic waveguides *Nat. Photon.* **14** 37–43

[112] Wang F F, Niu X X, Hu X Y, Gu T Y, Wang X Y, Yang J H, Yang H, Ao Y T, Wang S F and Gong Q H 2020 All-optical mode-selective router based on broken anti-PT symmetry *Phys. Rev. Appl.* **14** 044050

[113] Haffner C *et al* 2018 Low-loss plasmon-assisted electro-optic modulator *Nature* **556** 483–6

[114] Chai Z, Zhu Y, Hu X Y, Yang X Y, Gong Z B, Wang F F, Yang H and Gong Q H 2016 On-chip optical switch based on plasmon-photon hybrid nanostructure-coated multicomponent nanocomposite *Adv. Opt. Mater.* **4** 1159–66

[115] Chai Z, Hu X Y, Wang F F, Niu X X, Xie J Y and Gong Q H 2017 Ultrafast all-optical switching *Adv. Opt. Mater.* **5** 1600665

[116] Alam M Z, Leon I D and Boyd R W 2016 Large optical nonlinearity of indium tin oxide in its epsilon-near-zero region *Science* **352** 795–7

[117] Kinsey N, DeVault C, Boltasseva A and Shalaev V M 2019 Near-zero-index materials for photonics *Nat. Rev. Mater.* **4** 742–60

[118] Niu X X, Hu X Y, Sun Q, Lu C C, Yang Y M, Yang H and Gong Q H 2020 Polarization-selected nonlinearity transition in gold dolmens coupled to an epsilon-near-zero material *Nanophotonics* **9** 4839–51

[119] Qi H X, Wang X X, Hu X Y, Du Z C, Yang J Y, Yu Z X, Ding S Q, S S S C and Gong Q H 2021 All-optical switch based on novel physics effects *J. Appl. Phys.* **129** 210906

[120] N V Richardson and S Holloway (eds) 2008 *Handbook of Surface Science* (Amsterdam: Elsevier)

[121] Shen Y R 2016 *Fundamentals of Sum-Frequency Spectroscopy* (Cambridge: Cambridge University Press)

[122] Tian C S and Shen Y R 2014 Recent progress on sum-frequency spectroscopy *Surf. Sci. Rep.* **69** 105–31

[123] Ji N, Ostroverkhov V, Chen C-Y and Shen Y-R 2007 Phase-sensitive sum-frequency vibrational spectroscopy and its application to studies of interfacial alkyl chains *J. Am. Chem. Soc.* **129** 10056

[124] Ostroverkhov V, Waychunas G A and Shen Y R 2005 New information on water interfacial structure revealed by phase-sensitive surface spectroscopy *Phys. Rev. Lett.* **94** 046102

[125] Stiopkin I V, Jayathilake H D, Bordenyuk A N and Benderskii A V 2008 Heterodyne-detected vibrational sum frequency generation spectroscopy *J. Am. Chem. Soc.* **130** 2271–5

[126] Yamaguchi S and Tahara T 2008 Heterodyne-detected electronic sum frequency generation: 'up' versus 'down' alignment of interfacial molecules *J. Chem. Phys.* **129** 2981179

[127] Wen Y-C, Zha S, Liu X, Yang S, Guo P, Shi G, Fang H, Shen Y R and Tian C 2016 Unveiling microscopic structures of charged water interfaces by surface-specific vibrational spectroscopy *Phys. Rev. Lett.* **116** 016101

[128] Levin Y 2009 Polarizable ions at interfaces *Phys. Rev. Lett.* **102** 147803

[129] Le J M, Su Y, Tian C, Kung A H and Shen Y R 2023 A novel scheme for ultrashort terahertz pulse generation over a gapless wide spectral range: Raman-resonance-enhanced four-wave mixing *Light Sci. Appl.* **12** 34

[130] Dadap J I, Shan J, Eisenthal K B and Heinz T F 1999 Second–harmonic Rayleigh scattering from a sphere of centrosymmetric material *Phys. Rev. Lett.* **83** 4045–8

[131] Roke S and Gonella G 2012 Nonlinear light scattering and spectroscopy of particles and droplets in liquids *Annu. Rev. Phys. Chem.* **63** 353–78

[132] Florsheimer M, Brillert C and Fuchs H 1999 Chemical imaging of interfaces by sum frequency microscopy *Langmuir* **15** 5437–9

[133] Arnolds H and Bonn M 2010 Ultrafast surface vibrational dynamics *Surf. Sci. Rep.* **65** 45–66

[134] Chen S, Cai Y, Li G, Zhang S and Cheah K W 2016 Geometric metasurface fork gratings for vortex-beam generation and manipulation *Laser Photonics Rev.* **10** 322

[135] Liu X, Deng J, Jin M, Tang Y, Zhang X, Li K F and Li G 2019 Cassegrain metasurface for generation of orbital angular momentum of light *Appl. Phys. Lett.* **115** 221102

[136] Ren H, Fang X, Jang J, Bürger J, Rho J and Maier S A 2020 Complex-amplitude metasurface-based orbital angular momentum holography in momentum space *Nat. Nanotechnol.* **15** 948

[137] Li G, Chen S, Pholchai N, Reineke B, Wong P W H, Pun E Y B, Cheah K W, Zentgraf T and Zhang S 2015 Continuous control of the nonlinearity phase for harmonic generations *Nat. Mater.* **14** 607

[138] Li G *et al* 2017 Nonlinear metasurface for simultaneous control of spin and orbital angular momentum in second harmonic generation *Nano Lett.* **17** 7974

[139] Chen S, Li K F, Deng J, Li G and Zhang S 2020 High-order nonlinear spin–orbit interaction on plasmonic metasurfaces *Nano Lett.* **20** 8549

[140] Mao N *et al* 2022 Nonlinear wavefront engineering with metasurface decorated quartz crystal *Nanophotonics* **11** 797

[141] Berry M V and Balazs N L 1979 Nonspreading wave packets *Am. J. Phys.* **47** 264

[142] Siviloglou G A, Broky J, Dogariu A and Christodoulides D N 2007 Observation of accelerating Airy beams *Phys. Rev. Lett.* **99** 213901

[143] Efremidis N K, Chen Z, Segev M and Christodoulides D N 2019 Airy beams and accelerating waves: an overview of recent advances *Optica* **6** 686

[144] Kaminer I, Segev M and Christodoulides D N 2011 Self-accelerating self-trapped optical beams *Phys. Rev. Lett.* **106** 213903

[145] Jia S, Lee J, Fleischer J W, Siviloglou G A and Christodoulides D N 2010 Diffusion-trapped Airy beams in photorefractive media *Phys. Rev. Lett.* **104** 253904

[146] Wimmer M, Regensburger A, Bersch C, Miri M-A, Batz S, Onishchukov G, Christodoulides D N and Peschel U 2013 Optical diametric drive acceleration through action–reaction symmetry breaking *Nat. Phys.* **9** 780

[147] Batz S and Peschel U 2013 Diametrically driven self-accelerating pulses in a photonic crystal fiber *Phys. Rev. Lett.* **110** 193901

[148] Pei Y, Hu Y, Lou C, Song D, Tang L, Xu J and Chen Z 2018 Observation of spatial optical diametric drive acceleration in photonic lattices *Opt. Lett.* **43** 118

[149] Zhang P, Hu Y, Bongiovanni D, Li Z, Morandotti R, Chen Z and Xu J 2021 Unveiling the link between airy-like self-acceleration and diametric drive acceleration *Phys. Rev. Lett.* **127** 083901

[150] Alberucci A, Jisha C P, Peschel U and Nolte S 2019 Effective breaking of the action-reaction principle using spatial solitons *Phys. Rev. A* **100** 11802(R)

[151] Barh A, Rodrigo P J, Meng L, Pedersen C and Tidemand-Lichtenberg P 2019 Parametric upconversion imaging and its applications *Adv. Opt. Photonics* **11** 952–1019

[152] Dam J S, Tidemand-Lichtenberg P and Pedersen C 2012 Room-temperature mid-infrared single-photon spectral imaging *Nat. Photon.* **6** 788–93

[153] Zhou Q, Huang K, Pan H, Wu E and Zeng H 2013 Ultrasensitive mid-infrared up-conversion imaging at few-photon level *Appl. Phys. Lett.* **102** 241110

[154] Huang K, Wang Y, Fang J, Kang W, Sun Y, Liang Y, Hao Q, Yan M and Zeng H 2021 Mid-infrared photon counting and resolving via efficient frequency upconversion *Photon. Res.* **9** 259–65

[155] Mrejen M, Erlich Y, Levanon A and Suchowski H 2020 Multicolor time-resolved upconversion imaging by adiabatic sum frequency conversion *Laser Photonics Rev.* **14** 2000040

[156] Huang K, Fang J, Yan M, Wu E and Zeng H 2022 Wide-field mid-infrared single-photon upconversion imaging *Nat. Commun.* **13** 1077

[157] Liu P, Guo L, Qi F, Li W, Li W, Fu Q, Yao J, Xia M, Liu Z and Wang Y 2022 Large dynamic range and wideband mid-infrared upconversion detection with $BaGa_4Se_7$ crystal *Optica* **9** 50–55

[158] Wang Y, Fang J, Zheng T, Liang Y, Hao Q, Wu E, Yan M, Huang K and Zeng H 2021 Mid-infrared single-photon edge enhanced imaging based on nonlinear vortex filtering *Laser Photonics Rev.* **15** 2100189

[159] Junaid S, Kumar S C, Mathez M, Hermes M, Stone N, Shepherd N, Ebrahim-Zadeh M, Tidemand-Lichtenberg P and Pedersen C 2019 Video-rate, mid-infrared hyperspectral upconversion imaging *Optica* **6** 702–8

[160] Israelsen N M, Petersen C R, Barh A, Jain D, Jensen M, Hannesschläger G, Tidemand-Lichtenberg P, Pedersen C, Podoleanu A and Bang O 2019 Real-time high-resolution mid-infrared optical coherence tomography *Light Sci. Appl.* **8** 11

[161] Kawata S, Sun H-B, Tanaka T and Takada K 2001 Finer features for functional microdevices *Nature* **412** 697–8

[162] Chen N-K, Li X-B, Bang J, Wang X-P, Han D, West D, Zhang S and Sun H-B 2018 Directional forces by momentumless excitation and order-to-order transition in Peierls-distorted solids: the case of GeTe *Phys. Rev. Lett.* **120** 185701

[163] Wang X-J, Fang H-H, Sun F-W and Sun H-B 2022 Laser writing of color centers *Laser Photonics Rev.* **16** 2100029

[164] Wang L, Chen Q-D, Cao X-W, Buividas R, Wang X, Juodkazis S and Sun H-B 2017 Plasmonic nano-printing: large-area nanoscale energy deposition for efficient surface texturing *Light Sci. Appl.* **6** e17112

[165] Ouyang X *et al* 2021 Synthetic helical dichroism for six-dimensional optical orbital angular momentum multiplexing *Nat. Photon.* **15** 901–7

[166] Li Z-Z, Wang L, Fan H, Yu Y-H, Chen Q-D, Juodkazis S and Sun H-B 2020 O-FIB: far-field-induced near-field breakdown for direct nanowriting in an atmospheric environment *Light Sci. Appl.* **9** 1–7

[167] Zhang X-L, Yu F, Chen Z-G, Tian Z-N, Chen Q-D, Sun H-B and Ma G 2022 Non-Abelian braiding on photonic chips *Nat. Photon.* **16** 390–5

[168] Hua J G, Liang S Y, Chen Q D, Juodkazis S and Sun H B 2022 Free-form micro-optics out of crystals: femtosecond laser 3D sculpturing *Adv. Funct. Mater.* **32** 2200255

[169] Genty G, Salmela L, Dudley J M, Brunner D, Kokhanovskiy A, Kobtsev S and Turitsyn S K 2021 Machine learning and applications in ultrafast photonics *Nat. Photon.* **15** 91–101

[170] Hu Z Y, Jiang T, Tian Z N, Niu L G, Mao J W, Chen Q D and Sun H B 2022 Broad-bandwidth micro-diffractive optical elements *Laser Photonics Rev.* **16** 2100537

[171] Kosterev A, Bakhirkin Y A, Curl R F and Tittel F K 2002 Quartz-enhanced photoacoustic spectroscopy *Opt. Lett.* **27** 1902–4

[172] Wei T, Wu H, Dong L and Tittel F K 2019 Acoustic detection module design of a quartz-enhanced photoacoustic sensor *Sensors* **19** 1093

[173] Patimisco P, Scamarcio G, Tittel F and Spagnolo V 2014 Quartz-enhanced photoacoustic spectroscopy: a review *Sensors* **14** 6165

[174] Repond P and Sigrist M W 1996 Photoacoustic spectroscopy on trace gases with continuously tunable CO_2 laser *Appl. Opt.* **35** 4065

[175] Simandoux O, Prost A, Gateau J and Bossy E 2015 Influence of nanoscale temperature rises on photoacoustic generation: discrimination between optical absorbers based on thermal nonlinearity at high frequency *Photoacoustics* **3** 20

[176] Wu H, Dong L, Zheng H, Liu X, Yin X, Ma W, Zhang L, Yin W, Jia S and Tittel F 2015 Enhanced near-infrared QEPAS sensor for sub-ppm level H_2S detection by means of a fiber amplified 1528 nm DFB laser *Sens. Actuators* B **221** 666

[177] Wu H *et al* 2015 Quartz enhanced photoacoustic H_2S gas sensor based on a fiber-amplifier source and a custom tuning fork with large prong spacing *Appl. Phys. Lett.* **107** 111104

[178] Yin X, Wu H, Dong L, Ma W, Zhang L, Yin W, Xiao L, Jia S and Tittel F 2019 Ppb-level photoacoustic sensor system for saturation-free CO detection of SF_6 decomposition by use of a 10 W fiber-amplified near-infrared diode laser *Sens. Actuators* B **282** 567

[179] Patimisco P, Sampaolo A, Dong L, Tittel F K and Spagnolo V 2018 Recent advances in quartz enhanced photoacoustic sensing *Appl. Phys. Rev.* **5** 011106

[180] Wei T, Zifarelli A, Russo S D, Wu H, Menduni G, Patimisco P, Sampaolo A, Spagnolo V and Dong L 2021 High and flat spectral responsivity of quartz tuning for used as infrared photodetector in tunable diode laser spectroscopy *Appl. Phys. Rev.* **8** 041409

[181] Wu H, Dong L, Zheng H, Yu Y, Ma W, Zhang L, Yin W, Xiao L, Jia S and Tittel F K 2017 Beat frequency quartz-enhanced photoacoustic spectroscopy for fast and calibration-free continuous trace-gas monitoring *Nat. Commun.* **8** 15331

[182] Li B, Wu C Y, Wang M R, Charan K and Xu C 2020 An adaptive excitation source for high-speed multiphoton microscopy *Nat. Methods* **17** 163

[183] Zheng W *et al* 2017 Adaptive optics improves multiphoton super-resolution imaging *Nat. Methods* **14** 869

[184] Gao Y F *et al* 2022 Axial gradient excitation accelerates volumetric imaging of two-photon microscopy *Photon. Res.* **10** 687–96

[185] Yang C, Bi Y L, Cai E L, Chen Y G, Huang S L, Zhang Z H and Wang P 2021 Pulse-sheet chemical tomography by counterpropagating stimulated Raman scattering *Optica* **8** 396–401

[186] Tian S D *et al* 2020 Polydiacetylene-based ultrastrong bioorthogonal Raman probes for targeted live-cell Raman imaging *Nat. Commun.* **11** 81

[187] Ao J P, Fang X F, Miao X C, Ling J W, Kang H, Park S, Wu C F and Ji M B 2021 Switchable stimulated Raman scattering microscopy with photochromic vibrational probes *Nat. Commun.* **12** 3089

[188] Yang Y F, Yang Y L, Liu Z J, Guo L, Li S P, Sun X J, Shao Z M and Ji M B 2021 Microcalcification-based tumor malignancy evaluation in fresh breast biopsies with hyperspectral stimulated Raman scattering *Anal. Chem.* **93** 6223–31

[189] Shi K B, Li H F, Xu Q, Psaltis D and Liu Z W 2010 Coherent anti-stokes Raman holography for chemically selective single-shot nonscanning 3D imaging *Phys. Rev. Lett.* **104** 093902

[190] Hu C F, Field J J, Kelkar V, Chiang B, Wernsing K, Toussaint K C, Bartels R A and Popescu G 2020 Harmonic optical tomography of nonlinear structures *Nat. Photon.* **14** 564–9